2013

Development of Enhanced Lateral Flow test Devices for Point-of-Care Diagnostics

Roman Gerbers
University of Rhode Island, roman_gerbers@my.uri.edu

DEVELOPMENT OF ENHANCED LATERAL FLOW TEST DEVICES FOR POINT-OF-CARE DIAGNOSTICS

BY

ROMAN GERBERS

A THESIS SUBMITTED IN PARTIAL FULFILLMENT OF THE

REQUIREMENTS FOR THE DEGREE OF

MASTER OF SCIENCE

IN

MECHANICAL ENGINEERING

UNIVERSITY OF RHODE ISLAND

2013

MASTER OF SCIENCE THESIS

OF

ROMAN GERBERS

APPROVED:

Thesis Committee:

Major Professor Dr. Mohammad Faghri

Dr. Constantine Anagnostopoulos

Dr. Jason R. Dwyer

Dr. Nasser H. Zawia
DEAN OF THE GRADUATE SCHOOL

UNIVERSITY OF RHODE ISLAND

2013

ABSTRACT

Lateral flow Imunoassays (LFIA) are common, simple to use point-of-care devices for the diagnostic market. Conventionally LFIAs are limited in their complexity since they are optimized for minimally trained operators. Paper-based analytical devices (PAD) are advanced sensors based on a wide range of recently developed techniques for complex analytical methods. In this research, a point-of-care (POC) immunosensor was developed based on techniques adapted from lateral flow and paper-based analytical devices. Alternating layers of paper and tape were used to expand the common 2D design of lateral flow tests to 3D in order to enable complex fluid flow control. Four fluidic valves were integrated for automatic sequential loading of three different fluids to a detection area. Fabrication processes, reagent concentrations, materials and device geometries were optimized and a chip-yield of 92% was achieved. A three step alkaline phosphatase (ALP)-based enzyme-linked immunosorbent assay (ELISA) procedure with Rabitt IgG as model analyte was used to prove the working principle of the sensor. After optimization of crucial assay parameters practicability was verified by visual detection of signal development on nitrocellulose membrane after reaction of ALP and NBT/BCIP with a good detection limit of 4.8 fm.

Keywords: Lateral Flow Imunoassay (LFIA) Paper-based Analytical device (PAD), Alkaline Phosphatase (ALP), Enzyme Linked Immunosorbent Assay (ELISA), Point-of-Care (POC)

ACKNOWLEDGMENTS

It has been a wonderful and unforgettable experience spending the exchange year on completing my Master's thesis in the Department of Mechanical Engineering, University of Rhode Island.

First of all, I would like to thank Dr. Mohammad Faghri for his continuous guidance, encouragement and support throughout the course of this research. It has been a real pleasure to work with him, on this promising field.

I am grateful to Dr. Constantine Anagnostopoulos for his invaluable suggestions and continuous help. Furthermore, I would also like to thank Dr. Hong Chen, and Jeremy Cogswell. I learned a lot from them, such as sophisticated laboratory skills and the ability of developing new techniques to tackle the challenges in research. Great thanks to my lab colleague and good friend Wilke Föllscher without him it would not have been the same unforgettable experience.

Special thanks to Nadine Madanchi, who has been supporting and encouraging me from the beginning till the end, especially in the time of difficulties.

Finally, I want to thank my parents Kirsten Gerbers and Björn Gerbers. Without their enduring love, care and support in any situations of my life I could not have gone this path and reached the point where I am today.

TABLE OF CONTENTS

LIST OF TABLES

LIST OF FIGURES

LIST OF ABBREVIATIONS

POC	Point-of-Care
ELISA	Enzyme Linked Immunosorbent Assay
LFIA	Lateral Flow Imunoassay
LFT	Lateral Flow Test
LOD	Limit of Detection
LOQ	Limit of Quantification
PAD	Paper based Analytical Device
LOP	Lab on Paper
Ig	Imunoglubin
A3CS	Allyltrichlorosilane
AB	Antibody
AG	Antigen
GNP	Gold Nanoparticles
HRP	Horseradish Peroxidase
T20	Tween 20

LIST OF SYMBOLS

Latin Symbols

t	Time	s
KD	Antibody affinity	%
ΔP	Pressure difference	N/m^2
R_{eq}	Fluidic resistance	Ns/m^5
WH	Channel surface area	m^2
Q	Volumetric flow rate	m^3/s
q	Flow rate	m/s
V	Volume	m^3
L	Distance moved by fluid	m
D	Average pore diameter	m

Greek Symbols

μ	Viscosity	Ns/m^2
κ	permeability	m^2
γ	effective surface tension	N/m

CHAPTER 1 - INTRODUCTION

This chapter will introduce the background knowledge about point-of-care diagnostics and diagnostic devices, immunoassays and antibody recognition reaction advantages for paper as sensor substrate and lateral flow test devices.

1.1 Point of Care Diagnostics and Diagnostic Devices

Point-of-care (POC) devices allow rapid diagnostic tests to be performed at the site of patient care facility. This means the test can be done in the hospital, the emergency room, a physician's office or at home by minimally trained personnel. And, the results are available immediately rather than waiting for hours or days for the results to come back from a central facility [51].

Point of care testing is a fast growing area with a growth rate around 10% in clinical diagnostics which will be one of the biggest driving forces for the future of the in-vitro diagnostics market [54]. According to the market analyst Frost & Sullivan, the US market for Point-of-Care testing devices will increase from a revenue of $2.13 billion USD in 2009 to $3.93 billion USD in 2016 [11]. The market is thereby driven mainly by two high-growth segments, infectious diseases and coagulation monitoring. The infectious disease market is growing due to increasing infections, detection of new diseases and mutations. The coagulation monitoring market is growing dramatically because of expanded testing in patient homes and the growth of patient services [11].

Therefore, diagnostic testing devices have to be lightweight, portable and easy-to-use to perform complex biological tests at the site where they are most needed [54]. Microfluidic systems are suitable for those developments since they can be designed to operate from small volumes of complex fluids with efficiency and speed and without the requirement for highly trained personnel [31].

Several companies around the world market rapid tests. They have developed a variety of devices and technologies which reduce the test times to hours or even minutes [51]. Those technologies can be grouped in three different categories: Permanent integrated instruments; pure disposables; and permanent instruments that use disposable components [61].

Permanent integrated instruments are designed for a high-throughput work, with fast and accurate results but even when those devices would be cheap enough, they could not be considered as point of care devices because trained personnel are needed. Carry over between two tests has to be prevented by rinsing the component with cleaning solutions and also frequent calibration is necessary to keep the settings with the standards even when they use microfluidic components [61].

Disposables are analytical tests based on a disposable substrate (e.g. paper) they are normally based on a microfluidic device (e.g. Lateral flow test) and they rely on relatively inexpensive components and reagents which can be produced as commercial off-the-shelf (COTS) products on large-scale production methods, to be relatively affordable. They can be designed for detection of antigens or antibodies and are usable

with a wide range of specimens. Most of them are developed to be stable at ambient temperatures without refrigeration for more than a year and the analytical performance for some of them are comparable to reference-level laboratory methods [29].

Disposable tests provide POC diagnostics in areas without access to well-equipped and well-staffed clinical laboratories. Users can quickly learn to perform such disposable-based tests without the requirement to be repeatedly retrained. Because of this, disposable rapid tests are the one diagnostic technology which has been successfully used in the modern military and the developing world. However, complex and expensive approaches do not deliver the needs of the majority of the world's people suffering with infectious diseases, which have access mostly to poorly resourced health care facilities [60].

Disposable tests currently on the market have a number of disadvantages. They are still not as sufficiently sensitive, specific and accurate as laboratory results. They also usually provide just a yes/no answer.

Disposables with a reader are a compromise between disposables and professional instruments. The sample, the process reagents and the waste remain in the disposable while the reader is used to add more complexity to the test by using electrically driven valves and pumps to control the fluid flow of different fluids within the disposable. The advantage over integrated instruments is that the reader does not need to be cleaned between two samples and that calibrates can be stored on the

disposable. This compromise allows high performance with low per-test cost [61]. This approach is the perfect POC solution for hospitals where several tests have to be done daily at the patient's bedside. But the higher prices for the readers in comparison to just disposable tests keeps this approach from being widely accepted for at home use. And, the need for electricity for the pumps and valves is a disadvantage when the test has to be run in developing countries in places without easily available power sources. For a portable instrument the power could come from automobile generators, photocells, hand-generators, or stored in the disposable [61]. But all these points increase the complexity in comparison to disposable test devices.

Therefore, more complex diagnostic tests based on inexpensive disposables are needed to fulfill the requirements of POC applications at the patient's home and for the developing world.

1.2 Justification

One approach for more complex disposable devices with a better sensitivity is to use advanced lateral flow devices which are able to incorporate multiple fluids for the test. With multiple fluids, it is possible to perform more advanced Immunoassay protocols with disposable lateral flow tests. As example, for an ELISA immunoassay assay (*vide infra*) at least a substrate is needed as another input fluid in addition to the sample [23].

Devices on the market normally consist of a plastic housing with a developing solution pot which contains the second input fluid (e.g. substrate) that is heat-sealed with laminated aluminum film [23]. The user has to rapture the seal in order to release the developing solution. Their major disadvantage is that the user has to rapture the seal at the right time after the sample has been added to the strip test.

Using the paper based fluidic valve technology developed at the University of Rhode Island by Dr. Hong Chen et al. [3] at the microfluidics laboratory of Professor M. Faghri (*vide infra*), it is possible to develop lateral flow test devices with more than two fluids that are self-triggered after a certain amount of time. Such advanced lateral flow test strips are capable of conducting ELISA on paper without operator intervention, except for the application of the sample fluid.

1.3 Paper Based Analytical Devices

Advanced sensors based on a paper substrate are called paper based analytical devices (PAD) or lab on paper devices (LOP). They have recently gained increasing interest. For decades paper was used for analytical chemistry but lately it was rediscovered as substrate for sensors. This is because paper offers many advantages including biocompatibility, biodegradability, price and availability (see Table 1.1) which makes this material first-choice for development of disposable sensors and integrated sensing platforms [37].

Table 1.1: Paper as sensor substrate in comparison with traditional materials adapted from [37]

Property	Material			
	Paper	**PDMS**	**Glass**	**Silicon**
Structure	Fibrous	Solid	Solid	Solid
Fluid flow	Capillarity	Forced	Forced	Forced
Flexibility	+	+	–	–
Surface-to-volume ratio	+	–	–	–
Biocompatibility	+	+	+	+
Biodegradability	++	+	–	–
High-throughput fabrication	+	–	+	+
Sensitivity to moisture	+	–	–	–
Functionalization	++	–	–	+
Spatial resolution	–	+	+	++
Homogeneity of the material	–	+	+	+
Disposability	+	–	–	–
Price	++	+	+	–
Low initial investment	++	+	+	–

1.4 Immunoassays

Immunoassays are a suitable technique for the direct detection of targets of clinical Interest. They rely on the ability of an antibody to recognize and bind to a specific macromolecule in a lock and key mechanism.

1.4.1 Antibodies and Recognition Reaction

Antibodies (AB) are large Y-shaped glycoproteins produced by the B-cells of the immune system to identify and deactivate potentially harmful targets such as viruses or bacteria. They belong to the group of immunoglubins (Ig) and they possess the

ability to form specific binding sites by recognition of a unique part of the target, called an antigen (AG) [20].

To bind to an antigen the antibody binding-site contains a paratope that is specific for one particular region of 15–22 amino acids on the antigen called the epitope [13].

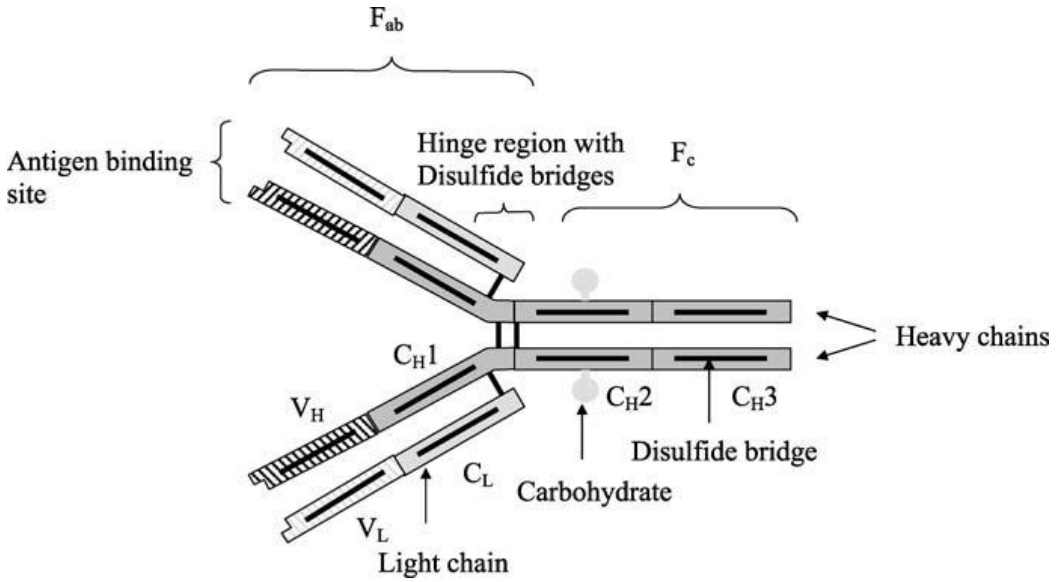

Figure 1.1: Schematic representation of an antibody. VL: variable part of the light chain, VH: variable part of the heavy chain, CL constant part of the light chain, CH1, CH2, CH3: constant parts of the heavy chain, Fab: fragment antigen binding, Fc: fragment constant/crystallyzable. Adapted from [44].

Besides the fragment antigen binding-region (F_{ab}) the antibodies consist of another binding region called fragment constant or crystallyzable region (F_c) which is used as contact region in the immune system for other molecules which can finally destroy the antigen. All antibodies are built on the same mirror-symmetrical Y-structure of four polypeptide chains, two of those chains are “light chains” (L-chains) and two of them are “heavy chains” (H-chains) They are linked by disulfide bridges (Figure 1.1) [44].

There are two types of immunoglubin light chains which are called lambda (λ) and kappa (κ) and five types of heavy chains (α, δ, ε, γ, and μ) [20]. The type of heavy chains defines the class of immunoglobulins (IgA, IgD, IgE, IgG, or IgM) [42].

In human serum approximately 85% of the antibodies belong to the IgG class at a concentration of 8–18 gL^{-1}, the dimeric IgA (0.9–4.5 gL^{-1}) and the pentameric IgM (0.6–2.8 gL^{-1}) can also be found [44]. The molecular weights of antibodies are 150 kDa for IgG and IgD, 900 kDa for IgM, 150 or 600 kDa for IgA and 190 kDa for IgE. The chemical composition of the reachable surface of an average antibody is 55% non-polar, 25% polar, and 20% charged [25]. Three groups of antibodies are typically produced: polyclonal, monoclonal and fragments of monoclonal antibodies [44].

Polyclonal antibodies are produced by vaccinating a mammal such as rabbit, goat, mouse, sheep or horse with the corresponding antigen. The blood serum isolated from these animals contains multiple antibodies which consist of different paratopes and recognize different epitopes on their respective antigen. Monoclonal antibodies are specific for only one single epitope of an antigen. They are produced by hybridoma cells which are isolated antibody-secreting lymphocytes from an animal and which are immortalized by fusing them with a cancer cell line [6]. Lately, genetically produced antibody fragments have played an increasing role, because of their characteristics to inhibit unspecific binding. The antibodies only consist of the Fab binding side while the Fc part is separated by enzymatic cleavage [44].

The recognition reaction between the paratope, the antigen-binding region (F_{ab}) and the eptitope, the surface structure on the antigen is mainly driven by four different non-covalent binding reactions. Those are electrostatic attraction between corresponding charges, van-der-Waals forces because of electron-density fluctuations, hydrogen bonds between electronegative atoms and hydrophobic interactions between nonpolar carbohydrates [44]. For example the usual number of hydrogen bonds in an Antibody-Antigen complex is acknowledged to be around 10 [21].

$$K_{\mathrm{D}} = \frac{k_{\mathrm{assosc}}}{k_{\mathrm{diss}}} = \frac{[AG][AB]}{[AGAB]} \tag{1.1}$$

The probability of an antibody to bind to a specific antigen is called affinity and it is described by a dissociation constant, K_D. K_D is the ratio of the association rate constant k_{assoc} and the dissociation rate constants k_{diss}. For monoclonal antibodies, studies [2 16, 17] have found that the dissociation rate constant has a wider variation than the association rate constant (k_{assoc} = 105–107 $M^{-1}s^{-1}$). The affinity can also be approximately derived from the law of mass action (Equation 1.1). The affinities for antibodies found in the literature vary between 10^{-5} M^{-1} and 10^{-12} M^{-1} [44].

1.5 Lateral Flow Test Strips

This section provides information on the key aspects of the design of lateral flow immunoassay (LFIA) also called lateral flow tests (LFT) with respect to the materials used and their integration with the assay conditions. Figure 1.2 shows the main parts

of a lateral flow test including the housing, membrane, sample-, conjugate- and absorbent pad.

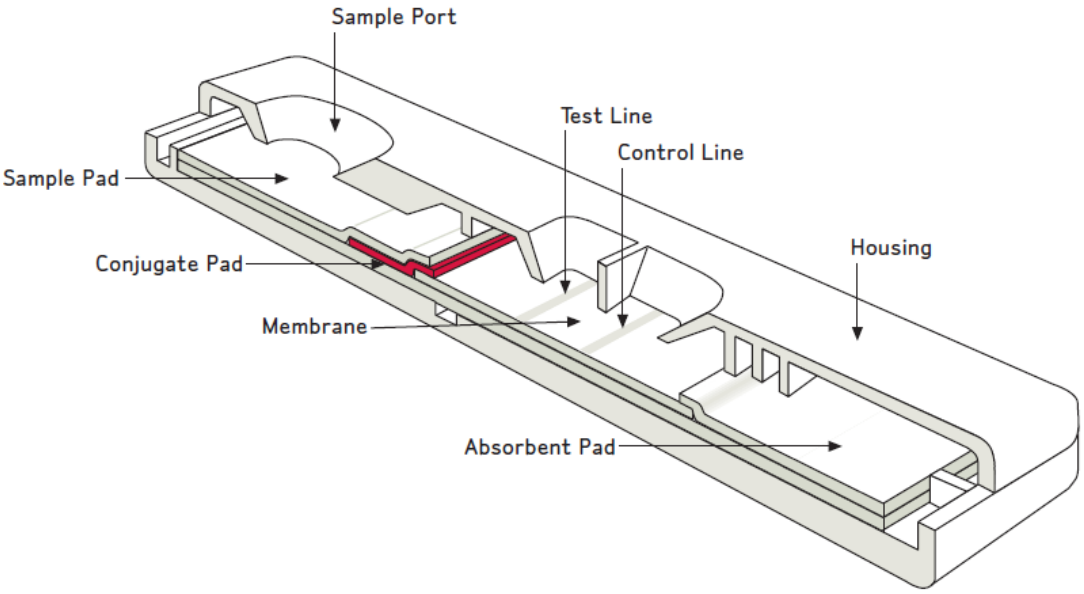

Figure 1.2: Schematic view of a lateral flow test strip [34]

1.5.1 Membrane

The membrane is the most important material used in a lateral flow test strip. For lateral flow test strips, the membrane must irreversibly bind capture reagents at the test or control lines. Physical and chemical attributes of the membrane affect its capillary flow properties which affects the reagent deposition, assay sensitivity, assay specificity, and test line consistency [34]. The binding characteristics of the membrane are defined by the polymer from which the membrane is made. Commonly used polymers and their binding characteristics are presented in Table 1.2.

Table 1.2: Binding properties of different membrane polymers [34]

Membrane polymer	Primary binding Mechanism
Nitrocellulose	Electrostatic
Polyvinylidene fluoride	Hydrophobic
(Charge-modified) nylon	(Ionic) electrostatic
Polyethersulfone	Hydrophobic

Because of electrostatically binding through interaction of strong dipole of nitrate ester with strong dipole of peptide bonds of the protein (Figure 1.3), nitrocellulose membranes are the most used membranes in the field.

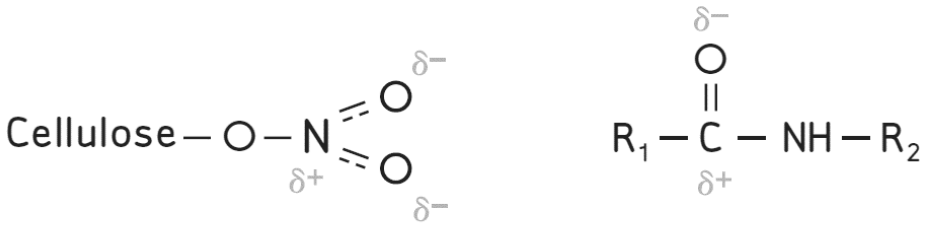

Figure 1.3: Structure of nitrocellulose ester and protein dipoles [34]

One important part for choosing the right membrane is the pore size, which is directly related to the capillary flow rate, and is therefore the most critical performance parameter. The concentration of analyte in the sample is inversely proportional to the square root of flow rate change (Figure 1.4). The result of this is a decreasing sensitivity and an increasing test time with decreasing flow rate.

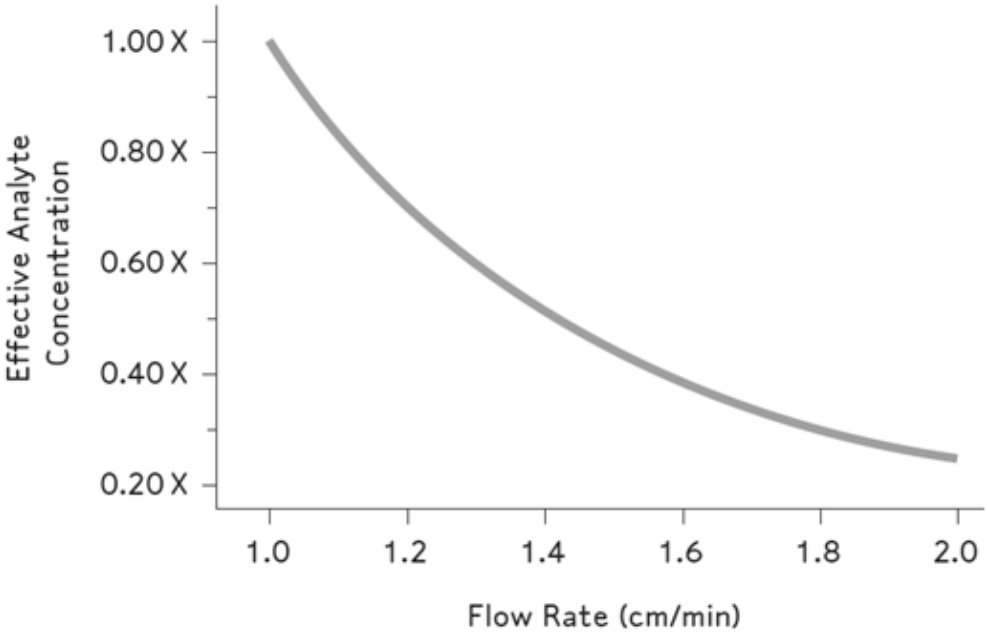

Figure 1.4: Effect of capillary flow rate on the effective Analyte concentration. X refers to Analyte concentration in the sample [34]

When reagent are applied to nitrocellulose membranes, chaotropic agents such as Tween 20, Triton X-100, glycerin, polyvinyl alcohol (PVA), polyvinylpyrrolidone (PVP), and polyethylene glycol (PEG), which might be used to inhibit unspecific binding or reduce the background noise should be minimized or avoided completely until after the capture reagents have been immobilized and fixed. Otherwise these compounds can physically interfere on molecular level between the protein and nitrocellulose and affect the signal development negatively [34].

1.5.2 Sample Pad

The main task of the sample pad is to ensure a uniform distribution and to control the flow rate of the sample to the conjugate pad. According to Millipore [34] the

sample pad can be treated with reagents such as proteins, detergents, viscosity enhancers, and buffer salts to perform multiple tasks:

- Increase sample viscosity to improve flow properties
- Enhance the ability of the sample to solubilize the detector reagent.
- Prevent nonspecific binding of the conjugate and analyte to downstream materials.
- Chemical modification of the sample to ensure immunocomplex formation at the test line

Woven meshes and cellulose filters are the two commonly used materials as sample pads. Woven meshes or also called screens have a very low bed volumes, which is why they retain small sample volume, normally around 1 – 2µl/cm^2 and they also have good sample distribution properties [34]. Because of this they are used for applications where limited sample volume is available. Besides this meshes are relatively expensive compared to other porous material and the low bed volume is also a disadvantage when the sample pad should be pretreated with different reagents.

Cellulose filters on the other hand are inexpensive and have large bed volumes, which is why they are used when large amount of blocking agents, detector reagents, release agents, pH and ionic strength modifiers or viscosity enhancers have to be loaded to the sample pad. The disadvantage of cellulose filters is the bad contact behavior with different materials because of this a sufficient and consistent contact might have to be ensured by compression with a housing.

1.5.3 Conjugate Pad

The main task of the conjugate pad is to store the dried detection reagents until a liquid test sample is applied to the sample pad and then ensure uniform transfer of the detection reagent and test sample onto the membrane.

According to the membrane manufacturer Millipore [34] the ideal conjugate pad material has to comprise the following attributes.

a) Low non-specific binding

   If the detector reagent or analyte binds to the conjugate pad, it is lost for the test and thereby reduce the signal intensity and sensitivity

b) Consistent flow characteristics

   Consistent flow properties are very important, otherwise it could happen that the detector reagent may be channeled onto the membrane and the membrane contaminates with streaks resulting into an uneven signal development at the test and control lines

c) Consistent bed volume.

   Normally the conjugate reagents are loaded by dipping the conjugate pad into the liquid. The amount of detection reagent in each test strip then depends on the bed volume of the material. The bed volume has to be consistent, to prevent variable signal intensities.

d) Low extractables.

   To prevent clogging at the connection between conjugate pad and membrane chemical extractables should be avoided and the material should be free of particles that

e) Consistent compressibility.

   This is important for consistent reagent transfer onto the membrane and for incorporation into test strip manufacture

Conjugate pads are commonly made of non-woven material such as cellulose, glass, or surface-treated (hydrophilic) plastic (polyester, polypropylene, or polyethylene) which are compressed into thin sheets. Those materials for conjugate pads are inexpensive compared to membranes. The different materials and there key properties are summarized in Table 1.3.

Table 1.3: Properties of conjugate pad materials adapted from [34]

Non-woven Material	Description	Advantages
Glass fibers	100 – 500 µm thick, can contain binders to hold fibers together	Good hold-up volumes, low nonspecific binding
Cellulose filters	300 – 1000 µm thick, compact fibers of consistent density	Very low nonspecific binding, normally very uniform
Surfacemodified polyester	100 – 300 µm thick, hydrophilic polyester filters	Low nonspecific binding, excellent tensile strength and web handling

1.5.4 Absorbent Pad

The absorbent or also called wick or waste pad is used to keep a uniformly capillary flow through the membrane in the right direction and at a proper flow rate. Without or with a too small absorption pad the sample will flow back in the membrane and could raise the background or possibly cause false positives [34]. Absorption pads are commonly fabricated from non-woven, cellulose fiber sheets in variety of thicknesses and densities to suit the needs of the assay

1.5.5 Housing

A housing is not required for accurate assay functionality but there a different reasons why many manufactures choose to place the lateral flow tests into a housing. The most obvious reason is, to ensure proper operation by forcing the user to apply the sample in the sample pad. For over-the-counter products it also protects the membrane from contamination through splashes. The Housing is also used for labeling to provide important information to the user (e.g. position of test and control line). Internal pins and bars in the housing are used to keep the strip test in the right place and compresses the materials together to ensure repeatable fluid flow conditions [34].

1.6 Objective and Outline of the Thesis

The overall goal of this project is to develop a highly sensitive ELISA based lateral flow test device by using fluidic valves to trigger multiple fluids automatically in a

sequential manner. As first step of the project, the knowledge for point-of-care diagnostics and paper based analytical devices is established, following by the development of a multifluid lateral flow test and the integration of an ELISA procedure. So, this thesis is comprised of six chapters in the following orders:

Chapter 1, background introduction covers the information of point-of-care diagnostics and diagnostic devices, possibility of paper as substrate for sensors and functionality of immunoassays.

Chapter 2, literature review, provides a review on the current approaches for paper based analytical devices and presents immunoassay techniques and validation methods.

Chapter 3, methodology, describes the principle and procedure of the sensor fabrication and immunoassay development. Sensor fabrication using wax printer and laser cutter and development of sandwich enzyme linked immunosorbent assay for lateral flow are described in detail.

Chapter 4, findings and discussion, presents and discusses the results of this study. Including different fabrication methods and variation of reagents.

Chapter 5, findings and future work, summarizes all the chapters of the thesis and addresses recommendations for future research.

CHAPTER 2 – LITERATURE REVIEW

This chapter reviews the current status of analytical methods based on Immunoassays including different labeling-detection techniques, designs for immunoassays and validation methods. Also paper as substrate for sensors is discussed and the newest approaches for paper based analytical devices including fabrication techniques and fluid flow manipulation and calculation are being presented.

2.1 Analytical Methods Based on Immunoassays

Immunoassays are an important technique for developing highly sensitive sensors. The targets cover hormones, proteins, metabolites, drugs, tumor products, antigens and antibodies to infectious agents [8]. Polyclonal or monoclonal [42] antibodies are used to detect the target. Current immunoassays have the ability to detect down to 10^{-13} mol/l of analyte [8]. Immunoassays have been developed since 1950 and the development still continues [20]. The most recent and commonly used immunoassay technologies and validation methods will be presented in this chapter.

2.1.1 Labeling-Detection Systems

In order to detect or visualize the antibody-antigen complex, which is typically bound to a surface, one of the antibodies needs to be labeled by a marker that can generate a signal. This is mostly the last antibody which is called the detection-antibody. Those detection markers can be of different structure and composition they

can be bound covalently or adsorptive and can generate direct (e.g., optical, absorption) or indirect signals (e.g., enzymatic reaction of colored products).

According to Seydack et. al. [44] the ideal detection marker has to meet the following requirements:

- Simple and sensitive detection
- No compromise of sensitivity and specificity of the antibody
- No disruption of the conjugation process as the assay progresses
- No effect to the long-term stability of the conjugate
- Binding to *F*ab part of the antibody is not dominant
- Simple removal of unbound markers is possible
- Not toxic

Several labeling-detection systems have been establish over the past decades. The major labeling systems used in the field are shown below:

Table 2.1: Common labeling-detection systems, adapted from [8]

Labeling-detection system	**Examples**
Radioactive nuclides	^{125}I, ^{32}P, ^{35}S, ^{3}H
Fluorescent labels	Fluorescein, Rhodamines, Phycobiliproteins, Rare-earth chelates, Ethidium, Quantum dots
Luminescent labels	Luminol derivatives, Acridinium esters, Dioxetane derivatives, Bacterial or firefly luciferace
Colored labels	Latex beads (blue color), nanometer sized gold particles (red color)
Enzymes	Alkaline phosphatase (ALP), Horseradish peroxidase (HRP), beta-Galactosidase

Since 1970 the Enzyme Linked Immunosorbent Assay (ELISA), is the most common diagnostic method. It involves reaction between an enzyme label and a substrate. The cascading character of the enzymatic reaction leads to a very good signal-to-noise (S/N) values. They are superior by several orders of magnitude to any non-cascading method values and consequently very low limits of detection are possible [44].

For lateral flow test devices particle based detection labels (e.g. 20–40 nm gold particles) are common. This is because only one fluid, the sample fluid, may flow through the device. The sample fluid contains the analyte or antigen which binds to an antibody labeled with gold or colored latex particles that have been previously dried onto the conjugation pad and the complex of the antigen and detection antibody flows to a nitrocellulose membrane where capture antibodies have been immobilized during the device manufacturing process in a narrow stripe perpendicular to the flow. The antigen-detection antibody complexes then conjugate with the immobilized capture antibodies. The end result is to concentrate a large number of the gold nanoparticles or color beads in the stripe, thus making the stripe visible to the naked eye. Recent studies [2] also report the use of fluorescent labels in lateral flow test devices instead of the colored particle labels that lead to a better Limit of Detection (LOD) but require the use of a reader box.

2.1.2 Immunoassay Designs

All Immunoassay protocols can be grouped into direct or indirect (Figure 2.1) and into competitive and not competitive assays (Figure 2.2). The majority of immunoassays are performed with three different general approaches: competitive assay with either immobilized antibody or immobilized antigen approach or noncompetitive two-site (sandwich) assay [50].

Figure 2.1: Indirect (A) and direct (B) immunoassay adapted from [50]

In a direct assay (Figure 2.1, B) the analyte is immobilized to a solid surface and the specific antibody is labeled to a marker. After incubation the antibody binds to the analyte. In an indirect assay (Figure 2.1, A) a primary antibody (capture antibody) is immobilized to a solid surface and a secondary antibody (detection antibody) is labeled with a marker. During the assay detection and capture antibodies bind to the analyte, since both antibodies are specific for the analyte but normally to different epitopes. This assay architecture is called sandwich assay because the analyte is “sandwiched”

between two antibodies. This design is reported to provide a better sensitivity and is the preferred method in the field [20].

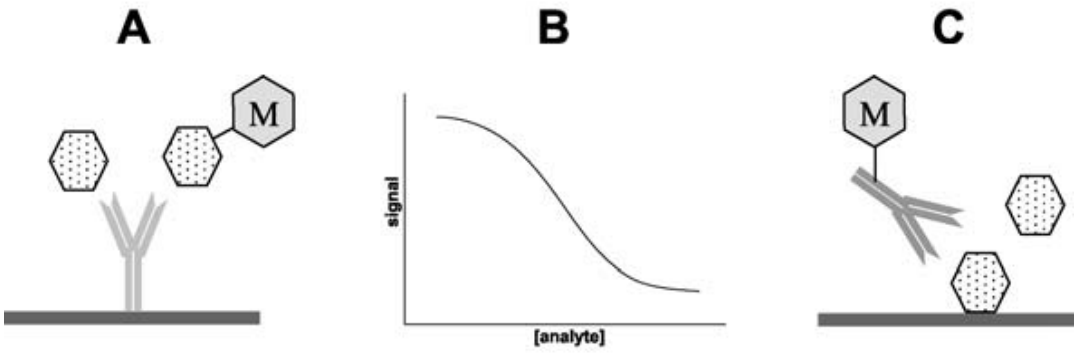

Figure 2.2: Competitive immunoassay is based on the competition of two reagents. A) Immobilized antibody approach, B) Decreasing Signal intensity with increasing analyte concentration for competitive assays, C) Immobilized antigen approach adapted from [50]

In a competitive assay the analyte competes with another antigen for the binding to the antibody. This principle leads to a decreasing intensity with increasing analyte concentration (Figure 2.2, B). The maximum signal is reached when the sample contains no analyte. For competitive assays either the antibody can be immobilized onto the surface (Figure 2.2, A) and the analyte competes with a labeled antigen that has to be added to each sample in the same concentration. When low-molecular weight analytes need to be detected the antigen can be immobilized on the surface (Figure 2.2, C) and the analyte competes with the antigen for the marker labeled antibody.

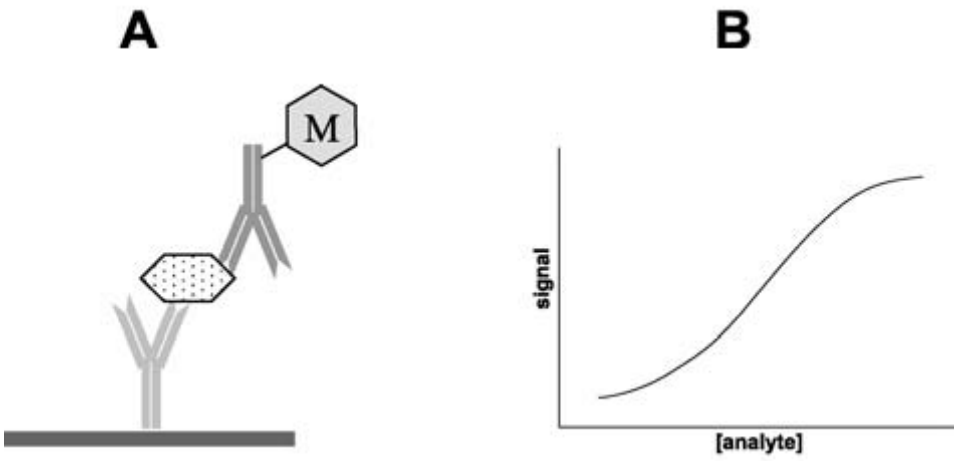

Figure 2.3: Non-competitive assay A) Sandwich assay with analyte sandwiched between capture and detection antibody B) Increasing signal with increasing analyte concentration for non-competitive assays adapted from [50]

In non-competitive assays the signal increases with increasing analyte concentration (Figure 2.3, B). The most common non-competitive assay is the sandwich assay (Figure 2.3, B), when more antigens are in the sample more labeled antibodies can form a sandwich complex with the capture antibodies.

For most immunoassays the sandwich design is preferred. But when the analyte has a too low molecular weight and can't react with to two antibodies at the same time one of the other presented methods has to be used [8].

2.1.3 Surface Binding Techniques

Immunoassays require one type of antibody or antigen to be immobilized on a solid surface while the other reagents remain in the reaction buffer or sample matrix [44]. Most used materials for the solid phase are nitrocellulose or nylon membranes

which are used for test strips and pre- or untreated polymer (as example polystyrene) which is used for microtiter plates [44]. To keep the functionality of the protein consistent, the binding to the solid has to be as adsorptive as possible. Therefore different surface modifications for the support material are used to allow molecules with different degrees of hydrophobicity to be absorbed. As example hydrophilic surface coatings (= O, – OH, – NH2 or = N) are commonly used for microtiter plates.

Direct immobilization of highly specific monoclonal antibodies to the surface can cause denaturing of the proteins. To avoid this circumstance indirect binding procedures have been developed as alternatives to the direct binding (Figure 2.4).

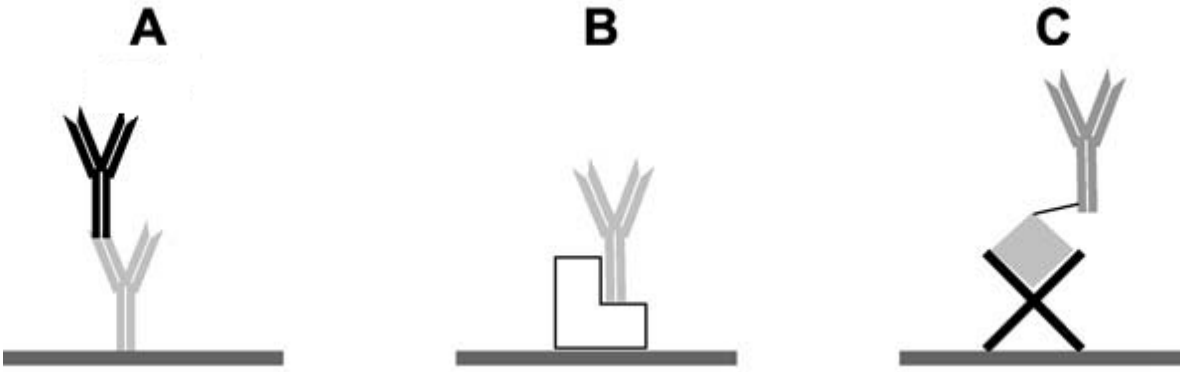

Figure 2.4: Different alternatives to immobilize antibodies on a solid surface A) Anti-antibody bounding B) Antibody binding proteins C) Streptavidin-modified surface and biotinylated antibody bounding [50]

For the anti-antibody approach less specific polyclonal antibodies, which bind to the F_c part of the desired monoclonal antibody are coated to the surface and the antibodies are bounded together. This approach can't be used in sandwich assays since the polyclonal antibody will react with every monoclonal antibody from the same

animal. In a different method antibody binding proteins (e.g. protein A, G, or L) can be immobilized on the surface to hold the desired antibody since these proteins bound to the F_c part (Protein A and G) or the K-type light chain (Protein L) of the antibodies. Sandwich assays are not possible with these techniques.

An indirect method to immobilize antibodies for sandwich assays can be applied by using the biotin-(strept)avidin system. Here the antibody is conjugated to biotin and the surface is coated with avidin or streptavidin. The antibody is then held by the biotin-(strept)avidin reaction. The advantage of this method is the simple and well understood process of labeling the antibodies with biotin which barely influences the recognition properties [14].

2.1.4 Assay Validation

Validating of immunoassay is an important tool during the development of immunoassay applications and it is also a requirement of the European Directive 98/79 EC on in vitro diagnostic tests approved by the European Parliament and Council to bring applications to the market [44]. The following definitions, in accordance to the ICH Guideline “Validation of Analytical Procedures: Text and Methodology Q2(R1)" will provide a background of the validation procedures:

Specificity or selectivity

Specificity is defined as the ability to clearly assess the analyte in the presence of components which could be expected to be present (e.g. impurities, degradants) [47].

Other literature [48] further differentiates between specificity and selectivity: Specificity is an evaluation of the response to a single analyte in contrast to selectivity which is the evaluation of a response to a group of analytes that may not be differentiated from each other.

It should be demonstrated, that the assay results are not affected by typical impurities therefore the pure analyte has to be contaminated with a specified amount of impurities and the test result of the purified and the contaminated analyte have to be compared.

Accuracy or Trueness

The accuracy or trueness of an immunoassay specifies the closeness of agreement between the value which is accepted either as a conventional true value or an accepted reference value and the value found. The accuracy should be determined by using at least nine trials over a minimum of three concentrations in the specified range. The accuracy is described as percent recovery by the assay of known added amount of analyte in the sample [44]. Otherwise the accuracy can be described with the difference between the mean and the accepted true value together with the confidence intervals [47]. If the accuracy is a controversial issue international reference material can be used to prove the accuracy of an assay [44].

Precision

Precision is defined as the closeness of agreement (degree of scatter) between a series of measurements obtained from multiple sampling of the same homogenous sample under the prescribed conditions. The precision should be described as standard deviation, variance or coefficient of variation obtained from a series of measurements [47]. The precision has to be calculated for three different levels:

f) Repeatability

   Repeatability is the precision determined under the same operating conditions over a short period of time. (e.g same operator, same day, same laboratory)

g) Intermediate precision

   Intermediate precision is determined within-laboratory variations. (e.g. different operators, different batch, different days, same laboratory)

h) Reproducibility

   Reproducibility is the precision determined between different laboratories. It can only be assessed by inter-laboratory trials or round robin tests.

The precision should be determined using a minimum of nine trials over the specified range for the procedure or using minimum of six determinations at the maximum test concentration. For all precision levels the conditions of the trials have to be included to the precision data as specific as possible.

Limit of Detection

The detection limit is the lowest concentration of an analyte in a sample that can be detected by the assay. The three most common approaches to determine the Limit of detection are listed below. Other Approaches than those listed may be acceptable too [47].

i) Visual Evaluation

Visual evaluation can be used for non-instrumental methods like lateral flow tests. The detection limit is thereby determined by the analysis of samples with known analyte concentrations and by evaluation of the minimum level at which the analyte can be reliably detected

j) Blank Determination

This method is simple and quick it can be used when the blanks have a non-zero standard deviation. The LOD is expressed as the analyte concentration corresponding to the sample blank value including three times the standard deviation [45].

$$LOD = X_b + 3\sigma_b \quad (2.1)$$

Where X_b is the mean concentration of the blank and σ_b the standard deviation of the blank.

k) Signal-to-Noise Approach

The Signal-to-Noise Ratio is determined by comparing the measured signal of samples with a negative control. The detection limit is reached, when, the Signal-to-Noise Ratio falls below a specified limit. A ratio between 3:1 or 2:1 is usually considered acceptable for determining the detection limit [47]

l) Standard Deviation of Response and Slope

A more accurate and refined method than the methods described above uses the Slope S of the calibration curve and the standard deviation σ of the response. The detection limit is then expressed with following equation:

$$LOD = \frac{3.3\ \sigma}{S} \tag{2.2}$$

Limit of Quantification

A quantitative or semi-quantitative assay relies on the opportunity to detect the exact or a range of the analyte amount in a sample in contrast to a qualitative assay which is only capable of detecting whether there is analyte in the sample or not. In order to develop a quantitative assay the Limit of Quantification is an important number for comparison of assays. The Limit of detection is defined as the lowest amount of analyte in a sample that can be quantitatively determined with suitable precision and accuracy [47]. The procedures to detect the LOQ are the same as for the LOD. A visual evaluation is applicable for non-instrument tests such as lateral flow test. A Signal-to-noise ratio of 10:1 is acceptable for the LOQ and for the method which is

using the standard deviation of the calibration curve and the Slope of the response following equation can be used [44]:

$$LOQ = \frac{10\,\sigma}{S} \tag{2.3}$$

Also the blank determination applies for the limit of quantification [45]. The LOQ is expressed as the analyte concentration corresponding to the sample blank value including ten times the standard deviation:

$$LOD = \frac{3.3\,\sigma}{S} \tag{2.4}$$

Linearity

The linearity of an analytical immunoassay is the ability to obtain linear test result in a given range which are directly proportional to the analyte concentration in the sample. The linearity can be evaluated by plotting the signal intensity response of different analyte concentrations. The regression line, correlation coefficients, slope of the regression line, and residual sum of squares can be used to compare assay configurations. For immunoassays which do not show linear behavior the response should be described with suitable nonlinear functions [47]

Range

The range describes the analyte concentration interval in which the immunoassay has been proven to have a suitable level of precision, accuracy and linearity [47].

Robustness

Robustness is defined as the resistance of an immunoassay against the influenced by variations of the assay parameters (e.g. temperature, pH, humidity). It is an indicator for the reliability during regular usage [47].

2.2 Limitations of Lateral Flow Immunoassay

Lateral flow immunoassay are the oldest technique for paper based analytical devices and can be traced back to the 1950s [57]. They were designed as easy to operate rapid diagnostic devices for the point of care market. Paper based analytical devices, can be classified as standard LFIA when they are composed according to section 1.5 and operated without prior sample preparation and without additional steps other than the sample application. Because of their simplicity LFIA have some major disadvantages compared to recent developments advanced paper based analytical devices (vide intra) such as miniaturization of sample volume requirements below microliter level, sensitivity or multiplexing [57]. To compare LFIAs with recent developed paper based analytical devices various performance parameters for LFIAs on the market or recent published in the literature were summarized in Table 2.2. The table list also some more advanced LFIA which are still based on the standard LFIA principle with a conjugate release zone and a reaction membrane but also with some more sophisticated principles to enhance the test results.

Table 2.2: Comparison of techniques and detection limits for state of the art LFIAs

	Analyte	Sample type	Label	Detection limit		Trademark\ Particularities	RR
				Mass	Molar		
Standard	Aflatoxin M1	Milk	Gold nanoparticles	0.3ng/ml	n/a	Extract-free	[63]
	Schistosoma circulating antigen	Urine	Colloidal carbon	0.2ng/ml	n/a	Alternative Label	[40]
	Hbs-Ag	Clinical samples	Gold nanoparticles	15ng/ml	n/a	Nanotrap Hemo™	[23]
Advanced	Cardiac Troponin I & Myoglobin	Standard Samples	Gold nanoparticles	1pg/ml 1ng/ml	n/a	Two conjugate pads & single-stranded DNA amplification	[65]
	PSA	Standards in female serum	Gold nanoparticles	1ng/ml	2.4fm	Mono-poly sandwich, wash step	[9]
	Hbs-Ag	Clinical samples	Alkaline Phosphatase	1ng/ml	n/a	ESPLINE™\ Button for substrate release	[23]
	Cholera toxin	Water	Ganglioside incorporated liposomes	0.1pg/ml	80zm	Premix necessary	[1]
	HBsAg	Clinical samples	Europium chelate loaded silica nanoparticles	30pg/ml	n/a	n/a	[58]

2.3 Sensing Approaches on Paper-based Devices

Nowadays, numerous examples of paper-based sensors are found in the literature. Compared to common lateral flow tests they are being developed to extend the range of application for point of care devices. According to Nery et. al. [37] paper based analytical devices can be classified into two different types of detection systems:

optical and electrochemical. The basic methods of optical detection are colorimetric, fluorescence, chemiluminescene, and transmittance based. For electrochemical detection the most commonly used methods are voltammetric, potentiometric, and conductivity based. Besides the type of detection system paper based sensors can be distinguished in the type of detector that is used (e.g. naked eye, scanners) the energetic principle (e.g. electricity, capillarity) and the analytical principle that is used (e.g. biological, chemical, physical). Paper-based analytical devices which are cited in this chapter are summarized in Table 2.3.

Table 2.3: Overview Paper-based Analytical Devices

	Sensor	Method	Detector	Analytical principle	Energetic principle	Analyte	LOD	RR
Optical	Tree-shaped paper strip	Colorimetric	Naked-eye or camera	Chemical	capillarity	BSA	0.08mg/ml	[53]
	Paper based ELISA	Colorimetric	Scanner	Imunoassay & Enzymatic	capillarity	Rabbit IgG	54fm	[5]
	Microfluidic paper-based chemiluminescence biosensor	Chemi-luminescene	Luminescence analyzer	Chemical	capillarity	Glucose & Uric acid	0.14mM & 0.52mM	[62]
	Temperature sensor	Colorimetric	Naked-eye	Chemical	Oxidation	n/a	n/a	[37]
Electrochemical	Paper based oxygen Sensor	Voltammetric	Multimeter	Chemical	Capillarity & electricity	Oxygen	0.0075%.	[43]
	PAD for el.chem. Flow-Injection Analysis	Voltammetric	Amperometer	Chemical	Capillarity, gravity & electricity	Glucose	200pmol	[24]
	Paper-Based Electrohemical ELISA	Potentiometric	Potentiostat	Imunoassay & Enzymatic	Capillarity & electricity	Rabbit IgG	3.9fM	[58]
	Potentiometric enzyme immunoassay	Potentiometric	Potentiostat	Imunoassay & Enzymatic	Capillarity & electricity	IgE	0.1ng/ml	[46]

2.3.1 Optical Detection: Methods and Detector Systems

Optical detection is the most inexpensive and universal method [22] and it is a perfect application for paper based analytical devices since this substrate offers a

bright, high-contrast, and colorless background for the read out of color intensity changes [59] . Several researcher groups [41] also discovered, that paper can give a better sensitivity and quantification than other substrate materials. The complex cellulose structure could also lead to some disadvantages. Researchers discovered, that high background signals (e.g. non-specific binding) or signal non-uniformity (e.g. liquid accumulating on the borders of the detection zone) can be a problem [37]. Chen et. al. [4] discovered that drying of reagent in an incubator at 37 °C can help to reduce background signal. And other research groups mentioned that treatment with poly(vinyl amine), gelatin, poly(acrylic acid), or poly(ethylene glycol) can help to stabilize color development [37].

A big advantage of optical detection methods is the simplicity of the detector systems. The least expensive detector which doesn't require to buy any further equipment is the naked eye. Detection based on the naked eye might be precise enough for the detection of non- or semi-quantitative assays such as Lateral flow immunoassays. For quantitative assays a reading device is essential. Those reading devices could be simple tools like scanners, digital cameras or phone cameras which are available all over the world and which are easily portable. These detectors are inexpensive and simple to use point of care devices. For application where a higher sensitivity, lower limit of detection or limit of quantification is needed, more specialized detector systems are being developed, including spectrophotometers, fluorimeters and gel documentation systems [2].

A notable device using colorimetric detection is a paper based protein detection system developed by Wang et. al. [53]. The group used bromophenol blue for semiquantitative analysis of bovine serum albumin in artificial urine in a tree-shaped (Figure 2.5, C) self-calibrating detection system. The design ensures uniform conditions of each assay.

2.3.2 Electrochemical Detection: Methods and Detector Systems

Compared to optical sensors, electrochemical sensors are not affected by dust, light or insoluble compounds [19]. Also different research groups found that using paper instead of solid materials for electrochemical sensors the influence of convection of liquids caused by random motion, vibration, or heating can be reduced [37]. Electrodes can easily be integrated into PADs. For example Hu et. al. [19] presented nanoporous gold electrode arrays on cellulose membranes which were used to develop a cost-effective and environment-friendly paper-based electrochemical gas sensor for the detection of oxide (Figure 2.5, A). Other researchers [43] also discovered that the large surface area of the paper on top of the electrode is able to increase the signal response of the sensor. An interesting PAD approach using electrochemical detection is a device based on potentiometric immunoassay to detect IgE [46]. The PAD is built from nitrocellulose paper sandwiched between two silicone rubber sheets connected to electrodes on both sides (Figure 2.5, B).

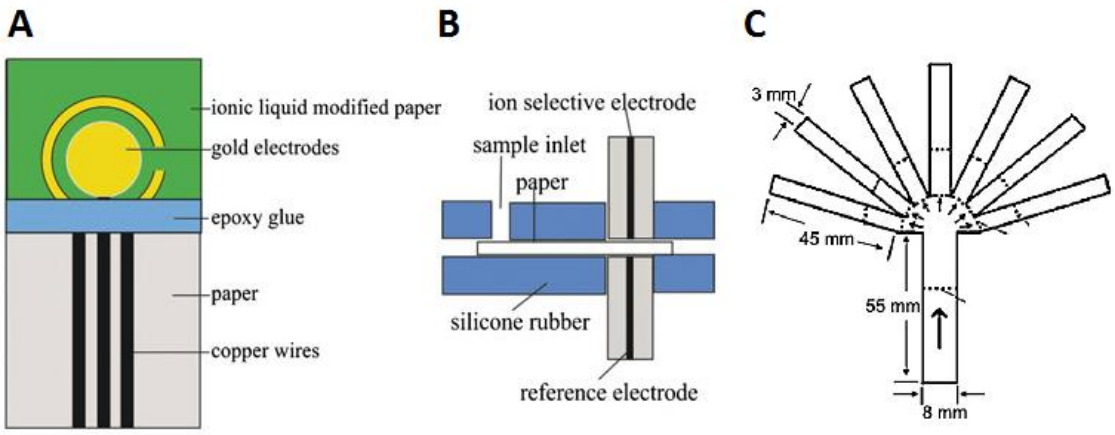

Figure 2.5: Paper based analytical devices: A) Oxygen sensor based on nanoporous gold [37] B) Potentiometric immunoassay [37] C) Tree-shaped self-calibrating detection system [53]

For electrochemical detection normally electrochemical scanning systems such as high-end potentiostats are used to measure very small signal changes. These devices can be used to develop highly sensitive and quantitative assays. In order to develop cheap and easy to use point of care devices without being forced to give up the benefits of electrochemical detection several groups worked on simpler and cheaper detector systems. Prof. George Whitesides group, for example, developed a PAD for Electrochemical Flow-Injection with low cost components for the detector system (amplifier, voltage regulator, voltage inverter & batteries) [24]. Also multimeters are being discussed to be the next generation of electrochemical detectors [37]. Liu et. al. [28] recently developed a paper based analytical device for electrochemical detection of adenosine using a digital multimeter for the readout (Figure 2.7).

2.3.3 Energetic Principles

Most paper based analytical devices are based on 2D or 3D microfluidic circuits using the advantage of capillarity for fluidic manipulations like transportation, sorting, mixing or separation of the needed reagents [26]. Also gravity is sometimes used to enhance the fluid flow [24]. The great benefit of this is, that these devices do not need additional energy sources to cause fluid flow and the analytical test will run on its own after the user has introduced the sample to the system. To accomplish multi-step-analysis and diagnostic procedures some PADs are based on mechanical manipulators like switches [30] or buttons [17] (*vide infra*). Also some paper based analytical devices need electric energy sources (e.g. to drive UV lamps or to enable electrochemical readout). Because of this several researchers are working on paper based batteries. For example Thom et al. [49] developed a disposable paper-based galvanic cell battery for diagnostic applications in resource-limited settings. The battery is composed of multiple galvanic cells and can be incorporated directly into a multilayer paper-based microfluidic device.

2.3.4 Analytical Principles

There are several analytical principles in the field, which are used to generate either an optical or electrochemical detectable signal. One main principle to generate a signal is chemical reactions. For example Yu et al. [62] developed a PAD based on chemiluminescence signal generation which is used for simultaneous quantification of

glucose and uric acid. Their system is based on generation of hydrogen peroxide through the chemical reaction of glucose and uric acid with oxidase enzymes. Hydrogen peroxide is then used to produce light by reacting with a rhodanine derivative (Figure 2.6, B).

Another important type of analytical techniques are biological reactions especially those which are based on immunoassays (see section 2.1). Immunoassays have the advantage of high selectivity, rapid detection, and the possibility to analyze complex matrices without pretreatment [37]. Using immunoassays on a paper substrate rather than on a solid surface also leads to a higher surface-to-volume ratio and shorter incubation times (e.g. 10 minutes for paper based ELISA [5] vs. hours on solid surfaces) and possibly better limit of detection. The Whitesides group [5] for example developed a paper based method to replace conventional 96-microzone microtiter plates with paper based ones. Their method requires smaller reagent volumes (e.g 3 µl of sample vs. 70 µl on microtiter plates) and less time (51 min vs. 213 min). Their limit of detection for Rabbit IgG was about 54 fm.

Other biological methods are using different strains of bacteria which are able to produce specific enzymes, which, for example have been used in a paper based colorimetric assays [18]. A different analytical principle is based on the piezoelectric effect discovered in oriented cellulose fibers. It was used to develop paper based strain and vibration sensors [37]. Also temperature dependent reactions are used to develop PADs. For example Nery et al. [37] described a method using thermochromic ink to

develop temperature sensors. The sensors consist of a series of pixels of various actuation temperatures. When the actuation temperature of the pixel is reached it turns colorless (Figure 2.6, C).

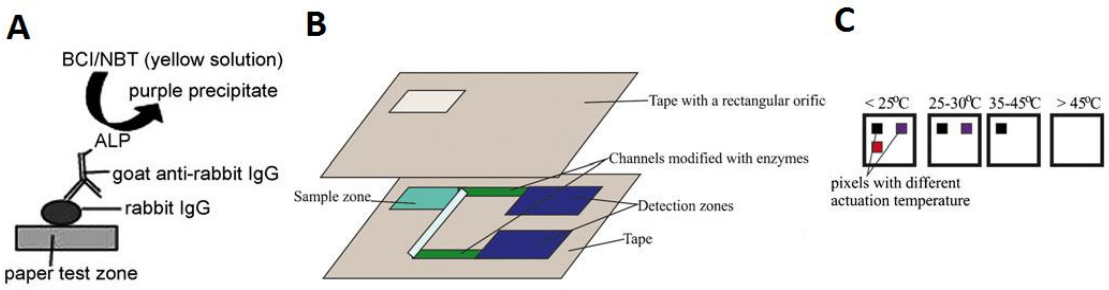

Figure 2.6: Paper based analytical devices. A) Paper based ELISA [5] B) Chemi-luminescence assay [37] C) Temperature sensor [37]

However many platforms are using combinations of those different principles. One example is a paper based electrochemical ELISA that was developed again by the Whitesides group. This analytical device uses the immunoassay technique combined with an enzymatic catalyzed electrochemical reaction. It was used to detect rabbit IgG with a detection limit of 3.9fm [58].

2.4 Fabrication Methods for PADs

Fabcrication of paper based analytical devices is fairly simple and inexpensive. The First PAD was introduced by the Whitesides Group of Harvard University [35] which used a photolithographic technique to fabricate their chips. The main goal of all fabrication processes is to create hydrophobic barriers on sheet of hydrophillic cellulose in order to generate millimeter-sized capillary channels [3]. Techniques

reported in the literature include cutting, printing, drawing, dip-coating, plotting, photolithography and laser treatment (Table 2.4). To protect the devices from contamination various enclosure methods like wrapping in adhesive tape, lamination and toner or polymer coating are used [37].

Table 2.4: Comparison of common fabrication techniques for resolution, cost and high throughput (HT) adapted from [37]

Technique	Resolution	Cost	HT
Cutting			
Manual Cutting	−−	++	−
CNC Cutting plotter	−	+	++
Laser cutter	++	−−	+
Mechanical drill	−	−	+
Printing			
Wax printing	++	+	+
Screen printing	+	++	+
Flexographic printing	++	−	+
Ink-jet printing	++	+	+
Laser printing	++	+	+
Transfer printing	+	+	+
Others			
Drawing	−−	++	−
Dip-coating	+	++	−
Plotting	−	+	+
Photolithography	++	−	+

2.4.1 Three-dimensional PADs

Compared to 2D paper based devices (e.g. dipsticks and lateral flow systems) that are based on lateral movement of fluids across paper strips, 3D paper based microfluidic systems are capable to distribute fluids both vertically and laterally. Using a 3D design it is possible to develop PADs with complex microfluidic paths and the

capabilities of those low-cost analytical systems can be expanded significantly. Two different approaches have been developed to build 3D PADs.

Layered paper and tape

Martinez et. al. [33] described a method stacking alternating layers of water-impermeable double sided tape and paper to create three-dimensional PADs. First they patterned the paper layers with hydrophobic wax in order to define the fluid channel and cut holes into the tape do define the area where the fluid has to flow vertically. Then they stacked the layers together, the holes in the tape were filled with a paste made from cellulose powder and water in order to ensure a good connection between the layers. The advantage of this approach is the simplicity with which these devices are assembled which makes the prototyping of new designs rapid.

Origami approach

Origami PADs (oPADs) first described by Liu et al. [27] are fabricated on a single sheet of paper (e.g. filter- or chromatography paper) and then assembled into a 3D fluidic architecture by folding and sealing. Prior to the assembly the paper is patterned with hydrophobic wax and heat treated in order to create the desired channels. Compared to 3D devices fabricated from stacked layers of paper and tape this approach is much simpler in particular for automated mass production. For sealing of those devices the group reported a method using a glossy plastic envelope sealed with an impulse thermal edge laminator [28]. That approach avoids adhesives which can lead

to contamination or nonspecific adsorption of reagents or targets [52]. They also reported that it is possible to integrate electrodes by screen printing in those devices (Figure 2.7).

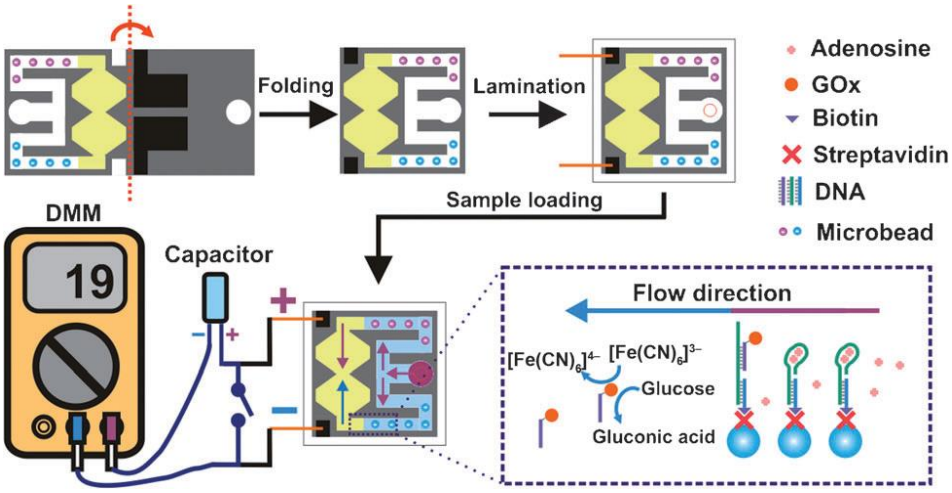

Figure 2.7: Origami paper based analytical device for electrochemical detection of adenosine [28]

2.5 Control of Fluid Flow in Paper-based Devices

In microfluidic PADs, movement of the various fluids is based on capillary flow, this is why mechanisms and equations developed for conventional microfluidic devices cannot be applied. To accomplish multi-step-analysis and complex diagnostic procedures (e.g. ELISA) the fluid flow in PADs has to be controlled and manipulated (e.g. valves). For designing and modeling, the fluid flow in PADs has to be described with suitable equations.

2.5.1 Single-use Buttons

Martinez et. al. [32] developed a single-use 'on' push-buttons for use in programmable 3D microfluidic paper based devices. A small gap between two layers of paper, which is created by a hole in the tape, is used to separate two channels (Figure 2.8, C). The gap is closed by pressing the two layers of paper together using mechanical force. The gap will stay closed due to in-elastic deformation of the paper.

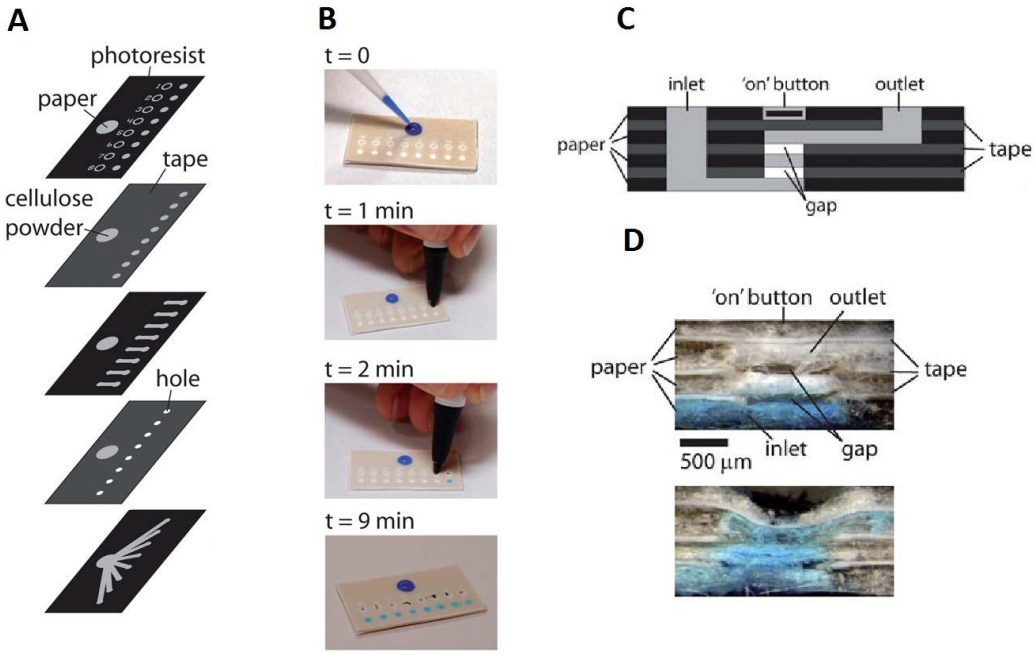

Figure 2.8: Programmable microfluidic paper based devices using push buttons adapted from [32]. A) Schematic of the layers in a fluidic de-multiplexer B) Use of the fluidic de-multiplexer C) Schematic of the cross-section of an button D) Photographs of the cross-sections before and after use

To demonstrate the functionality of the buttons and the capabilities of programmable PADs, the group developed a fluidic de-multiplexer. The device was able to directed fluid from a single inlet into any combination of outlets (Figure 2.8, A, B). This device is particularly useful in situations where only a limited quantity of sample

is available, where analytical standards require multiple duplications of an assay, or where reagents and samples must be combined in a timed sequence.

2.5.2 Fluidic Timers

Noh et. al. [38] develop a fluidic timer which does not require starting, stopping, reset buttons, batteries, or maintenance. The fluidic timers can be integrated in any 3D or 2D PADs. They are made using paraffin wax and the timing function is made possible by the specific time required for a fluid to wick through a region coated with this wax. The time period can be anywhere between 1 min and 2 h and is defined by the amount of paraffin wax coated in the region. The group integrated their invention into a 3D PAD (Figure 2.6, B) for the detection of glucose. They used the timer in combination with a colorimetric signaling component (1µl of a dye solution) to pinpoint the time when the test has to be read out.

2.5.3 Mechanical Switch

Zhong et. al. [64] developed a mechanical switch which can be integrated into a PAD to stop the fluid flow through a channel until the switch is pulled mechanically. The switches were produced from rectangular holes in the channels and a paper strip that was patterned with wax leaving out an area with the same width as the fabricated channels. After heating, the paper strip was inserted into the cut-out area of the paper

device. Pulling on the paper strip could then be used as a switch that restricts or allows the fluid to flow through the fluidic channel.

2.5.4 Fluidic Valve

Chen et. al. [3] developed a fluidic valve which acts like a electric diode. The valves consists of two functionalized discs fabricated of paper. One disc is made hydrophobic by soaking the paper in Allyltrichlorosilane (A3CS) and the other is infused with surfactant. If the fluid enters the valve from the hydrophobic side it is stopped. If it enters from the side containing the surfactant, the fluid goes through the valve, because the surfactant transforms the surfaces of the fibers in the hydrophobic disc from hydrophobic to hydrophilic. Once the fluid passes the diode the valve is open for fluid flow in both directions.

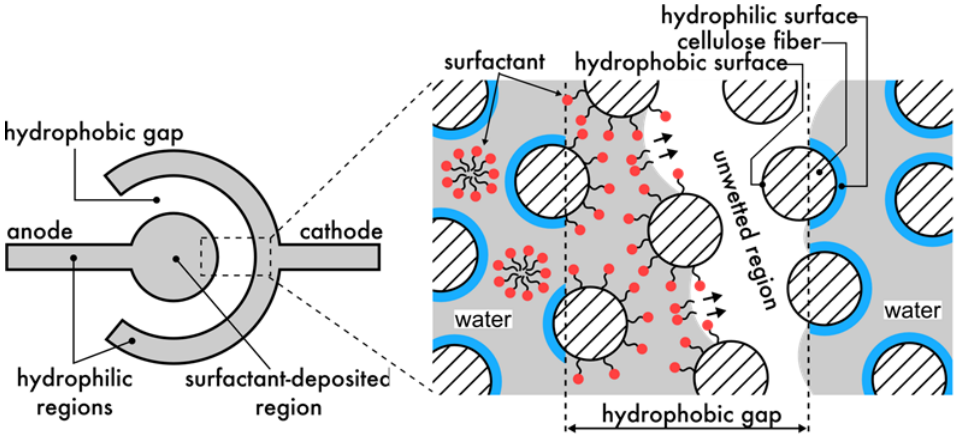

Figure 2.9: Two-dimensional representation of the valve principle [15]

The principle behind this is a simple reaction of two reagents (Figure 2.9). The hydrophobic side of the valve is treated with Allyltrichlorosilane and the surfactant side is treated with Tween 20. Treating filter paper with A3CS coats the cellulose fibers with

thin hydrophobic film and fluid cannot flow in the pores. Tween 20 on the other hand makes the cellulose fibers hydrophilic again thus allowing fluid flow. Using this device, fluidic networks can be developed which can sequentially pass different fluids through a detection area. Chen et. al. [3] for example proposed the circuit shown in Figure 2.10 with two valves and a triggering channel to sequentially pass two different reagents by a detection area. In this fluidic network or circuit the enzyme alkaline phosphatase was used as the model analyte. It was deposited and dried at the detection spot. At one of the input pads a color agent, such as a substrate was deposited, and at the same time a stop buffer was pipetted in the other pad. At first the substrate solution travels through the detection region and reacts with the immobilized enzyme to produce a color. When the substrate solution reaches diode 2 it opens it and allows the stopping buffer to begin flowing. However, this solution cannot at first go through the test spot because diode 1 blocks the flow. Instead, it travels around the fluidic channel with a clock indicator and after some time arrives at the forward end of diode 1 causing it to open. Now the stop buffer can flow through the test spot and end the color producing enzymatic reaction.

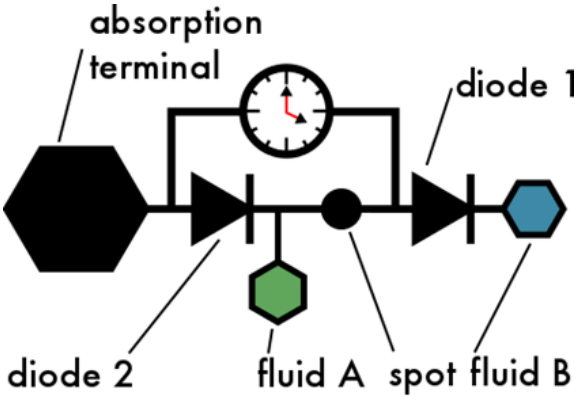

Figure 2.10: Colorimetric assay with triggering system using fluidic valves [3]

2.6 Modelling of Fluid Flow in Cellulose Substrates

Fluid flow in cellulose substrates can be distinguished for either flow in dried (paper wet-out) or wetted (fully-wetted flow) materials. Bose cases have two be addressed with different mathematical approaches.

2.6.1 Paper Wet-out

For the simplest case, the one-dimensional fluid flow in a porous cellulose matrix (e.g. paper strip) during wet-out follows the Washburn equation [55]:

$$L = \sqrt{\frac{\gamma D t}{4\mu}} \tag{2.5}$$

where L = the distance moved by the fluid front, γ = the effective surface tension of the liquid, D = the average pore diameter, t = time, and μ = the viscosity of the liquid. For water the surface tension at room temperature is estimated to be 0.0728 N/m and the viscosity 1.002 x 10^{-3} Ns/m^2. The application of the Washburn equation for the fluid flow in a cellulose membrane follows the assumption of a constant cross-section and a non-limiting source. Zhong et. al. [64] verified the Washburn equation in uncovered paper-based fluidic channels with a constant width of 1.2, 1.6 or 2 mm, fabricated by wax printing on Grade 1 chromatography paper. The results showed that the flow characteristics are independent of the width of the fluidic channels, when a non-limiting source is given. They also showed that it is possible to deduce the average pore

diameter with a good estimation by flow experiments using the rearranged Washburn equation:

$$D = \frac{4L^2\mu}{\gamma t} \tag{2.6}$$

2.6.2 Fully wetted Flow

A flow in a pre-wetted paper channel of constant width can be described by Darcy's law [7]:

$$Q = -\frac{\kappa WH}{\mu L}\Delta P \tag{2.7}$$

where Q = the volumetric flow rate, κ= the permeability of the paper to the fluid, μ = the viscosity of the fluid, WH = the area of the channel perpendicular to flow, and ΔP = the pressure difference along the fluid flow direction over the length L. The flow rate of the fluid, q can be derived by assuming a constant cross-sectional area and by division of WH on both sides of the equation:

$$q = -\frac{\kappa}{\mu L}\Delta P \tag{2.8}$$

According to the principle of conservation of mass, the volumetric flow rate, Q has to be constant along a channel. Therefore the time a fluid front needs to travel a certain distance can be calculated from the ratio of volumetric flow rate and the volume of the geometry and substituting in Darcy's law [12]:

$$t = \frac{V}{Q} = \frac{V\mu L}{\kappa W H \Delta p} = \frac{\mu L^2}{\kappa \Delta P} \quad (2.9)$$

where V = the volume of the fluid at the time t. For most fluid flow calculations the fluid flow can be approximated with following parameters [64]: The viscosity of water at the room temperature 1.002 x 10^{-3} Ns/m^2 ;The pressure variation ΔP which is assumed to be constant in capillary driven flow and estimated to be 4,560 N/m^2 for paper [12]; The permeability of paper can also be assumed to be constant, in the range of 3 x 10^{-13} m^2 [12]. Since all constants are known the fluid flow only depends on the geometry. For more accurate calculations the permeability for a specific paper can be developed through iteration.

2.6.3 Abundant vs. Constricted Flow

Zhong et.el [64] also studied the condition for abundant (Figure 2.11, A) and constricted (Figure 2.11, B) fluid flow. They discovered that an abundant flow (from a channel with a larger width to a channel with a smaller width) does not affect the fluid flow rate. This is because a flow from a larger width channel acts as a non-limiting source for the flow entering into a smaller width channel. In contrast a constricted flow (from a channel with a smaller width to another channel with a larger width) constricts the fluid flow rate at the transition point.

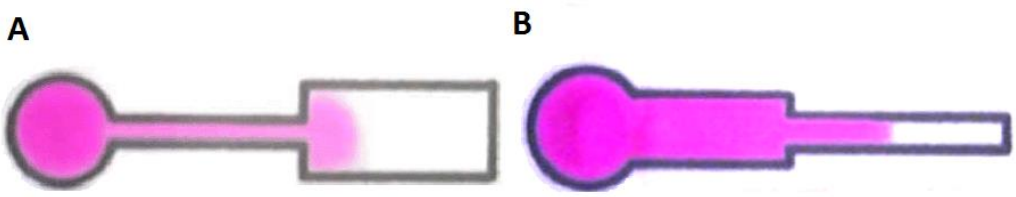

Figure 2.11: Fluid flow in channels with variation of the width adapted from [64] A) Abundant flow B) Constricted Flow

2.6.4 Electrical Circuit Analogy

For the purpose of simplified mathematical calculations of complex fluid flow in 2D or 3D paper networks, the fluid flow can be calculated with the analogy to an electric circuit:

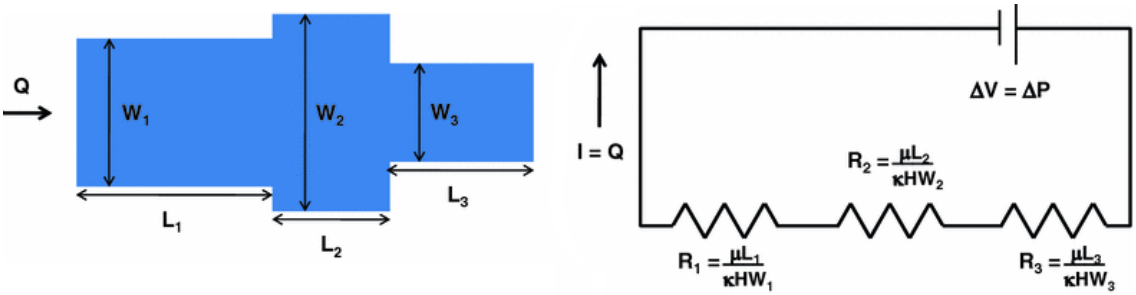

Figure 2.12: Schematic of the fluidic network analogy to electrical resistance. The total volumetric flux through a paper network of N segments in series, during fully wetted flow, follows the same form as Ohm's Law for a circuit with N resistors in series. [12]

The total volumetric flow through a paper network of N segments of varying widths in series, during fully wetted flow, follows the same form as Ohm's law for calculating the electric current through a circuit with N resistors in series [12]. By extension of the simplest case of Darcy's law and by imposing equality of the volumetric fluxes in the segments of different widths the fluid flow in N connected channels can be calculated:

$$Q = -\frac{\Delta P}{\frac{\mu}{\kappa}\sum_{i=1}^{N} {L_i}/{W_i H_i}} = \frac{\Delta P}{R_{eq}} \tag{2.10}$$

where W_iH_i = the area of segment i of the channel perpendicular to flow, L_i = the length of segment i of the channel in the direction of flow, and ΔP = the absolute magnitude of pressure difference in the direction of flow. ΔP is thereby the fluidic counterpart to voltage change, Q the fluidic counterpart to current, and R_{eq} the fluidic equivalent to the resistance. As consequence of Darcy's law, also fluidic channel connected in parallel can be reduced to a single element by adding the fluidic resistances in reciprocals.

CHAPTER 3 - METHODOLOGY

This chapter is used to present the methods and experiments used to develop and optimize a fluidic circuit and an immunoassay based on the ELISA procedure for lateral flow. Fabrication methods for the device, different circuit designs, assay development, and housing development are addressed.

3.1 Chip Fabrication Method

Fabrication of all chips for this study was done using the layered paper and tape method described in section 2.4 [33]. Briefly, all 3D fluidic circuits were built to contain at least three layers consisting of two layers of filter paper with wax printed fluidic channels held together by one layer of double-sided tape. Holes in the double-sided tape filled with hydrophilic material were used to connect the flow layers (Figure 3.1).

Additional layers of one-sided tape were used to cover the channels to prevent contamination, contact, or evaporation. All chips were fabricated in batches of 4 - 6 chips. The channels were printed on filter paper using a solid ink printer (Xerox® ColorQube® 8570) with solid wax ink (Xerox® Genuine Solid Ink Black). All Flow channels were cured for 60 seconds at 120^{o}C using a Vacuum Oven (Isotemp® Model 280A, Fisher Scientific). Cut outs were made using a CO_2 laser cutter (Epilog® Mini 24) and cutting and printing masks were designed using vector graphic programs such as *Inkscape* and *Corel Draw*®. To protect the adhesive sides of the tape during handling and cutting processes tape was covered with wax paper (Parchment Paper, Reynolds®).

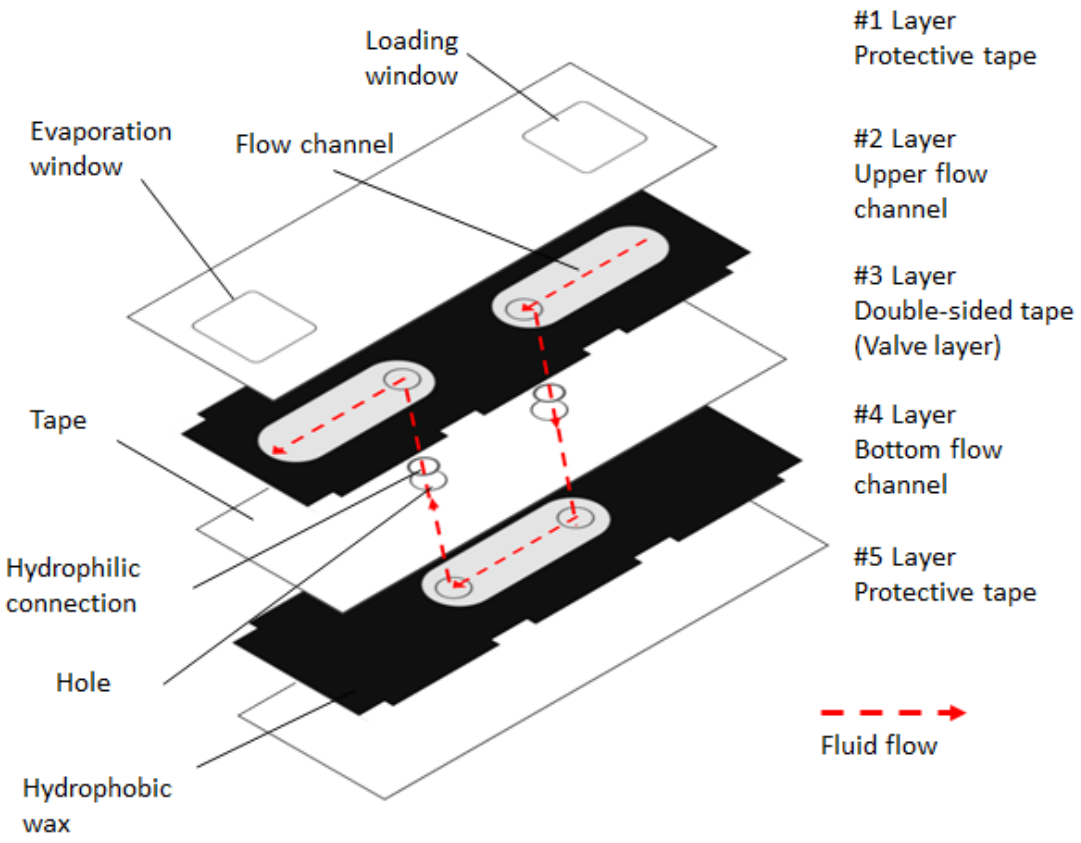

Figure 3.1: General principle of chip fabrication

3.2 Valve Fabrication Methods

To fabricate 3D fluidic valves two parts are needed: a hydrophobic anode and a surfactant treated hydrophilic cathode (see section 2.5.4). Cellulose material was treated with Allyltrichlorosilane (A3CS) to create a hydrophobic cathode and then treated with Polysorbate 20 commonly known as Tween 20 (T20), a surfactant.

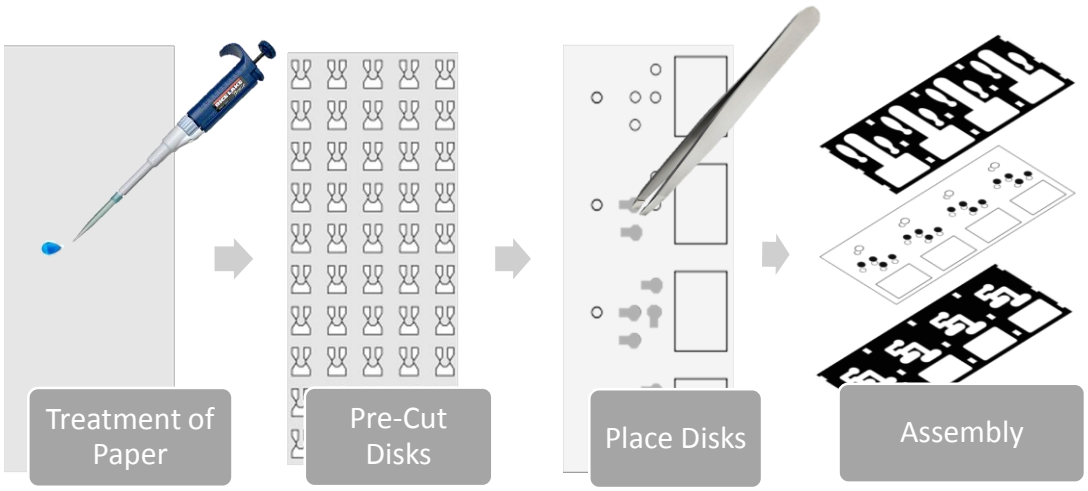

Figure 3.2: Flowchart for the valves fabrication initaly developed at the labarotory of professor Faghri

The first chips were fabricated following the initial method developed and optimized at the laboratory of Professor Faghri (Figure 3.2) [3]. The procedure to fabricate these chips is summarized as follows:

- Dilution of 5 ml 16.6 µl/ml Allyltrichlorosilane in Perfluro-compound FC-72[1]
- Dilution of 5 ml 0.04 g/ml Tween 20 in Ethanol
- Treatment of 8x10 in filterpaper sheets with A3CS solution using a transfer pipette
- Dried on hotplate at 60°C (3 hours)

[1] Perfluorohexane (C_6F_{14}) fluorocarbon, with the structure of a helical carbon backbone. Biologically inert and chemically stable. Used to dissolve reagents to a high concentration [16].

- Treatment of 8x10 in filterpaper sheets with entire amount of T20 solution using a transfer pipette (dried at room temperature)
- Cutting of 3 mm (hydrophobic) and 2.2 mm (surfactant) disks including a gap and handling area
- Cutting of 2.2 mm holes in double sided tape (middle layer of chip)
- Manual assembly of valves using tweezers to place disks

For assembly (see Figure 3.2) on protective sides of the double sided tape was removed and the surfactant disks were placed into the holes of the tape using tweezers and the gap and handling area to position and attach the disks. Then the respective flow layer was attached to the tape and the other protective side of the tape was removed. Next the bigger hydrophobic disks were placed on top of the holes to completely cover them. For the last step the missing flow layer was attached to the tape.

To improve the fabrication process three advanced methods based on the one described have been developed during this study.

3.2.1 Disk Punching

This method uses the same treatment for the disks as described before. However, the method of manually handling the disks was replaced with a semi-automatic tool to place all disks at once. The tool (Figure 3.4) consists of three parts: alignment, disk holding, and punching.

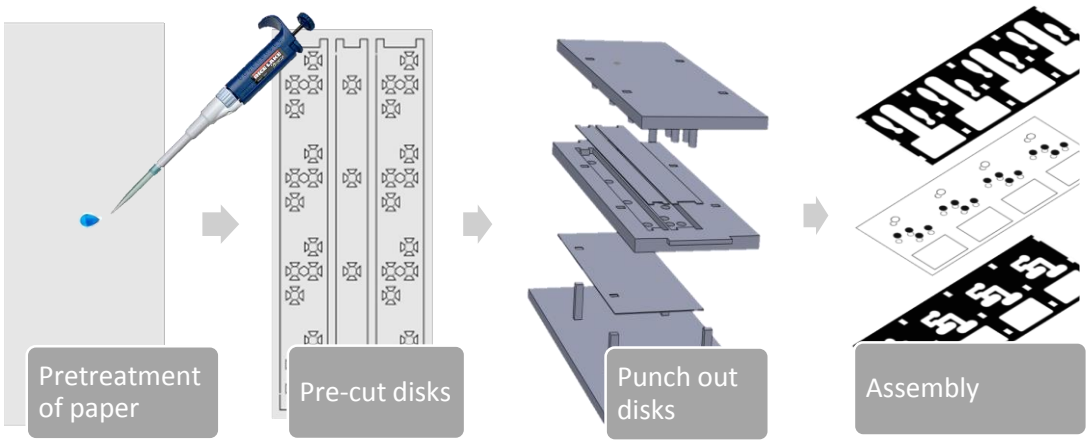

Figure 3.3: Flowchart for valve fabrication using a tool to punch-out the disks

The CAD model of the tool was designed with SolidWorks (Dassault Systèmes®) and the fabrication was done using rapid prototyping with fused deposition modeling of ABS (Stratasys - Dimension Elite). The procedure to fabricate disks with the tool is shown in Figure 3.3 and the necessary steps are as follows:

- Pretreatment of filterpaper with Allyltrichlorosilane and Tween 20
- Cutting of round shaped disks keeping attachment points to hold multiple disks in strips
- Fixation of disk holding strips in tool
- Placing of double sided tape into alignment tool
- Insertion of disk holding tool into alignment tool
- Push out of disk by punching tool
- Attachment of flow layer and slewing
- Repeat of procedure for disks on the other side of the chip
- Assembly of layers

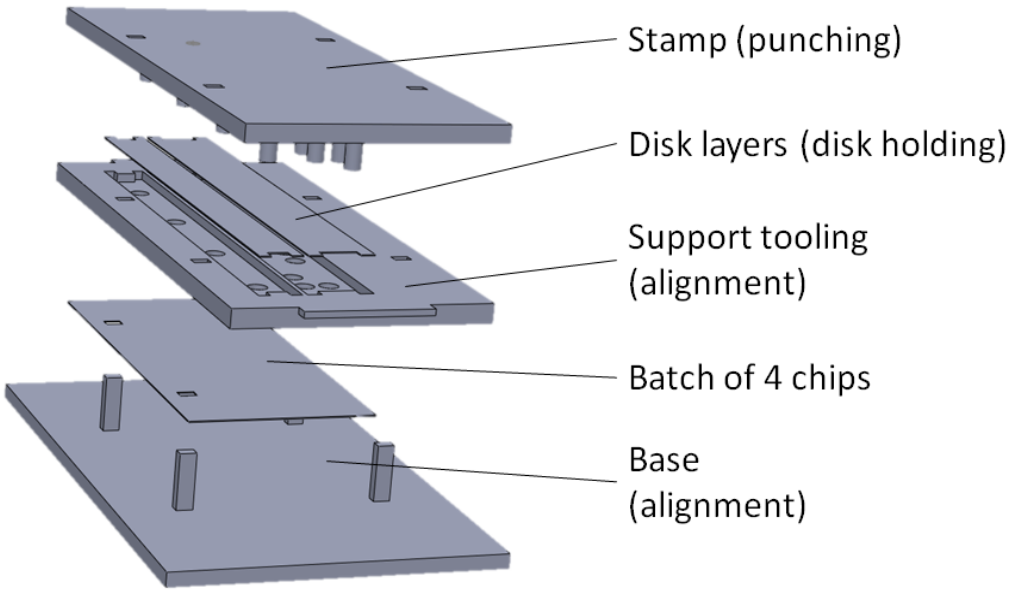

Figure 3.4: Tooling to punch out and place several valve-disks at once

3.2.2 Disk-holding Layers

This Method is based on four additional layers (two layers of tape and two layers of filter paper) to incorporate the disks into the chip. The layers of filter paper are used to fabricate and hold the disks during assembly for multiple disk placement in one assembly step. The additional layers of double-sided tape are used to attach these layers to the flow layers of the chip.

The geometry of hydrophobic disk, surfactant disks, and the hole in the double-sided middle layer was maintained according to the method described above. In contrast to the methods described above each disk is printed and treated separately. Circles were printed for each disk on layers of filter paper (2.5 mm for surfactant disks and 3 mm for hydrophobic disks) and after heating of the wax treated with Tween 20

or Allyltrichlorosilane. The amount of reagents needed for each disk was optimized using additional experiments (*vide infra*).

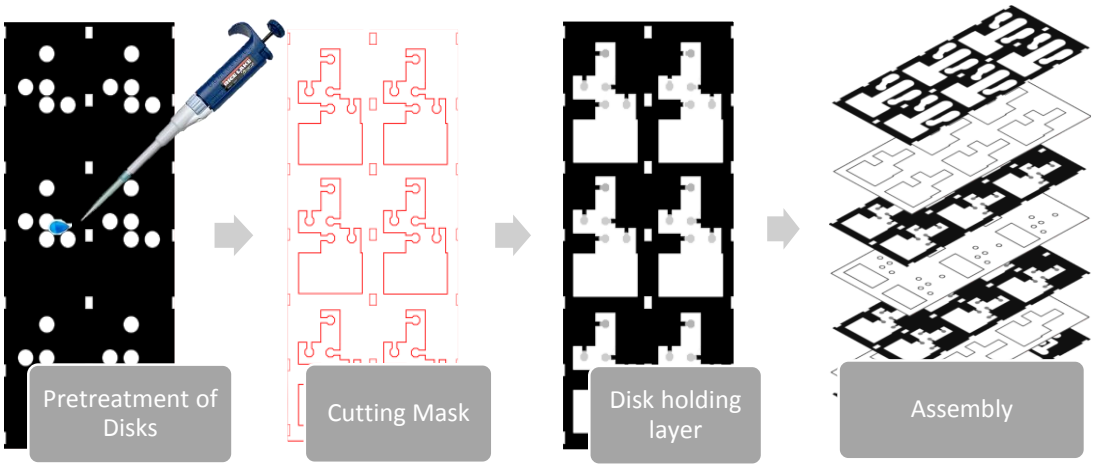

Figure 3.5: Flowchart for valve fabrication using layers to hold and align disks

The minimum amount of Allyltrichlorosilane for each disk needed to generate hydrophobic disks was determined in an parallel study at the laboratory of microfluidics of Professor Faghri by W. Föllscher [10]. It was discovered that each hydrophobic disk has to be treated four times with 2 ul of 4.76 vol.% A3CS in Perfluro-compound FC-72 in order to achieve permanent hydrophobicity.

After pretreatment the disks were cut out using a laser cutter while a bridge was kept to hold the disks in the layers. The excised area was made as large as possible in order to guarantee tight contact of the flow layer with the middle tape layer. Additionally, layers of double-sided tape were placed on-top/underneath of the disk-holding layers to attach them to the flow layers. The fabrication procedure is shown in Figure 3.5 and the steps needed for fabrication are summarized as follows:

- Printing of 3 and 3.5 mm circles for hydrophobic and surfactant disks on filter paper with wax
- Heat treatment of disks in vacuum oven at 120^{o}C for 60 s
- Dilution of 35 Wt. % Tween 20 in Ethanol
- Dilution of 50 µl/ml Allyltrichlorosilane in Perfluro-compound FC-72
- Pretreatment of hydrophobic disks with 4 X 2 µl A3CS solution and surfactant disks with 1 X 2 µl Tween 20 solution
- Drying of disk holding layers at 60^{o}C (at least 10 min)
- Cutting of disk holding layers and double-sided tape using laser cutter
- Assembly by stacking tape and paper layers

3.2.3 Surfactant Cellulose-Powder

This method is similar to the method described in section 3.2.2 but the number of layers needed for fabrication is reduced. Instead of using disks made of surfactant treated filter paper to fill the holes in the middle layer of the chips. The holes are filled with a treated paste made from cellulose powder. Also the disks holding layers for the hydrophobic part of the valve is replaced. In this method the hydrophobic layer is prepared in the same way retaining the equivalent amount of Allyltrichlorosilane for the disks as before but the disks are not cut out anymore.

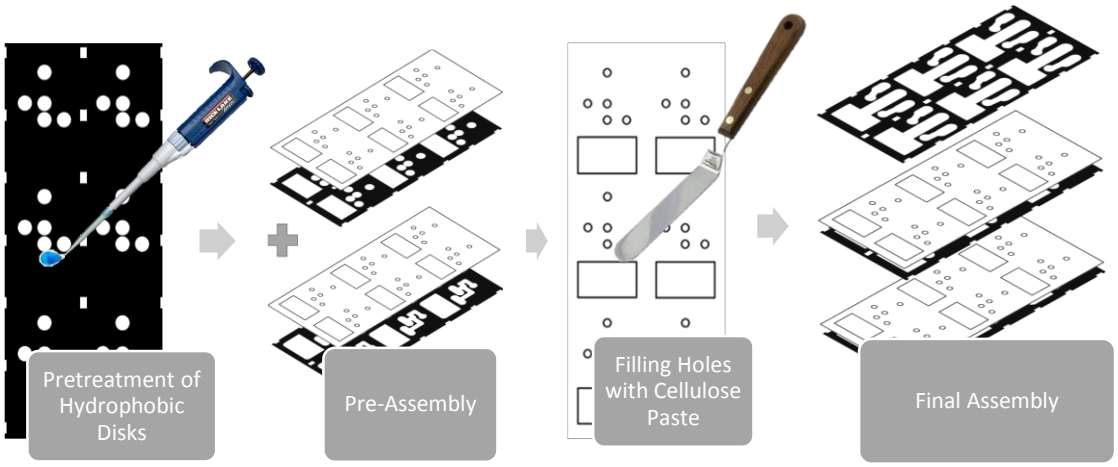

Figure 3.6: Flowchart for valve fabrication using layers to hold and align disks

In the previous method flexibility of the disks and compression was used to connect the hydrophobic disks to the next layer. In this method double-sided tape with holes filled with untreated cellulose paste is used to connect the hydrophobic layer to the flow layer.

The amount of surfactant per disks optimized for the method described earlier (section 3.2.2) was maintained. To fill 2.2 mm holes in double-sided tape approximately 455 µg cellulose is needed. To reach the same amount of surfactant per disk a paste with 154 mg/g surfactant modified cellulose was prepared and filled into the holes using a spreader before removing the protective side of the tape. The preparation procedure for this method is summarized as follows:

- Printing of 3.5 mm circles for hydrophobic disks on filter paper with wax
- Heat treatment of disks in vacuum oven at 120^{o}C for 60 s
- Dilution of 50 µl/ml Allyltrichlorosilane in Perfluro-compound FC-72

- Pretreatment of hydrophobic disks with 4 X 2 µl A3CS solution
- Dilution of 35 wt.% Tween 20 in Ethanol
- Dilution of 0.25 ml/ml surfactant solution in ultra-pure water
- Mixing of cellulose powder with the Water-Ethanol-Surfactant solution (0.5 g/ml)
- Mixing of cellulose powder with ultra-pure water (0.5 g/ml)
- Pre-assembly of one tape to hydrophobic disk layer and one tape to bottom flow layer
- Filling of holes in double sided tape with cellulose powder (with or without surfactant) using a spreader
- Drying of layers at room temperature (approximately 10 min)
- Final assembly of missing layers

3.2.4 Optimization of Surfactant

The amount of surfactant was optimized with the experimental setup shown in

Figure 3.7. Simple valves were fabricated with the preparation according to section 3.2.2 and different amounts of Tween 20 (40-286 µg) for the surfactant disks. The amount of surfactant per disk was reached by treating the disks with surfactant solutions between 10-60 wt.% Tween 20 in Ethanol. Each valve was wetted with 4 µl of water with food coloring and the time was measured until the fluid was completely

absorbed by the hydrophilic area on the other side of the valve. The experiment was repeated 18 times for each measured concentration of Tween 20.

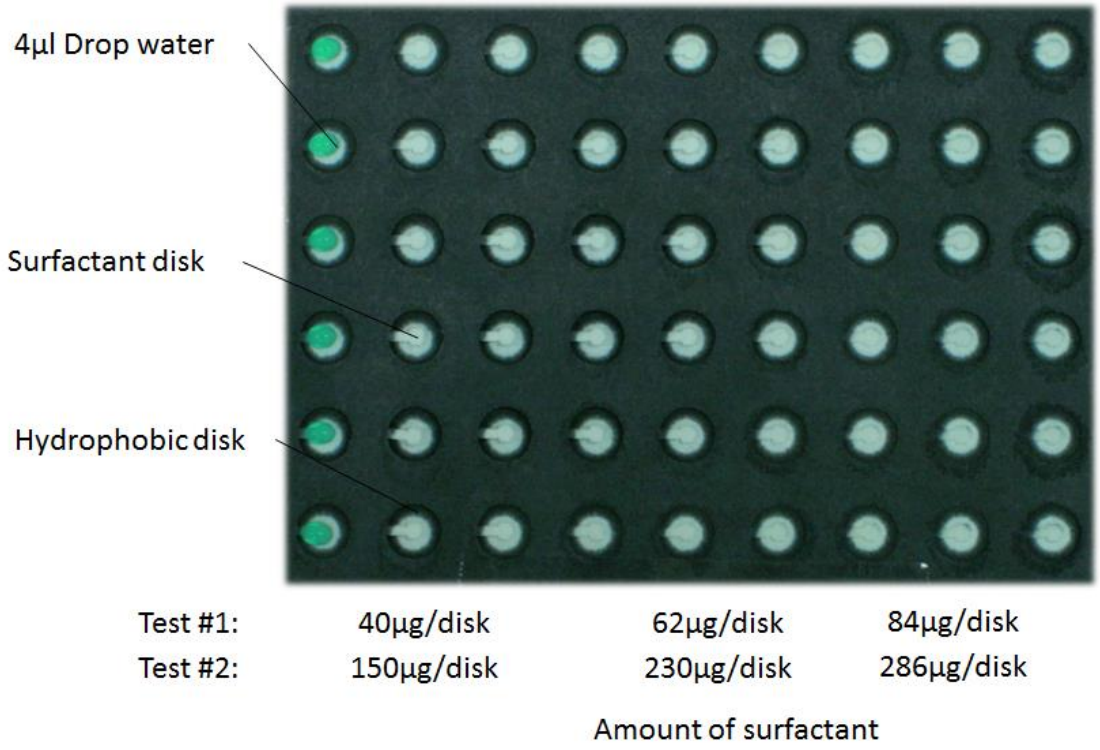

Figure 3.7: Experimental setup for the optimization of the surfactant amount per disk in fluidic valves

3.3 Material Selection and Processing

Material was selected according to section 1.5 and knowledge gained during the study. Filter paper (Grade 41, 20 µm, Whatman®) was chosen for printing the layers because of good wax absorption and the common use as a sample pad in regular lateral flow tests. Glass fiber was chosen for the conjugate pad material because of good hold-up volumes and low nonspecific binding. Different glass fiber materials were studied for the best conjugate release (*vide infra*). Absorption experiments (*vide infra*) were

conducted for different cellulose materials to estimate the hold-up volumes and the absorption potential in order to select suitable materials for the absorption area. Nitrocellulose (AE100, 12 µm, Whatman®) was chosen as a membrane.

Processing of the materials especially cutting and alignment were optimized during the study. The cutting parameters of the Laser cutter (power, speed and fan-support) were altered for all materials until a straight cut without burnt edges at the highest possible cutting speed was achieved.

Specifications and the manufacturer for cellulose or adhesive materials used during the study are listed below:

Table 3.1: Specifications and manufacturer for materials used during the study

Material	**Specification**	**Vendor**
Filter paper	Grade 41, 20 µm	Whatman®
Nitrocellulose membrane filters	AE100, 12 µm	Whatman®
Glass fiber membrane filters	GA-55	Sterlitech®
Gel blot paper	GB003	Whatman®
Double-sided tape	n/a	Ace®

3.4 3D Lateral Flow Test Strip Development

The 3D multi-fluid lateral flow tests presented in this study were developed by modifying the common strip test design presented in section 1.5. Briefly, the basic structure of a lateral flow test including membrane, sample pad, conjugate pad and absorbent pad was maintained and the lateral flow test was transferred to a 3D PAD by adding additional channels, inlets, and a valve mechanism.

3.4.1 One Valve two Inlets Design

As a base for the design preliminary test results for 3D lateral flow test conducted by J. Cogswell at the laboratory of Prof. Faghri were used [15]. The preliminary design (Figure 3.8) was based on two inlets and one valve fabricated in three layers. The valve operates according to the previously described mechanism (section 2.5.4).

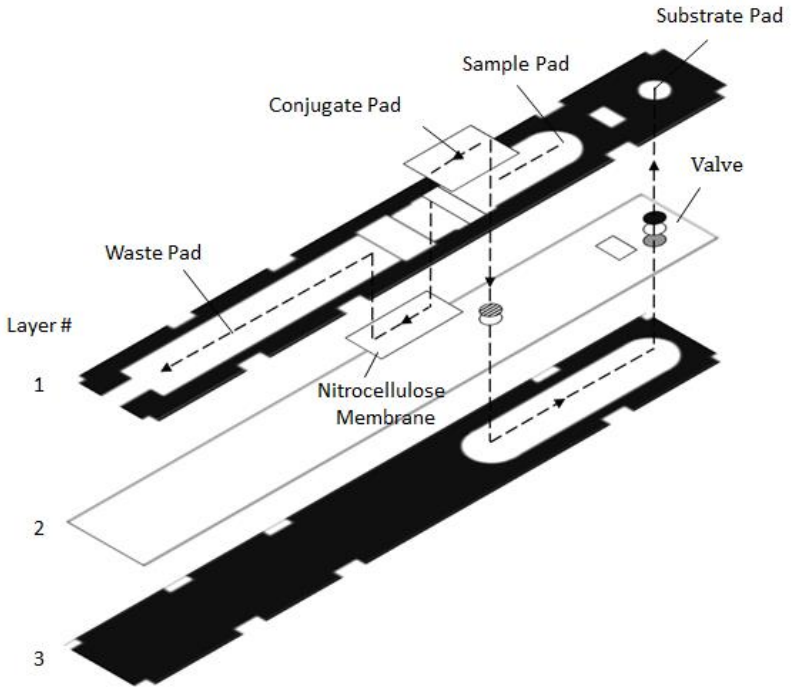

Figure 3.8: Two fluid lateral flow test based on fluidic valve

The first layer of the device consists of a 5 mm wide main channel and an input pad for the second fluid. Two windows are cut into the first layer where the 5x8 mm membrane and the 5x5 mm conjugate pad are placed. The windows above the membrane or conjugate pad are needed to force the fluid through the material and in case of the membrane are also necessary to allow a free view onto the signal. A double-

sided tape in which two holes were cut builds the second layer of this design. The hole underneath the main channel is filled with a hydrophilic disk fabricated from filterpaper to connect the main channel with the channel in the bottom layer. The second hole is used for the valve and placed underneath the substrate input pad. The hydrophobic side of the valve is placed on the upper side of the tape directly underneath the substrate inlet to keep the substrate in the reservoir. The third layer consists of a trigger channel connecting the valve with the hydrophilic disk. Once the sample is applied onto the sample pad, the upper layer works like a common lateral flow test. The biggest difference is that a part of the fluid is channeled through the hydrophilic disk into the bottom layer where the fluid flows towards the valve. Once the fluid reaches the valve, it opens the inlet and the substrate flows into the bottom channel traveling into the opposite direction. The capillary force from the waste pad pulls the substrate into the main channel where it moves through the strip like the sample before.

3.4.2 Two Valves two Inlets Design

Two main disadvantages were found for the design described in section 3.4.1. Firstly the substrate has to travel back through the already wetted trigger channel, and secondly the substrate has to flow through the conjugate pad. The test is slowed down by the fact that the substrate has to travel in the already wetted channel and enzyme labeled antibodies which may have remained in the conjugate pad can cross-contaminate the substrate. To avoid these disadvantages a new design (Figure 3.9) based on two valves was developed. The main geometries of the preliminary design

and the hydrophilic connection in the beginning of the strip where thereby maintained. The substrate input pad with the first valve underneath was moved to the side of the test close to the nitrocellulose membrane and a second valve (valve #2) was placed before the nitrocellulose membrane underneath the main channel.

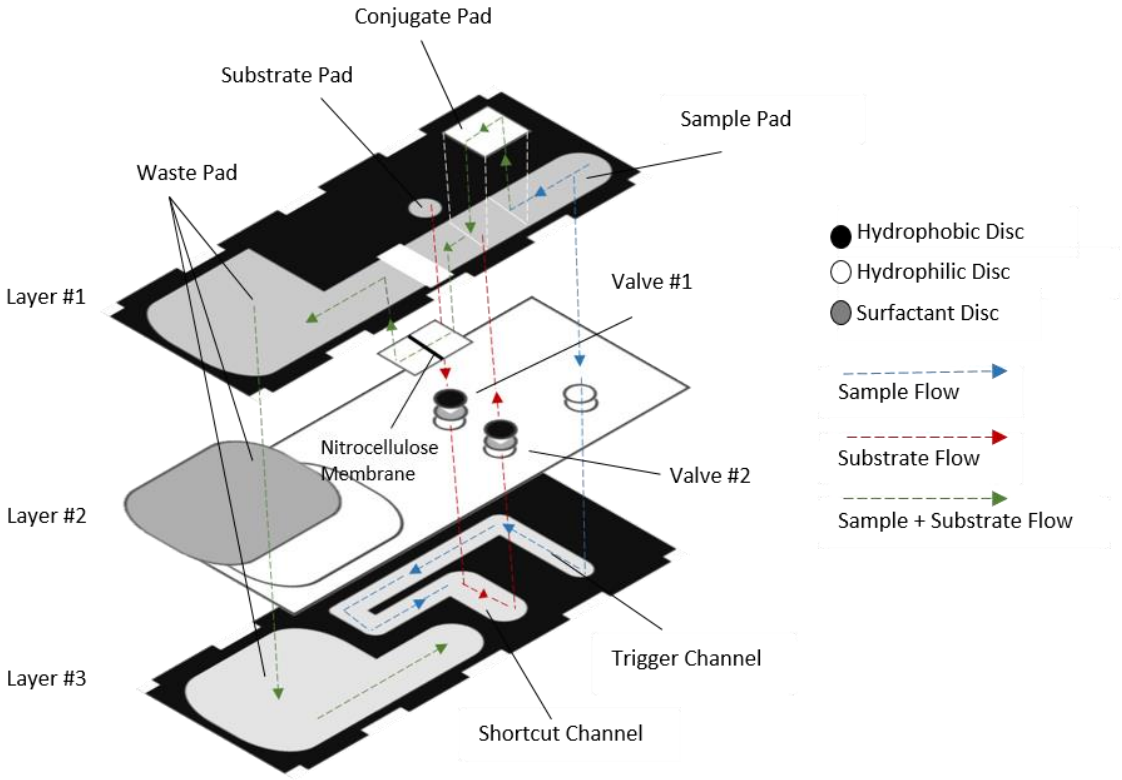

Figure 3.9: Two fluid lateral flow test based on two fluidic valves

The bottom layer of the new design contained three different areas in contrast to the simple bottom layer of the old design: A trigger channel, a shortcut channel, and a waste area. The trigger channel is directly connected to the sample pad through a hydrophilic disk, which is placed in the first hole of the double sided tape. The trigger channel length was determined in that way, that valve #1 opens when the entire sample volume is consumed by the test. Once valve #1 is open and the substrate is

released, the fluid will flow through the shortcut channel and eventually open valve #2. The bigger amount of fluid will flow through the shortcut into the main channel where it passes the nitrocellulose membrane. In order to reduce the surface area of the waste pad the unused space in the bottom layer was used as absorbent pad. A relatively huge hole was cut out from the double sided tape and filled with glass fiber as connection between the waste pad in the upper and in the bottom layer.

3.4.3 Four Valves three Inlets Design

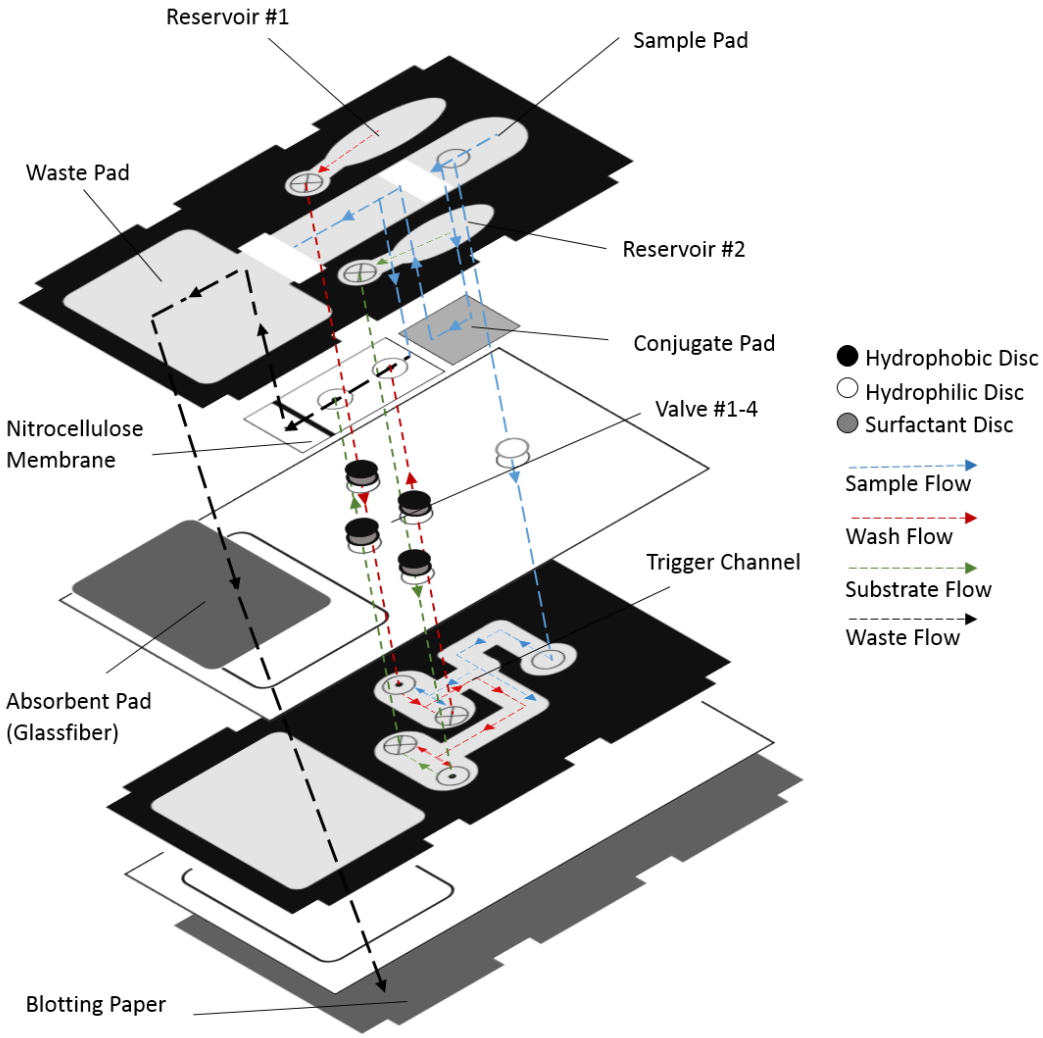

Wash steps are commonly used in immunoassay procedures to wash away unbound antibodies and increase the signal intensity by lowering the background noise [8]. Because of this several researchers are working on methods to integrate wash steps into lateral flow test devices. For example Fernández-Sánchez et. al. [9] reported a significant improvement of the signal intensity using a wash step in a standard LFIA. Using a wash step the group was able to lower their limit of detection to 2.4fm. Also preliminary results at professor Faghri's laboratory [15] showed that a wash step can wash away unbound antibodies in cellulose substrates.

Because of this, the design presented in section 3.4.2 was extended to three inlets including the sample a wash and the substrate. Two additional valves were added in order to incorporate the third input into the strip test. The principle for the third input is the same as described earlier. The difference is, that the fluid which vertically flows into the trigger channel of the bottom layer divides into two separate channels. The trigger channel is designed in that manner, that the fluid divides shortly before the first two valves with a longer channel to the third and fourth valve. The length of the trigger channel was determined so the second inlet opens after the sample is consumed and the third inlet opens after the fluid from the second inlet traveled into the waste pad. Additionally, a sheet of blotting paper was placed underneath the bottom layer using another layer of double sided tape for attachment to extend the absorption area and to stabilize the chip. To prevent bridging of the fluid the conjugate pad was placed underneath the channel instead of above. The length of the main channel was kept as short as possible in order to prevent fluid flow that was too slow.

3.5 Chip Optimization

Different trigger channel designs were used during the study (Figure 3.10). The length of the trigger channels were calculated assuming paper wet-out (see section 2.6.1). The parameters for the fluid flow timings were found during the assay development and material parameters were determined using flow experiments (*vide infra*).

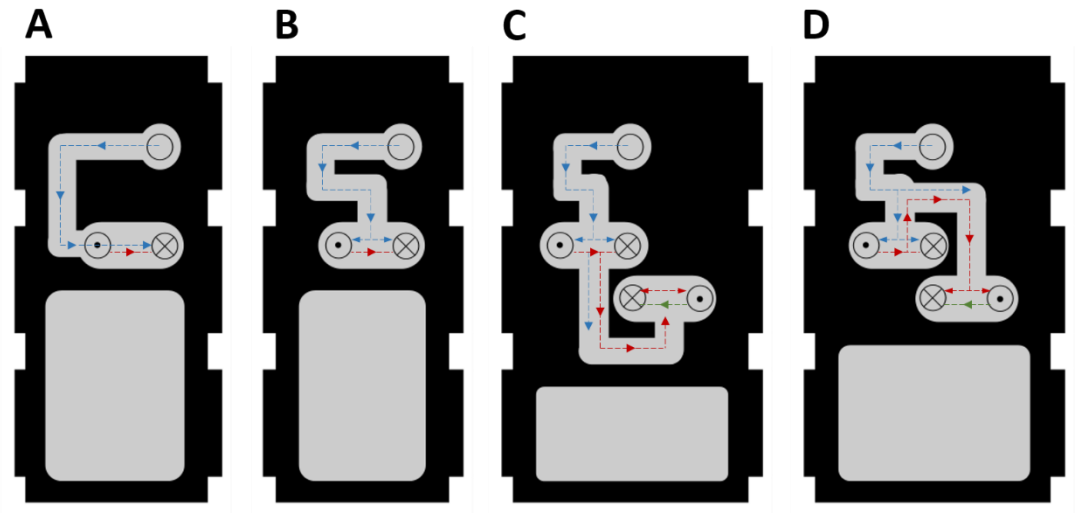

Figure 3.10: Trigger channel designs used during the study

The different trigger channel and valve fabrication methods configurations were compared and evaluated for repeatability and reliability using water colored with food coloring. The chip-yield and the valve opening deviation were determined in order to compare the different methods and designs. Chips were failed under two conditions: a leaking valve or a malfunctioned or delayed valve opening (+30 seconds).

Different materials were evaluated for their flow and absorption behavior, in order to optimize the waste absorption and the fluid flow and to generate data to calculate the channel length. To test the flow behavior, 70x6 mm strips were fabricated for each tested cellulose material. The strips were continuously wetted with colored water from an unlimited fluid source and the travel time until the fluid traveled 60 mm into the strip was measured. The retention volume of the material was also determined by measuring the necessary amount of fluid to completely wet a sheet of 20x20 mm of the tested cellulose material.

The chip design was also optimized with regards to waste material, size minimization, complexity of fabrication, and manufacturing time by changing the geometry of the chip and fabrication batch.

3.6 Assay Development

The developed assay was built on the alkaline phosphatase based enzyme linked imunnoabsorbent assay procedure.

The following section describes the procedure shown in Figure 3.11 in detail and addresses the techniques used for preparation and implementation of the assay. Also the optimizations conducted during the study are described. The section can further be used as a manual for repeating the experiments.

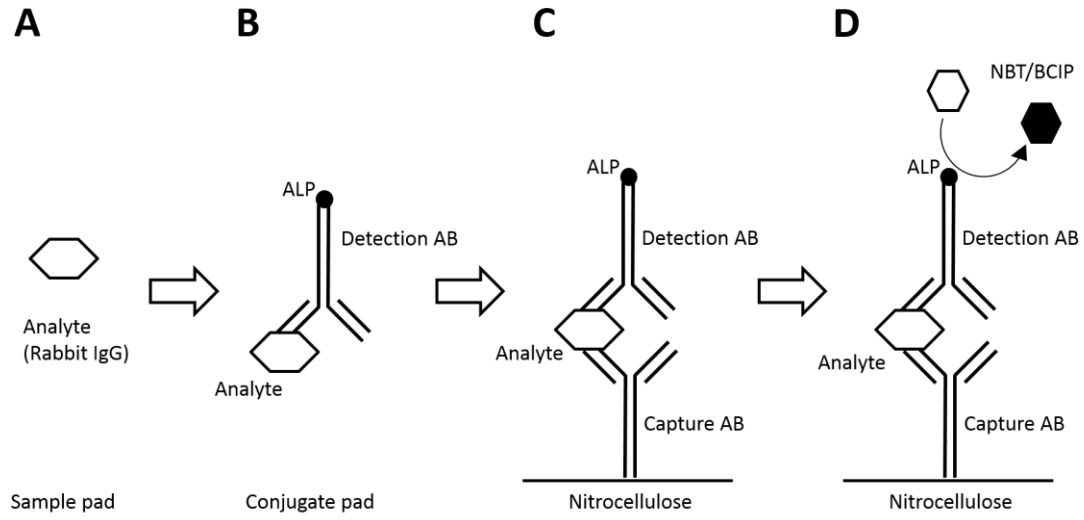

Figure 3.11: ELISA procedure in lateral flow: A) Analyte (Rabbit IgG) is applied to sample pad B) Analyte binds to detection AB labeled to ALP (in conjugate pad) C) Complex of analyte and detection antibody is captured by capture antibody (on nitrocellulose) D) Color is produce by reaction of ALP and NBT/BCIP.

3.6.1 Assay Preparation Procedure

Mouse monoclonal (SB62a) and polyclonal antibodies to rabbit IgG labeled with alkaline phosphatase were purchased from abcom® as detection and goat polyclonal and mouse monoclonal (31213) antibody to rabbit IgG were purchased from Pierce® as capture antibody. For blocking of unspecific sites SuperBlock® blocking buffer in TBS was purchased from Thermo Scientific.

In order to enable the highest possible sensitivity, the stock solution of capture antibodies was used for preparation of the detection area. The capture antibodies were placed drop by drop (0.6 µl) in the middle of the membrane with a 2.5 µl pipette in contrast to a line in conventional applications due to the lack of a dispenser. Dilution

of all reagents was performed in a blocking buffer solution and the procedure for preparation of the assay was conducted as follows:

- Preparation of chip material (printing, cutting & treatment with reagents)
- Blocking channels twice with Blocking Buffer Solution (fully wetted and dried at 37 ^{o}C on hotplate)
- Dispensing 0.6 µl drop by drop at 1.8 mg/ml of monoclonal or polyclonal capture antibody onto the membrane (dried at 37 ^{o}C in covered petri dish)
- Blocking of membrane for 8 minutes with blocking solution (fully wetted in petri dish) dried at 37 ^{o}C in covered petri dish
- Treatment of conjugate pad with 10 µl of blocking reagent
- Dilution of 20 wt.% (trehalose/sucrose) in blocking buffer
- Treatment of conjugate pad with 10 ul at 40 µg/ml of goat polyclonal or monoclonal anti-rabbit IgG labeled with alkaline phosphatase diluted in blocking/sugar solution (dried at 37 ^{o}C in covered petri dish)
- Chip assembly (after drying of material)

3.6.2 Assay Implementation Procedure

Rabbit IgG was purchased from Thermo Scientific and diluted in blocking buffer for the sample solution. Dilutions with antigen concentrations from 1 µg/ml to 1 ng/ml were prepared and dilution factors covered three orders of magnitude (1 X 10^{3}) to reduce the deviation error. The solutions were vortexed in between each dilution step

for at least 60 seconds in order to ensure homogeneous distribution of the antigens. Blocking buffer was used as sample fluid for negative controls.

BCIP®/NBT tablets[2,3] were purchased from SIGMAFAST™ as specific substrate to the alkaline phosphatase label and one tablet of BCIP®/NBT was dissolved in 10 ml ultra-pure water to produce the substrate solution.

The first assay experiments were conducted with the two fluid design described in section 3.4.2. The volume for the sample (80 µl) and the volume substrate (120 µl) was adapted from preliminary results obtained at Professor Faghri's laboratory. For the assay experiments, first the substrate and the wash were applied to the reservoirs of the test. Afterwards the test was started by applying the sample to the sample pad. The experiments were used as proof of concept, to test the repeatability in particular the reliability of the valves and to optimize variable parameters.

Optimization of the regents was conducted using the three fluid chip design presented in section 3.4.3. Experiments including this design were performed with 130 µl of sample, 60 µl of wash and 120 µl of substrate. The volume for the sample was adjusted for optimal conjugate release (*vide infra*), and the substrate volume was

[2] BCIP = 5-Bromo-4-chloro-3-indolyl phosphate (artificial chromogenic substrate)

[3] NBT = Nitro blue tetrazolium (oxidant)

adapted from the preliminary result. The amount of washing buffer was fixed at the maximum possible amount of 60 µl to keep the test duration under 12 minutes.

To document the results of the experiments all tests were recorded using at least 600 dpi scans. The images were taken immediately after finishing of the tests. The signal intensity was measured as mean grey value using the image processing program ImageJ.

3.6.3 Optimization of Conjugate Release

The conjugate release was optimized by changing various parameters, such as sugar concentration in the pad, geometry of the conjugate pad, blocking and materials. The impact of sugar to the assay was investigated, in a parallel study in this topic and the results showed that a sugar concentration of 20wt.% in the antibody dilution with equal proportions of trehalose and sucrose leads to the optimal antibody release [10]. To achieve optimal antibody release, all conjugate pads for this study were prepared using these previously determined amounts of sugar.

In addition, the conjugate release was optimized by valuating glass fiber material with binders and without binders for the conjugate pad, blocking of conjugate pads before applying antibodies, the amount of fluid needed to release the conjugate and the size of the conjugate pad. In order to compare the release for different conjugate pads, an experiment was designed where the conjugate pad was washed with increasing amounts of fluid and the signal intensity of the release was measured.

Therefore, the tested conjugate pad was first prepared with the antibodies according to section 3.6.1 and placed onto blotting paper. Afterwards the conjugate pad was washed several times with steps in the range of 20-40 µl of fluid. After each washing step the conjugate pad was moved to a different place on the blotting paper. Next, 10 µl of substrate was applied to each place where the conjugate pad was washed and the signal intensity of the developed signal was observed.

3.6.4 Optimization of Detection Antibody

The detection antibody has an important impact on assay sensitivity and background noise. To optimize this parameter the concentration of the anti-rabbit IgG antibody in the conjugate pad was varied between 10 µg/ml to 80 µg/ml while all other assay parameters were kept constant. The assay was run using triplicate 500 ng/ml samples per detection antibody concentration. To further optimize the signal polyclonal and monoclonal antibodies were evaluated as detection antibodies. To compare the results the signal-to-noise ratio was determined by reading out the mean grey value of the scans using ImageJ.

3.6.5 Optimization of Capture Antibody

In order to enable the highest possible sensitivity the stock solution of capture antibodies were used for preparation of the detection area. To further optimize the signal polyclonal and monoclonal antibodies were evaluated as capture antibodies.

Triplicate sets with at least five different analyte concentrations for both kinds of antibodies were conducted. The results were examined for the quality of signal development and the nonspecific binding on the detection spot.

3.6.6 Dose Response

After optimization of the immunoassay, the performance of the system was tested by observing of the dose response and by estimating the limit of detection and the limit of quantification. To do this, the signal response for triplicates of 8 different concentrations ranging from 1 ng/ml to 5 µg/ml was measured using the methods described earlier.

3.7 Housing Development

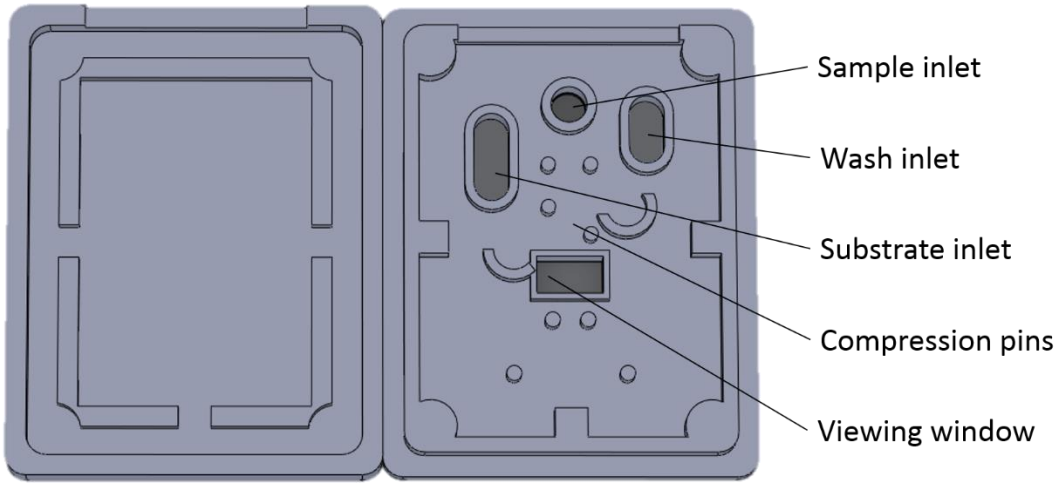

Figure 3.12: Housing design with valve compression adapted from [10]

In order to develop a POC device a housing was needed to store the substrate and wash solutions and according to section 1.5.5 a housing is also necessary to compress different materials together and ensure consistent assay conditions. Experimental results (*vide infra*) also showed that compression of material can increase the valve performance particularly for the valve fabrication method described in section 3.2.2. A basic housing design with compression for the valves and the connection between the materials was developed by Föllscher [10]. The design was adapted and modified to be compatible with the lateral flow test strip design presented in section 3.4.3 (Figure 3.12). The housing was designed with SolidWorks (Dassault Systèmes®) and the fabrication was done using rapid prototyping with fused deposition modeling of ABS (Stratasys - Dimension Elite).

3.7.1 Reagent Storing

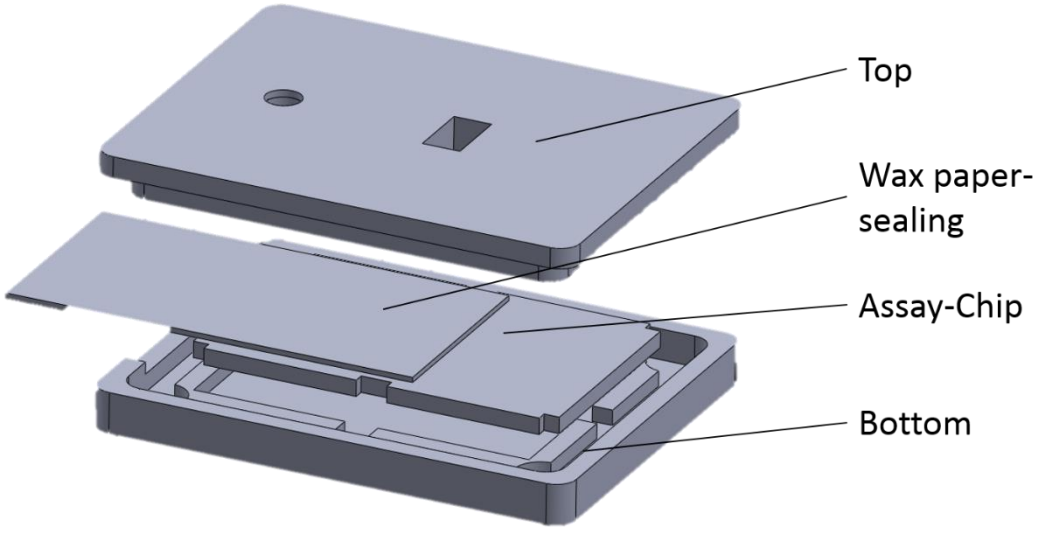

Figure 3.13: CAD model for housing with reagent storing

The CAD model of the housing with reagent storing is shown in Figure 3.13. In contrast to the design described earlier the inlets for the substrate and wash solution is sealed from above. In order to store the reagents in the housing 60 µl of blocker are added into the first and 120 µl of substrate in the second reservoir. Next, a piece of wax paper is placed on top of the inlets with one end penetrating through the housing. Then, the bottom layer of the housing with the inserted chip is placed onto the upper layer sealing the inlets by pressure. The wax paper strip has to be pulled to activate the immunoassay sensor after which the sample can be added to start the test.

CHAPTER 4 – FINDINGS AND DISCUSSION

This chapter presents the knowledge gained during the development of a paper based analytical devices, which uses fluidic valves to trigger multiple fluid flows in order to autonomously conduct ELISA procedure. Different fabrication methods are compared and the results of the immunoassay optimization are addressed.

4.1 Material Processing

Proper cutting parameters are very important for the fabrication process and the lateral flow test itself. Cutting power that is too high or too low can lead to burned edges of the material. Particles resulting from the burned material can be dissolved from the fluid flow and be transferred into the channels or detection area leading to discoloration. The various materials used in this study have a different tendency to burn, for example, a relatively low cutting power (3%) is needed to cut nitrocellulose membranes because of the high affinity to burn, whereas slightly different cutting parameters (+2% cutting power) can cause nitrocellulose to burn. Also the cutting speed is an important parameter for fabrication. Since many masks (channels, absorption, membrane, tapes etc.) have to be cut and one cutting process can take up to 15 minutes (e.g. cutting of disks holding layers) rapid cutting is preferable. On the other hand, the accuracy decreases with increased cutting speed resulting in rough edges. Fan support can help to prevent burning of material but it can also ruin the cutting process and make it inaccurate due to shavings and particles that have been

dislodged. In cases where those parts cannot be secured with tape or weighed down, the fan support should be deactivated. For some materials, especially tapes or glass fibers with binders, cutting can result in smoke development. In those cases cutting without fan support is not possible. The parameters presented in Table 4.1 are the results of the optimization process. Cutting using the listed parameters results in sharp unburned edges at the highest possible speed without smoke development.

Table 4.1: Optimized cutting parameters for materials used during the study

Material	**Manufacturer**	**Speed**	**Power**	**Fan Support**
Filter Paper	Whatman®	55%	12%	No
Glass fiber with binder	Whatman®	85%	7%	No
Glass fiber without binder	Sterlitech®	45%	13%	No
Nitrocellulose membrane filters	Whatman®	39%	2%	Yes
Gel Blot Paper	Whatman®	40%	17%	Yes
Double-sided tape	Ace®	50%	22%	Yes
One-sided transparent tape	Scotch®	50%	20%	Yes

4.2 Development and Optimization of the Fluidic Circuit

Optimization for the fluidic circuit was done with regards to reliability and repeatability of the fluid flow, particularly with reference to the valve opening performance. Different fabrication methods were investigated for their impact to the valve performance as well as different trigger channel designs. Also the amount of surfactant was optimized to improve the system reliability and repeatability.

4.2.1 Comparison of Fabrication Methods

The methods for the production of valves presented in section 3.2 have different advantages and disadvantages (Table 4.2) which will be discussed in the following. Assembling a chip with four valves using the initial method by manually placing each disk for the valves one after another takes about 50 minutes for a batch of 6 chips. The accuracy of placing the disks is highly dependent on the experience of the constructor and a consistent alignment over different chips is not possible. These circumstances result in high deviations in the valve opening and therefore in high valve failure rates (*vide infra*).

Table 4.2: Comparison of valve fabrication methods used during the study

	Manual	**Disks-Punching**	**Disk-Holding Layers**	**Cellulose Disks**
Layers needed (Paper/Tape)	3 (2/1)	3 (2/1)	7 (4/3)	5 (3/2)
~Preparation Time (for 100 Valves)	30 min	30 min	60 min	45 min
~Assembly Time (for 6 chips)	50 min	13 min	17 min	15 min
Advantages	Small waste	Small waste	Design changes easily possible	Less Cutting needed
	Easy design & development	Good possibility of automating	Small reagent deviations	Very easy Alignment
	Mass production of valves	Mass production of valves		
Disadvantages	Very difficult alignment	Complicated design changes	Compression needed	Messy fabrication
	High chip deviation	Time consuming development	High waste	Drying needed during assembly
	High reagent deviation		Brittle Layers	

Also the manner of pretreating a whole paper with the reagents could lead to variations of reagent concentration in the material itself resulting in poor valve opening behavior. However, the design and preparation of the fluidic circuit design and valves is quick, easy and very little waste is produced. Another benefit is that the valve disks can be mass produced for future use.

Using the disk punching method for fabrication of valves is advantageous because the chip design with three layers reduces the assembly time for a batch of 6 chips from 50 to 13 minutes. However, the valve placing with this method is still not accurate enough. Assemblies done with this method sometimes resulted in misplaced disks or the disks remained stuck to the tool. Possible explanations are a rough surface, low fabrication tolerances for the tool, and insufficient alignment either of the disks in the tool or the tool alignment itself. Even when those problems are solved the biggest disadvantage for this method is the tool itself. Once the tool is designed and fabricated it can only be used for one particular chip design. If the chip has to be changed the tool has to be redeveloped and refabricated as well. Also it has been found, that the fabrication with rapid prototyping is not satisfactory with respect to tolerance accuracy.

Although more layers are needed for the fabrication of valves with the “disk-holding” method and the design for printing and cutting masks are more complicated, it still offers the opportunity to place several valve disks in one assembly step without the need of a specific tool. Once a chip design for this method is established, changes to this design are easily possible. Since this methodology requires treatment of each

individual disk, it offers the opportunity to control the amount of reagents very precisely. This approach was used to optimize the exact amount per disks needed for optimal valve opening behavior (*vide infra*).

The major disadvantage of the “disk-holding” method is the relatively large gap between the layers caused by the extra tape layers needed to connect the disk holding layers to the channels. Because of these gaps no repeatable valve opening behavior could be reached (*vide infra*). But in another study [10] it was found, that compression of the layers using a housing can help to improve valve performance. The “disk-holding” layers are also very brittle and difficult to handle and align. This can lead to reduced chip yield due to broken disks. And compared to the methods presented earlier, this fabricating uses a lot of hydrophobic ink and filterpaper.

The last developed method dispenses the conventional art of using disks for the production of valves. No more cut outs are necessary and gaps between the layers are filled completely with cellulose paste. The biggest advantage of this is, that no additional compression is needed for reproducible valve opening behavior. It also reduces the time needed for preparation because of less cutting and treatment with reagents. On the other hand, fabrication is messy because of particles that result from crumbling during drying of the cellulose paste. But those disadvantages are marginal compared to the disadvantages of the other methods.

4.2.2 Impact of Fabrication on Reliability and Repeatability

Reliability and repeatability are important factors for analytical devices, particularly for the market admission of medical products [47]. They can only be assessed with constant assay results and without defective products. In order to have consistent test results for paper based microfluidic analytical devices, constant flow characteristics over all fabricated devices are required. Otherwise the results can lead to high deviations in the signal intensity and background noise (*vide infra*), making it impossible to have reliable results. For the developed paper based analytical device it was found, that the fabrication of those devices and the preparation of the valves has a great impact on the reliability and repeatability of the fluidic circuit. Alignment of the different layers, valve disks, conjugate pad, or membrane is crucial. It was observed, that small deviations in placing of the membrane or conjugate pad can result in an assay duration deviation of about 1-2 minutes. This is because the fluid flow is blocked when the above mentioned parts are not placed perfectly in the channel. Also, bridging of fluid flow on the sides of the material was observed for misplaced conjugate pads resulting in a much faster fluid flow than normal. An even greater impact on the repeatability has the preparation and the alignment of disks for the valves. Misplaced hydrophobic disks can cause the fluid to wick into a gap between the tape and the disk, which results in a leaking valve. This leaking occurs more often when manually placing the disks and could be prevented almost completely with the method where layers with hydrophobic spots are used instead of disks (see Figure 4.1).

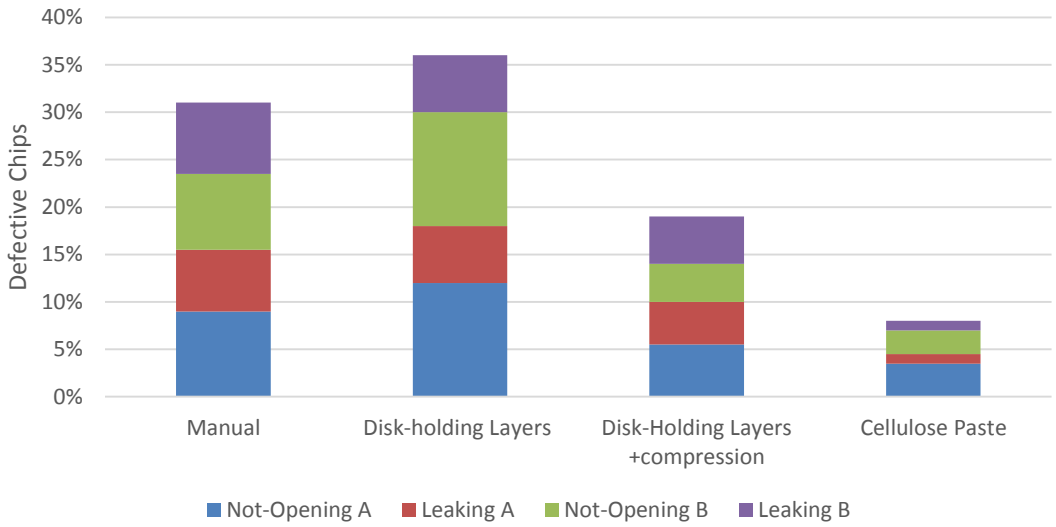

Figure 4.1: Chip yield for different fabrication methods with respect to valve failure probability for at least 18 replicates for each method. A refers to valve complex of valve 1&2 and B to the complex of valve 3&4.

Misalignment of the tape which holds the surfactant disks or misalignment of the disks itself can lead to unsuccessful contact between the hydrophobic and the surfactant disks causing the valve not to open. Because of this, it was found that compression of the chip (e.g. with housing) helps prevent valves from not opening (see Figure 4.1).

It was also observed, that the method of fabrication for the valves has an impact on the valve opening performance. This is probably due to the transfer of surfactant to the hydrophobic disk, which is dependent on the amount of surfactant, the material, and the contact between surfactant and hydrophobic disks.

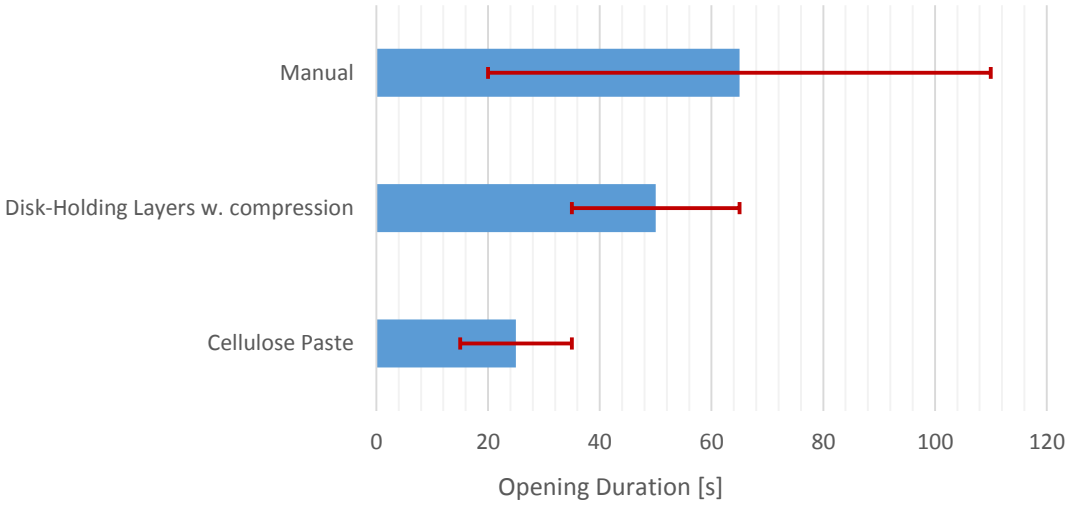

Figure 4.2: Valve opening performance for different fabrication methods. Opening duration and standard deviation of opening for at least 18 replicates.

As presented in Figure 4.1, the worst valve opening behavior was achieved with the manual method. It takes over 65 seconds with a standard deviation of ±45 seconds for the average valve to open. The explanation for this is that only a limited amount of surfactant can be used for this method, since amounts of surfactant that are >50 µg per disk prevent the disks from sticking to the tape, making alignment almost impossible.

For the other methods, the amount of surfactant per disk was optimized (*vide infra*). As seen from Figure 4.1, this optimization results in faster valve opening with smaller opening deviations. It was found that cellulose powder for the surfactant disks results in the best valve opening behavior. A possible explanation for this is that there are better contact or improved surfactant release characteristic for this material.

4.2.3 Optimization of Surfactant

Figure 4.3 shows the results of the surfactant optimization. It can be seen that a minimum amount of surfactant per disk (~20-35 µg) is needed to open the valves. It should be noticed, that with decreasing amount of surfactant per disk the time to open the disks exponentially increases. This is also true for the deviation of the valve opening.

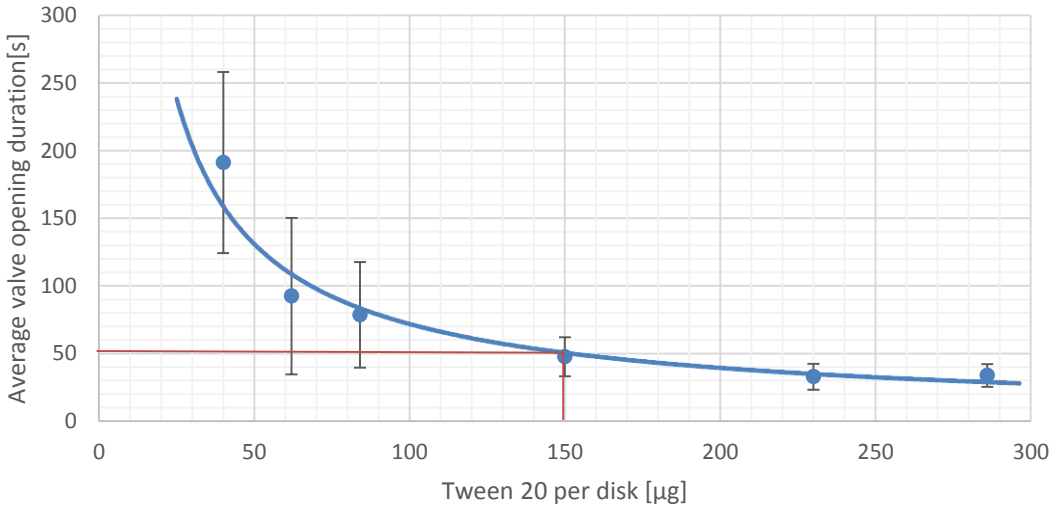

Figure 4.3: Average valve opening duration and standard deviation in dependence of the amount of surfactant per disk for at least 18 replicates. Rectangular indicates optimized amount.

A saturation point for the curve can be observed for approximately 220 µg surfactant per disk. At this point the cellulose material is probably oversaturated with the surfactant. A high deviation of the valve opening can decrease the reproducibility of the immunoassay due to different incubation times or fluid flow conditions. Thus, higher concentrations of surfactant can result in more consistent assay results. However, it was also found that concentrations that were too high in surfactant load

(close to the saturation point of the cellulose material; >170 µg per disks), could lead to diffusion of the surfactant. It should also be noted, that valves in chips assembled with such high concentrations of surfactant load failed after storage that lasted longer than three days. Due to this, approximately 150 µg of surfactant per disk can be considered as an optimal amount that will allow consistent valve opening, but also allows for extended storage.

4.2.4 Optimization of Trigger-channel Design

As discussed above, the biggest impact on the chip-yield, and therefore the assay reliability, is the probability of bad valves in a chip. Only one bad valve results in failure of the entire chip. Therefore, a decreasing chip yield with an increasing number of valves was found (cf. Figure 4.4, Design B & D). Because of this, the design of the trigger channel is crucial during development.

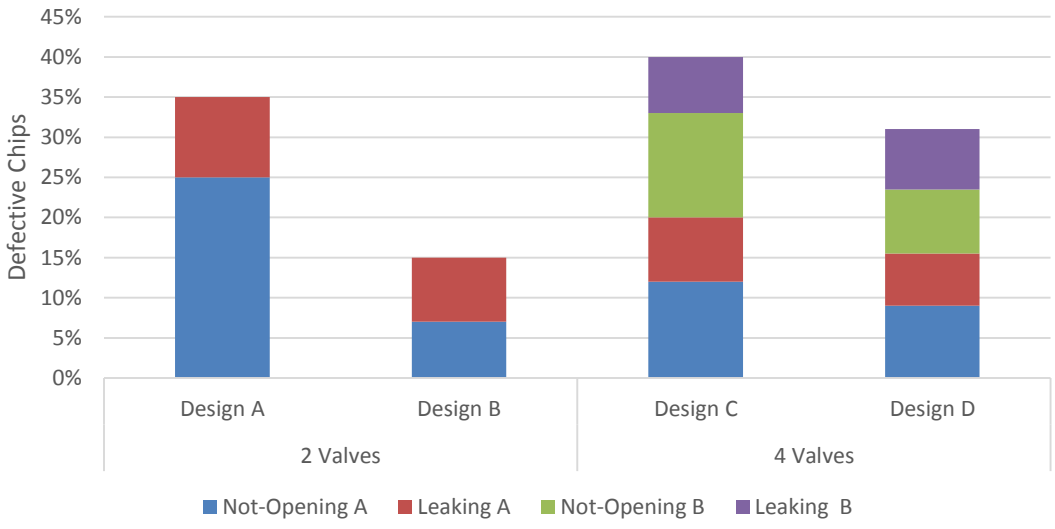

Figure 4.4: Chip yield for different trigger channel designs. Chips were fabricated with the manual method and at least 18 replicates were observed.

During development of the two valve fluidic circuit, it was found that the probability of a valve to open properly increases when the valve is located in a dead end of the trigger channel. This is likely due to the fact that a minimum volume of fluid is needed to open the valve and that the valve itself has a higher fluid flow resistance than the flow channel. If the valve is placed in the middle of a flow channel the fluid will more likely flow through the channel then into the valve and the valve will not open. A similar effect was observed by comparing valve failure of the four fluid designs (cf. Figure 4.4, Design C & D): valves that are placed in a dead end close to the flow will be more likely to fail than valves that are placed in a separate channel.

4.3 Determination of Chip Geometry and Materials

The required trigger channel length has been determined to allow for the correct valve timing and to reduce waste. In order to improve the fabrication time, the optimal chip geometries were determined. Finally the developed fluidic circuit was tested with water containing food coloring.

4.3.1 Trigger Channel Length

To calculate the trigger channel length assuming paper-wet out (see section 2.6.1) the effective pore diameter of the used material has to be known. The effective pore diameter for the materials used in the device are presented in Table 4.3. They were derived by the conducted flow experiments and calculated according to section 2.6.

Table 4.3: Retention capacity and effective pore size for selected materials

Material	Retention capacity [ml/m^2]	Effective pore size [10^{-7}m]
Filter paper	110	3.2
Glass fiber	280	8.3
Blotting paper	630	6.6

The observed times for fluid wicking are 120 s for the sample and 180 s for the wash. The deviation of the valve opening complicates the calculation of the trigger channel length. Due to these circumstances and the fact that a specific amount of fluid is needed to completely open the valve, the trigger channel has to be designed to be shorter than calculated for the best-case scenario. Otherwise a valve may need too long to open and the fluid is completely wicked into the main channel and the valve does not open at all, resulting in chip failure. Due to this, the average valve opening duration (50 s) was subtracted from the observed timings for reliable valve opening. Including these parameters in the calculation, the trigger channel length to the first valve should be 20 mm to the first valve and 27.5 mm to the second valve.

Values gained from this method are a good basis for determining the trigger channel length but it was found, that additional experiments with fully assembled chips are needed to optimize those parameters. This is due to the fact that the trigger channel design used for the experiments diverges at some point and the Washburn equation is limited for use in constant cross-sections, making it impossible to apply this model in accurately determining the trigger channel length. Therefore the channel length estimated with the experiments were slightly shorter than the calculated length.

The final results for the channel length to the first valve is 20.5 mm and 30 mm for the second valve (Figure 4.6) which still matches very well with the calculated lengths.

4.3.2 Chip Geometry and Absorption Area

In order to reduce waste of materials the height of the chip was fitted to the width of the double-sided tape (35 mm) and the width of the chips was optimized to fit as many chips as possible to one sheet of filter paper (8x10 in). The batch size was included in the consideration of the chip geometry in order to reduce fabrication time. It was found that one layer for a batch of 6 chips (2x3) with the geometry shown below (Figure 4.5) could be fabricated 8 times with one sheet on filter paper producing as little waste as possible.

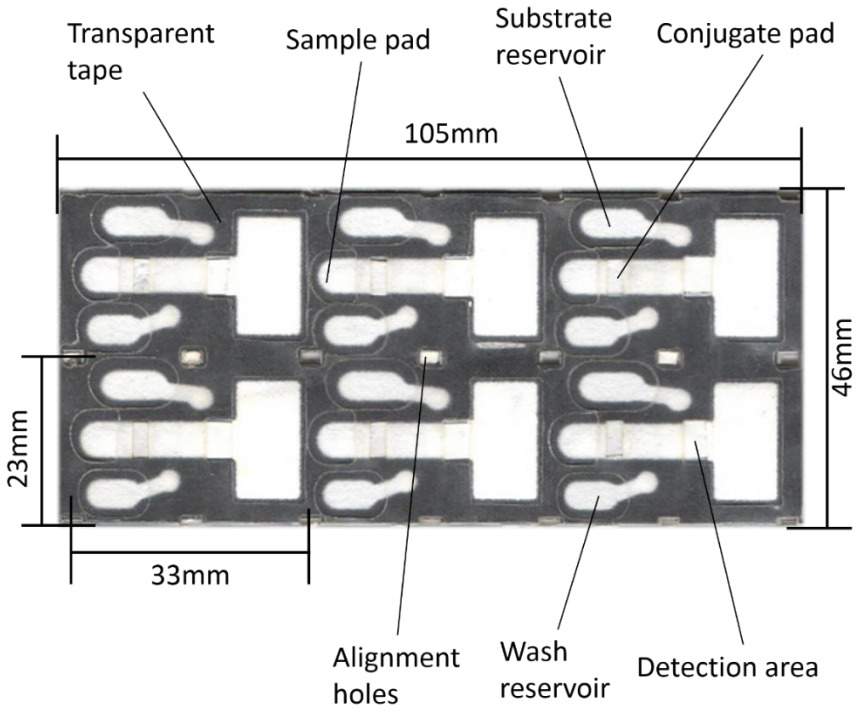

Figure 4.5: Description and geometries for a batch of 6 chips after fabrication

Since the maximum chip height was determined by the width of the double sided tape the unused space not taken up by the chip was used for the absorption area. The tape between the various flow layers was cut out in the same geometry as the waste pad and filled with cellulose material to increase the waste pad area. In order to keep a constant fluid flow, fluid congestion at the waste pad has to be avoided. Therefore rapid absorption from the main channel is essential and glass fiber was chosen as material to fill up the gaps in the tape due to of the largest available pore size, which results in the fastest absorption rate (Table 4.3).

Four layers of glass fiber are used to fill the gaps in the tape this results in a total area of 646 mm^2. The area of the filter paper for the chip, including the main channel, trigger channel, and the inlets is about 610 mm^2. For both materials together the retention volume for the chip can be approximated to 245 µl.

Since this retention volume is not enough to hold the volume of 310 µl used during the test, the waste pad is increased by a blotting paper underneath the chip (total area of 760 mm^2). This has two advantages, firstly the blotting paper provides for stability of the chips and secondly blotting paper offers particularly high retention volumes (see Table 4.3). The blotting paper increases the retention volume for the entire chip to 725 µl (+196%), allowing the sample to be captured and also preventing backflow of fluid into the main channel.

4.3.3 Geometry and Proof of Concept

The pictures taken during a test with water colored with food coloring after 5, 300, 310 and 600 seconds (Figure 4.6) show the functionality of the sequential loading circuit and the calculated parameters for the trigger channel and waste pad. The first picture (5 s) shows the circuit with the three filled inlets: sample (clear), wash (orange) and substrate (green). The second picture after 300 s shows that the first two valves have opened and that the wash has wicked into the absorption area without opening the third inlet prematurely. The picture taken 10 s later (at 310 s), shows that the third inlet has opened and that the substrate started to wick into the waste area. To consume all the fluids it takes about 600s.

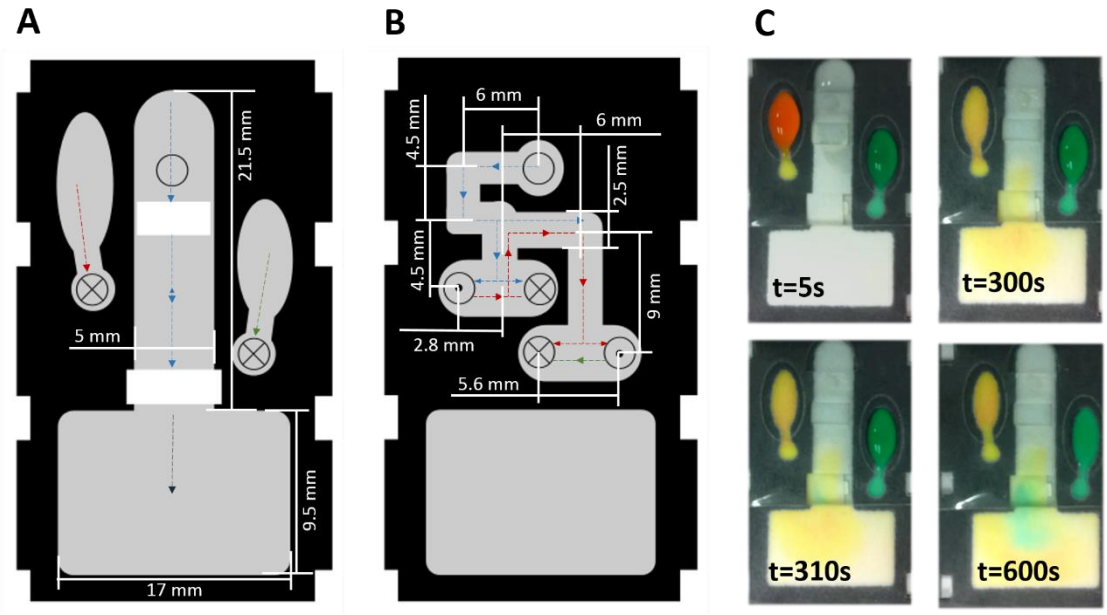

Figure 4.6: Results of the development process. A) Main channel geometries B) Trigger channel geometries C) Proof of concept with food coloring

4.4 Optimization of Assay Parameters

This section presents the results of the assay development and optimization process. The overall goal was to achieve a particularly low limit of detection. Therefore the conjugate release, the detection antibody concentration, and the kind of capture antibody have been improved.

4.4.1 Optimization of Conjugate Release

Influence of sample pad blocking to conjugate release

Blocking the conjugate pads prior to adding the detection antibody solution decreases the amount of fluid needed to wash out the conjugate. As can be seen from Figure 4.7 the amount of fluid needed to wash out the conjugate from the blocked pad is about 130 µl whereas 230 µl are still not enough to release the conjugate from the unblocked pad.

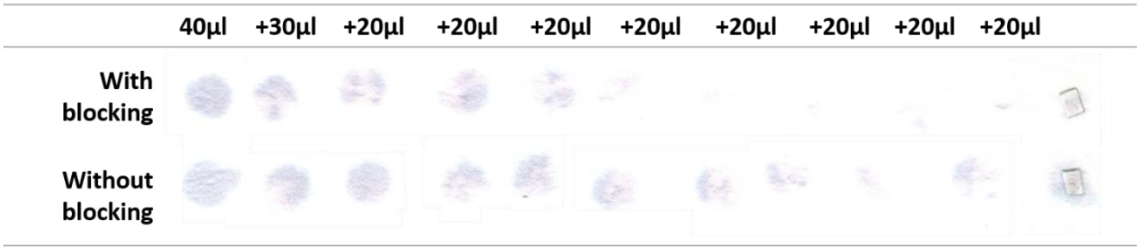

Figure 4.7: Comparison of conjugate release for non-blocked glass fiber pads to blocked glass fiber pads

This may be due to less non-specific interaction between the cellulose fibers and the antibodies for the blocked pad in comparison to the unblocked pad take place.

Conjugate Pad Size

The results (Figure 4.8) for conjugate pads with different sizes show that antibodies can be released more easily from smaller conjugate pads. It can be also seen, that 130 µl of fluid are needed to wash out the smaller conjugate pads and that about 80-100 µl of extra fluid is needed to wash out the larger ones.

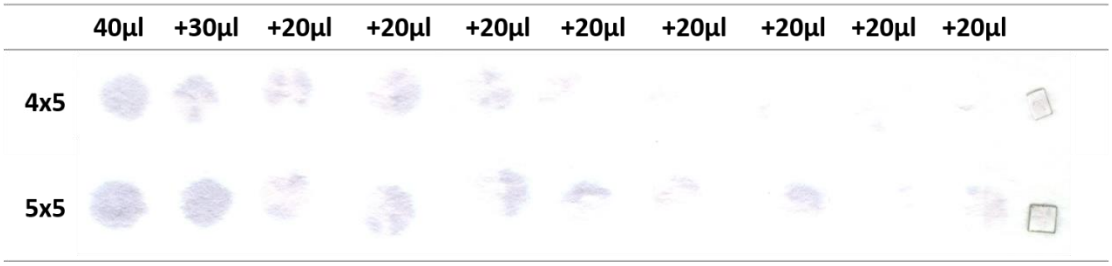

Figure 4.8: Comparison of conjugate release for 4x5 mm glass fiber pads to 5x5 mm glass fiber pads

This is probably due to non-specific interactions between the cellulose fibers and the antibodies. In larger conjugate pads more surface area is available for the same amount of antibodies resulting in a higher probability of non-specific interactions causing more antibodies to stick to the fibers. But it should be noted that it is not possible to reduce the size of the conjugate pad too much, as smaller conjugate pads are more difficult to handle and align and the contact to other materials can be problematic. An insufficient contact between the channel and the conjugate pad can result in a slow fluid flow or prevent the conjugate release. Because of this, 4x5 mm conjugate pads were assumed to be optimal for the developed test.

Conjugate Material

The comparison of glass fiber material with and without binder (Figure 4.9) for the conjugate pad indicates that the choice of material has an important impact on the conjugate release characteristics. From the evaluated materials it can be seen, that glass fiber with binders offers better release properties than without. For the conjugate pads containing glass fiber with binders the release is constantly higher than for the ones without binder, resulting in a faster release (approximately after 130 µl of fluid) of the entire amount of antibodies.

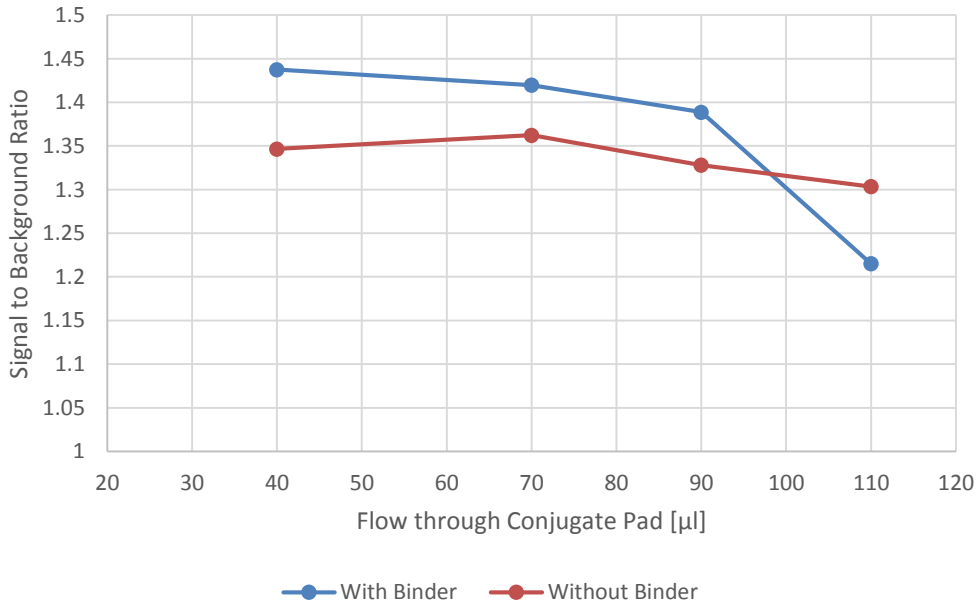

Figure 4.9: Comparison of conjugate release for glass fiber with and without binder

4.4.2 Polyclonal vs. Monoclonal Antibodies

The use of polyclonal antibodies for the detection zone and the conjugate pad lead to higher signal intensities for lower analyte concentrations than the monoclonal antibodies (cf. Figure 4.10, 10 ng/ml & 1 µg/ml). But the usage of polyclonal antibodies led to false positive results of the negative control (cf. Figure 4.10, NC). This could be due to non-specific interactions of the polyclonal antibodies which each other. To avoid non-specific interactions, monoclonal antibodies were used for preparation of the capture zone and the conjugate pad for further experiments.

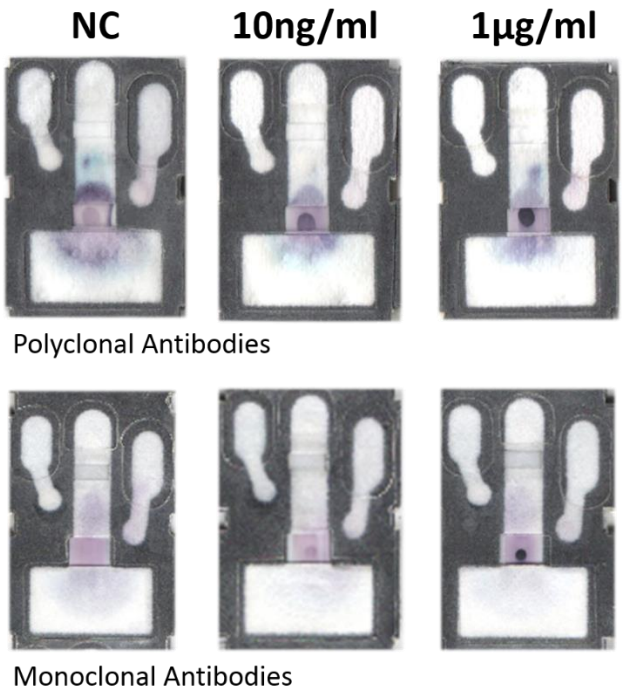

Figure 4.10: Comparison of signal intensities for monoclonal and polyclonal capture antibodies

4.4.3 Optimization of Detection Antibody Amount

It was found that the amount of detection antibody in the conjugate pad has an important impact to the signal quality and therefore also determines the limit of detection. As can be seen from Figure 4.11, 320 ng is the optimal amount of detection antibody per conjugate pad in order to get the best possible signal to noise ratio. Too little of an amount of detection antibody leads to decreasing signal quality because of decreasing probability of antibody - antigen binding reactions and therefore decreasing signal intensity. Too high amounts of detection antibodies lead to higher background signals without contributing to the actual signal intensity.

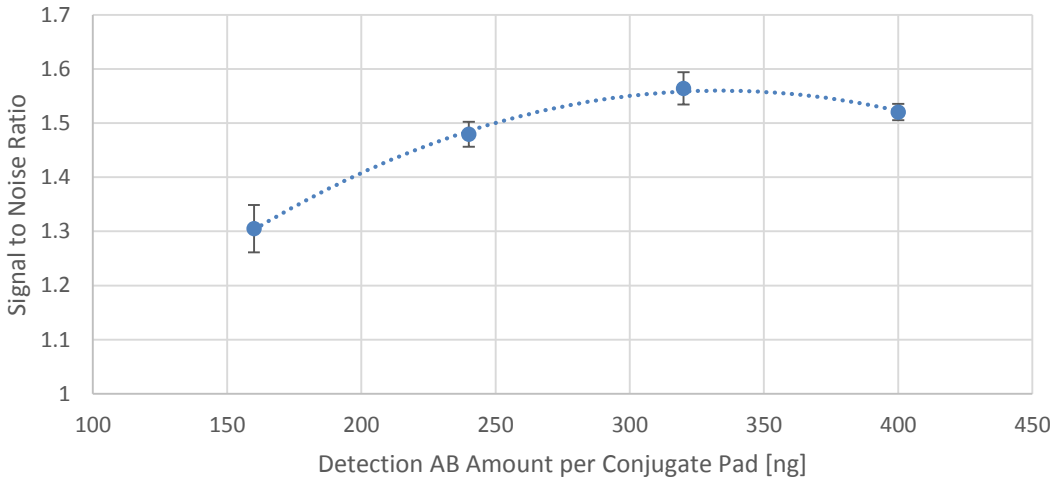

Figure 4.11: Signal quality in dependence of detection antibody amount per conjugate pad

4.4.4 Assay Results and Dose Response

The results for the response of the developed immunoassay to different analyte concentrations are shown below:

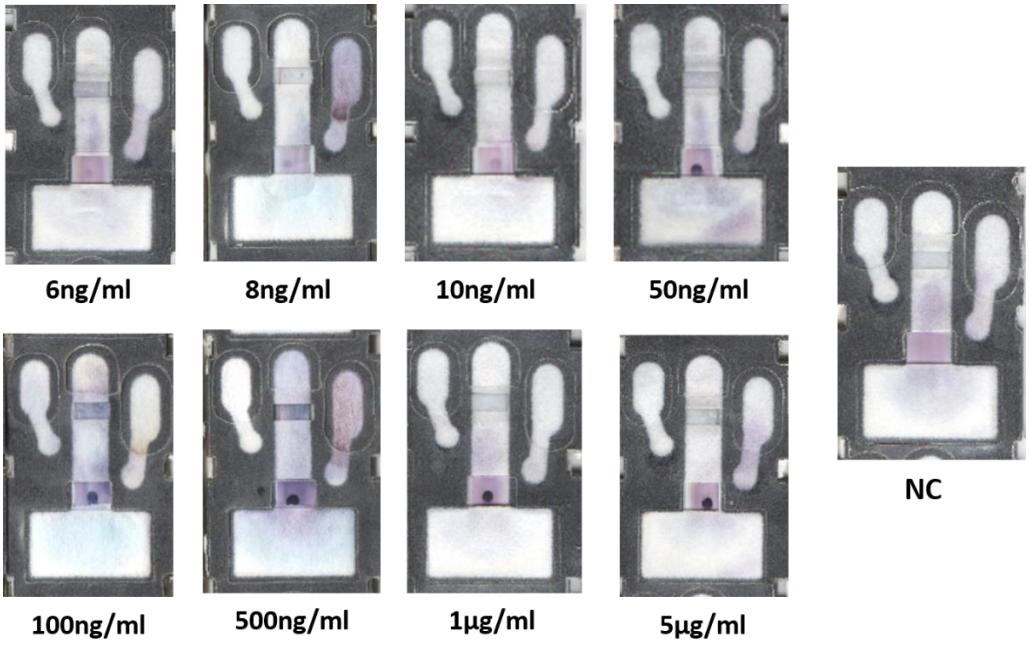

Figure 4.12: Assay response to different analyte concentrations

The lowest analyte concentration that that could still be discerned from human observation was reached with 6 ng/ml. The next lower concentration that was carried out was 2.5 ng/ml and no visible signal was achieved. It can be seen that the mean intensity of the background varies. This is due to the fact that the fluid flow is not uncompromisingly even, especially for the last fluid, the substrate. Since the substrate contributes in equal proportions to the signal and the background intensity, it is possible to smooth the results by calculating out the background signal. This was done by computing the signal to background intensity ratio.

By plotting the signal to noise ratio, a curve was generated (Figure 4.13) that could be fitted with good accuracy using the Weibull equation, a common sigmoid function in biochemistry for dose response curves:

$$y = a - be^{-cx^d} \tag{4.1}$$

where the parameters for this curve iteratively calculate to a=2.55, b=1.54, c=3.25x10^6 and d=0.98. The linear range can be estimated between the response to 100 ng and 1 µg. None of the negative controls showed a false-positive signal therefore the negative control is not shown in the graph.

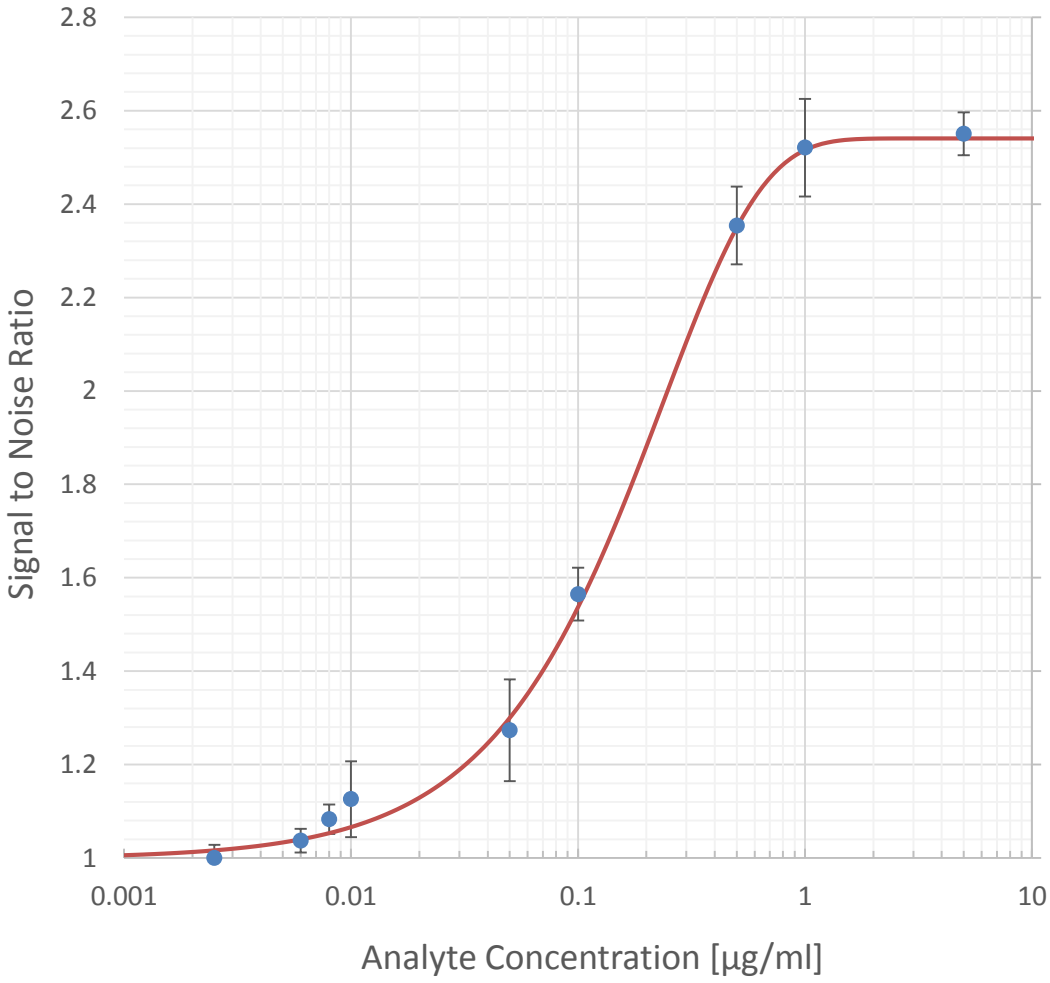

Figure 4.13: Dose response for different analyte concentrations and three replicates fitted with the Weibull equation

With the approach presented in section 2.1.4, which uses the standard deviation of the blank (3%) the LOD is estimated to 5.5 ng, which match very well with the signal that can still be discerned from human observation. Using the same approach the limit of quantification is estimated to be 21 ng. Since Rabbit IgG has a molecular weight about 150 kda [39] and 130 µl of sample were used for the assay, the detection limit can be converted to a molarity about 4.8 fm.

CHAPTER 5 – CONCLUSION AND FUTURE WORK

The research demonstrated that automatic sequential loading of multiple fluids to a detection area with enhanced lateral flow test devices was achieved. Using enzyme-linked immunosorbent assay (ELISA) and Rabbit IgG as model analyte it was proved, that complex diagnostic procedures can be proceeded autonomously in lateral flow. A prototype of a low cost, time efficient and easy-to-operate point-of-care device based on the developed test was achieved by storing the necessary reagents and the device into a housing.

First, different designs and fabrication methods for paper based devices with fluidic valves were developed and their influence to the valve performance explored. Fabrication processes, reagent concentrations, materials and device geometries were optimized and the valve opening deviation was reduced to 10 s. Also a Chip-Yield of 92% for devices with four valves was achieved.

Second, the developed methods were used to incorporate a three step ALP-based enzyme-linked immunosorbent assay procedure with Rabitt IgG as model analyte into a lateral flow test. Four fluidic valves were used to control the sequential loading of sample, wash and substrate to the detection area. The feasibility was verified by visual detection of signal development on nitrocellulose membrane after reaction of ALP with NBT/BCIP. Immunoassay parameters were optimized including conjugate release, amount of reagents, detection and capture antibodies.

Through optimization a proof-of-concept device with a good limit of detection at 4.8 fm was achieved. The results may not show as promising as expected since the sensitivity is still limited in the range of common gold-nanoparticle based lateral flow test devices (see section 2.2). But compared to other available methods based on ELISA for example microtiterplates which can reach down to 4 fm [58], this system offers resemblance in the detection limit with simplified operation.

5.1 Recommendations for Future Work

This section is used to propose several ideas to further improve the developed system such as signal enhancement, signal amplification multiplexing, fabrication methods or electrochemical detection.

5.1.1 Signal Enhancement

As first step the signal development due to background noise, signal deviation and non-specific binding should be addressed. Further research should be performed for different materials, blocking reagents and blocking duration. One promising material that should be investigated is Fusion 5^{TM} produced by Whatman [56] the material, based on a single layer matrix technology, was developed to perform all the functions of a lateral flow strip on a single substrate. The manufacturer advertises that this material has outstanding non-specific binding properties resulting in conjugate release of >94%. Therefore this material could be used to replace the conjugate pad and the

flow channels to attempt lower background noise and the loss of analyte and antibodies in the conjugate pad or channels due to nonspecific binding. According to Whatman their materials also acts as a membrane for striping antibodies as test and control lines. The antibodies have to be conjugated to latex beads, in order to allow binding of the antibodies to the membrane. With this method the upper layer of the developed multifluid lateral flow test could be completely fabricated from one material reducing fabrication time and fluid flow deviation due to insufficient alignment.

5.1.2 Signal Amplification

To improve the sensitivity and to lower the limit of detection gold nanoparticles (GNP) could be used to amplify signal development. In the current Immunoassay structure the signal development is limited by the restraint to label only one alkaline phosphatase (ALP) enzyme to the detection antibody (Figure 5.1, A). Several researchers are working on amplified systems for ELISA based immunoassays. For example Munge et. al. [36] are using massively labeled superparamagnetic particles to improve the sensitivity for their detection system based on Horseradish peroxidase (HRP)-electrochemical ELISA. A similar setup to their detection system could be used to improve the developed ELISA based optical immunosensor. Commonly used nanometer sized gold particles could be labeled to the detection antibody and several ALP-enzymes could be conjugated to the particle using the biotin-(strept)avidin system. (Figure 5.1, B) Such a structure would have three advantages: it would keep the benefits of common lateral flow tests with gold nanoparticles and signals for higher

analyte concentration could be seen immediately without the need of an substrate; it would keep the advantage of the cascading character of the enzymatic reaction; and in addition it would amplify the signal through a greater amount of ALP-enzymes in the detection zone.

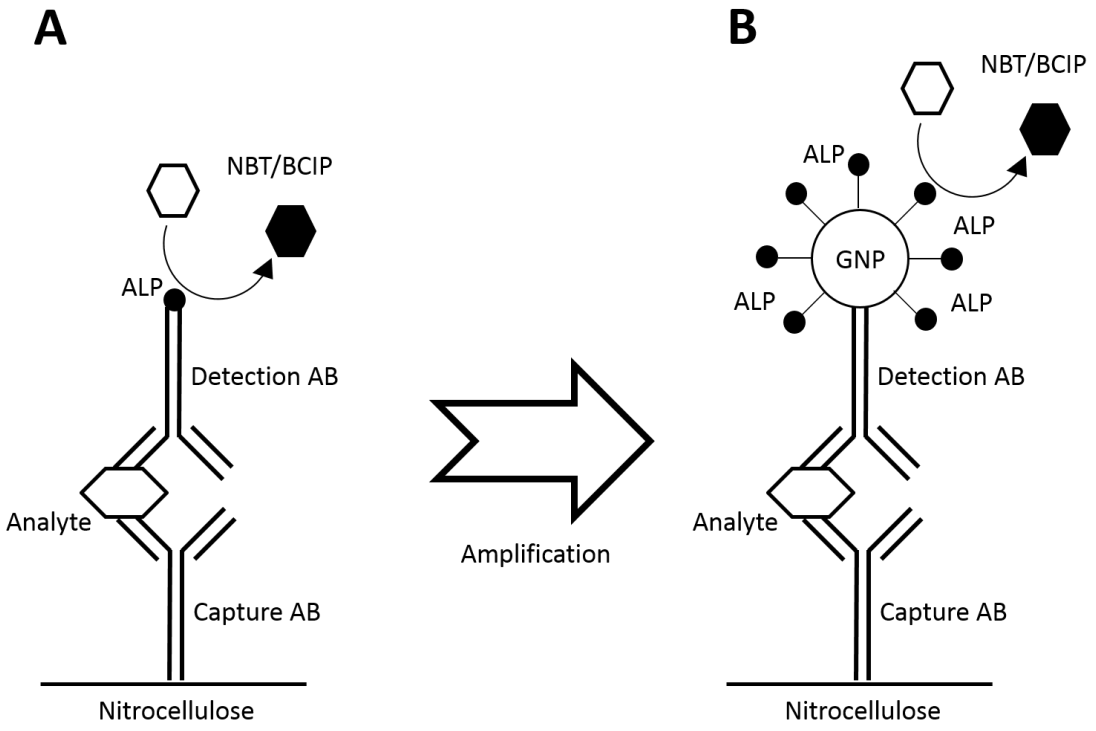

Figure 5.1: Signal amplification using gold nanoparticles to incorporate several ALP enzymes

5.1.3 Multiplexing

Martinez et. al. [32] reported, that 3D Paper based analytical devices, such as the one developed during this study, are perfect platforms for simple integration of multiplexing. Multiplexing for diagnostic devices encounters increasing interest in the literature since those devices can be used to detect multiple analytes simultaneously

in one sample or generate calibration curves for the assays with one test [32]. Integrating multiplexing into the developed platform can easily be done by expending the device with additional layers on-top of the current layers to distribute the reagents. Figure 5.2 presents an example for a possible solution to integrate multiplexing. Since this approach will increase the test area concepts for minimization have to be developed.

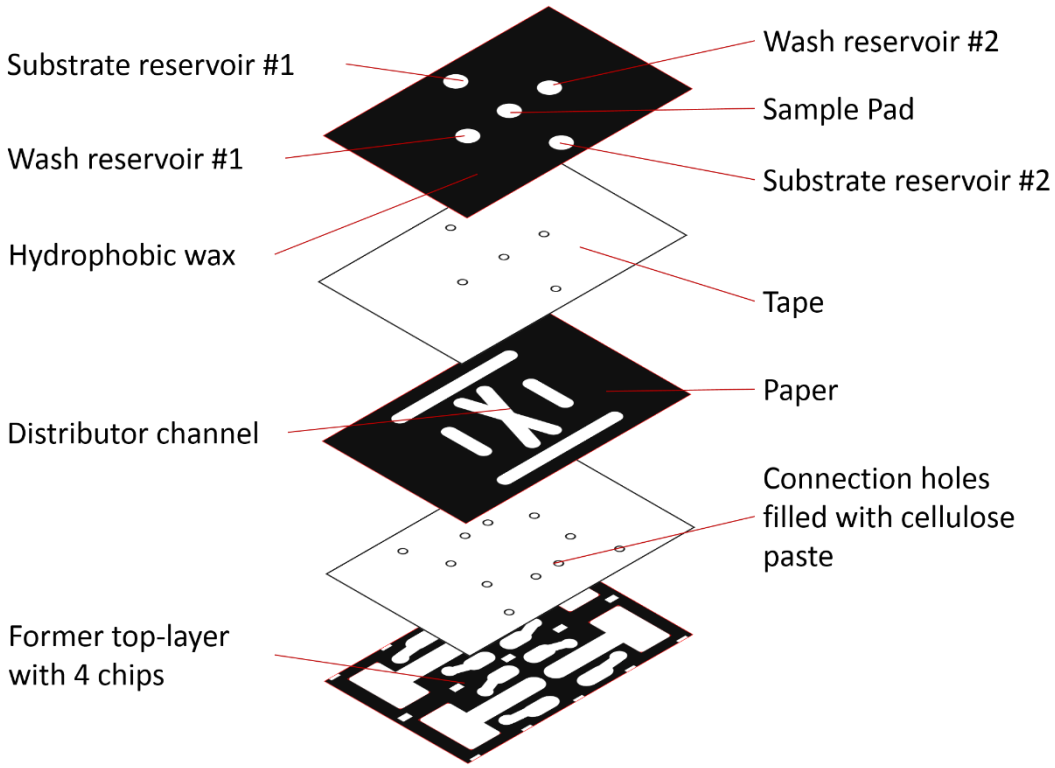

Figure 5.2: Proposed system to integrate multiplexing into the developed lateral flow test device

5.1.4 Origami Fabrication Method

Although the fabrication for paper based devices with fluidic valves was optimized and simplified during this study it still takes hours to fabricate a huge amount of prototypes. Liu et. al. [27] developed a method for fabrication of paper based analytical devices which they call origami approach and which does not require double-sided tape to hold the various layers together. They fabricate their devices on only one layer of paper, fold it and laminate it in order to obtain a 3D fluidic device (see section 2.4.1). This fabrication method could be adapted for paper based devices with fluidic valves. Disk layers for the valves could be fabricated with the approach presented in section 3.2.2 with the distinction that the disks are not cut out anymore. With this method fabrication could be limited to four layers of paper for channels and disks leading to further optimization of the fabrication time and decrease of the probability of alignment defects.

5.1.5 Electrochemical Detection

By printing electrodes on paper electrochemical detection could be integrated to enable quantification in a simple to operate paper based analytical device. For fabrication of the electrodes screen-printing with conductive carbon ink as reported by Liu et. al. [28] Dr. Constantine Anagnostopouloscould be used. The paper substrate should be nitrocellulose because of the superior biding properties compared to other materials [34]. This also would have the advantage that the developed lateral flow test

does not has to be modified to integrate the electrodes since the test is already optimized for nitrocellulose membrane in the detection area. Therefore the electrodes should have a design similar to the one presented in Figure 5.3. The geometry is chosen in that way to simply replace the standard membrane of the test with the one printed with a common electrode for immunoassay applications. The electrode and the wiring is screen printed on the same substrate to have a simple as possible fabrication process. Areas in which fluid flow has to be prevented are covered with hydrophobic wax.

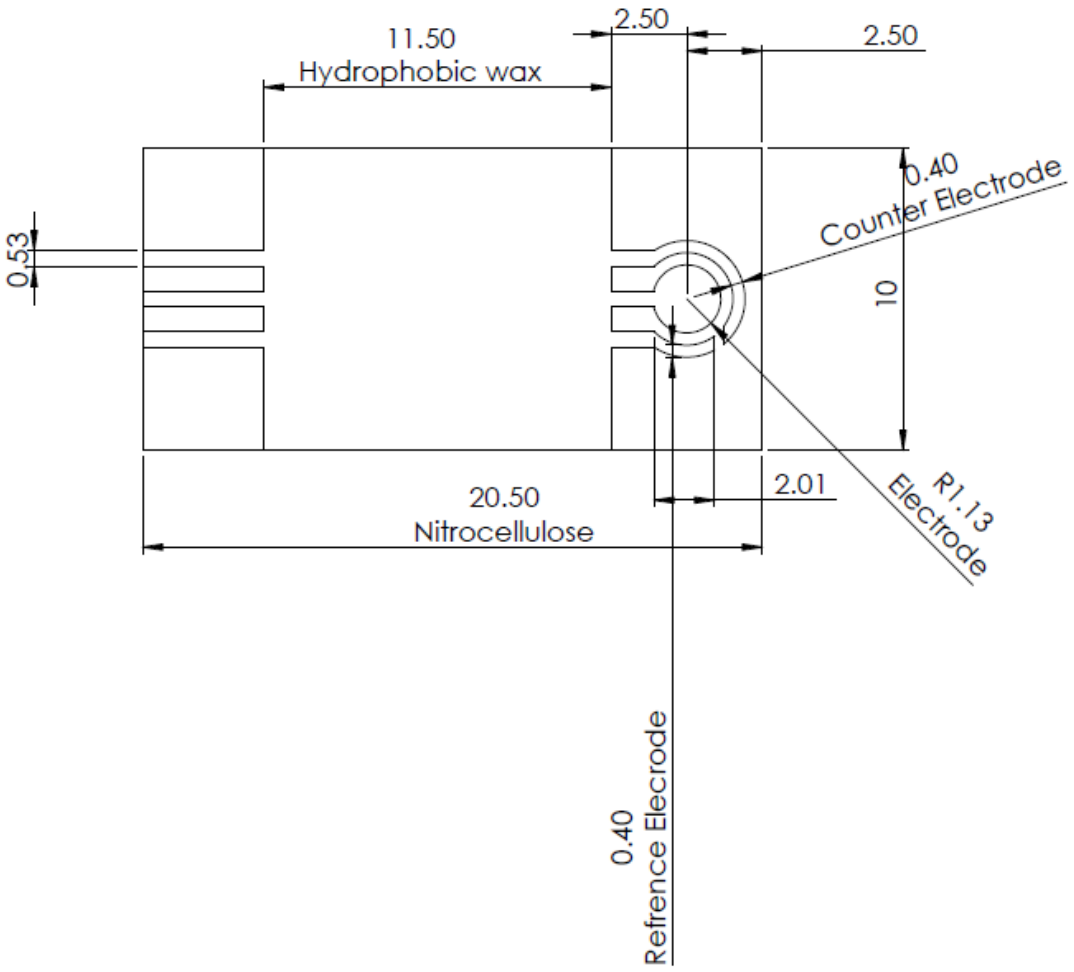

Figure 5.3: Proposed geometries [mm] for electrodes printed on nitrocellulose. Hydrophobic wax is used to prevent fluid flow to wiring area

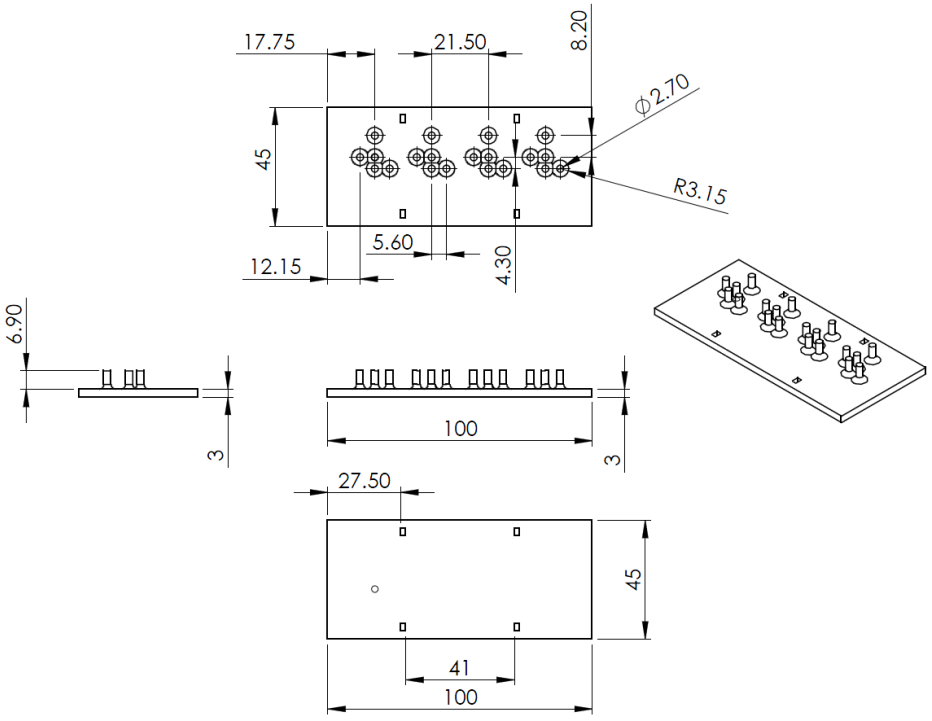

Figure A.1: Dimensions [mm] for fabrication tooling (Punch-out unit)

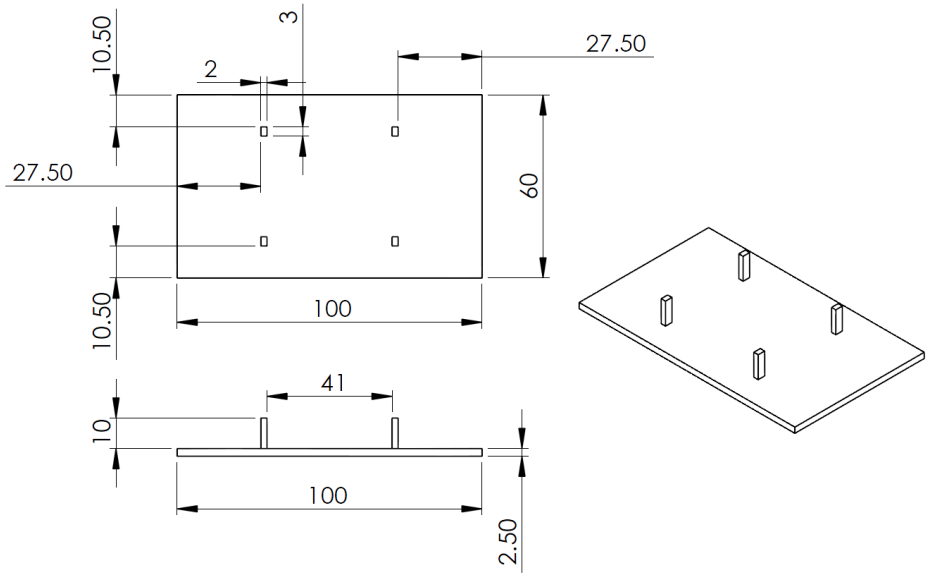

Figure A.2: Dimensions [mm] for fabrication tooling (Base-alignment unit)

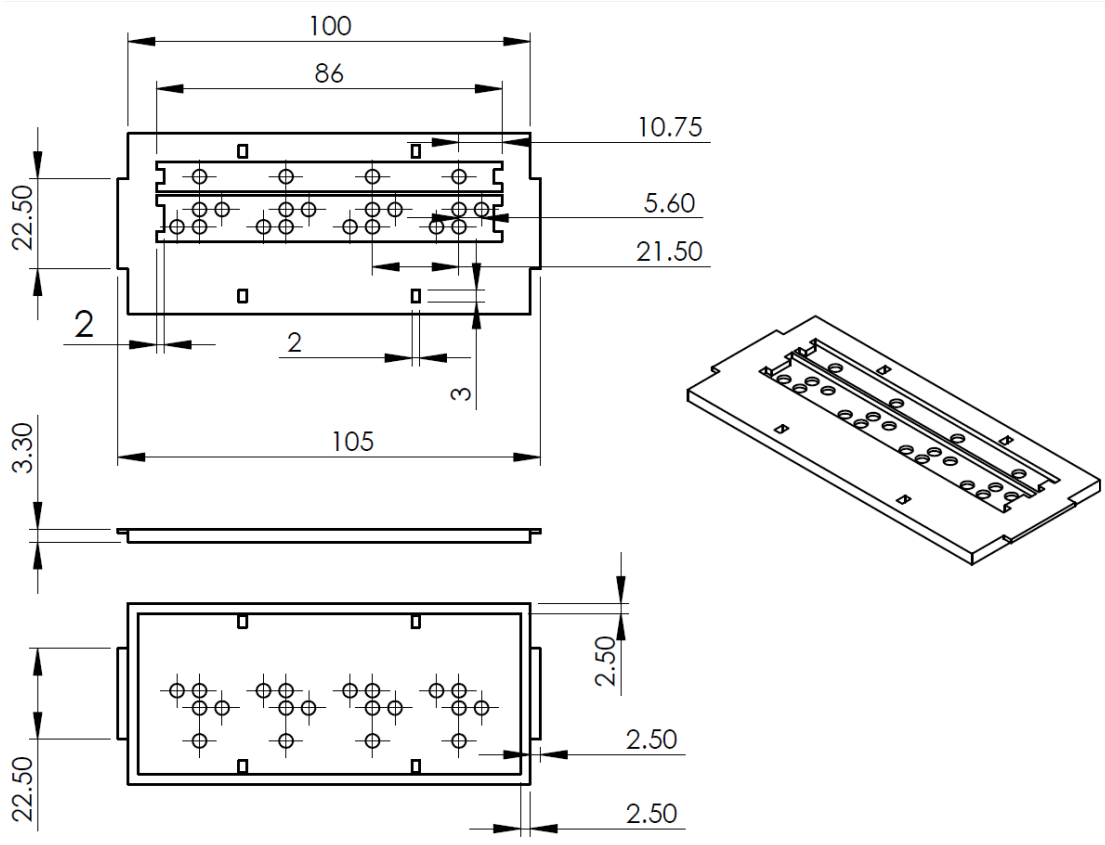

Figure A.3: Dimensions [mm] for fabrication tooling (Support-alignment unit)

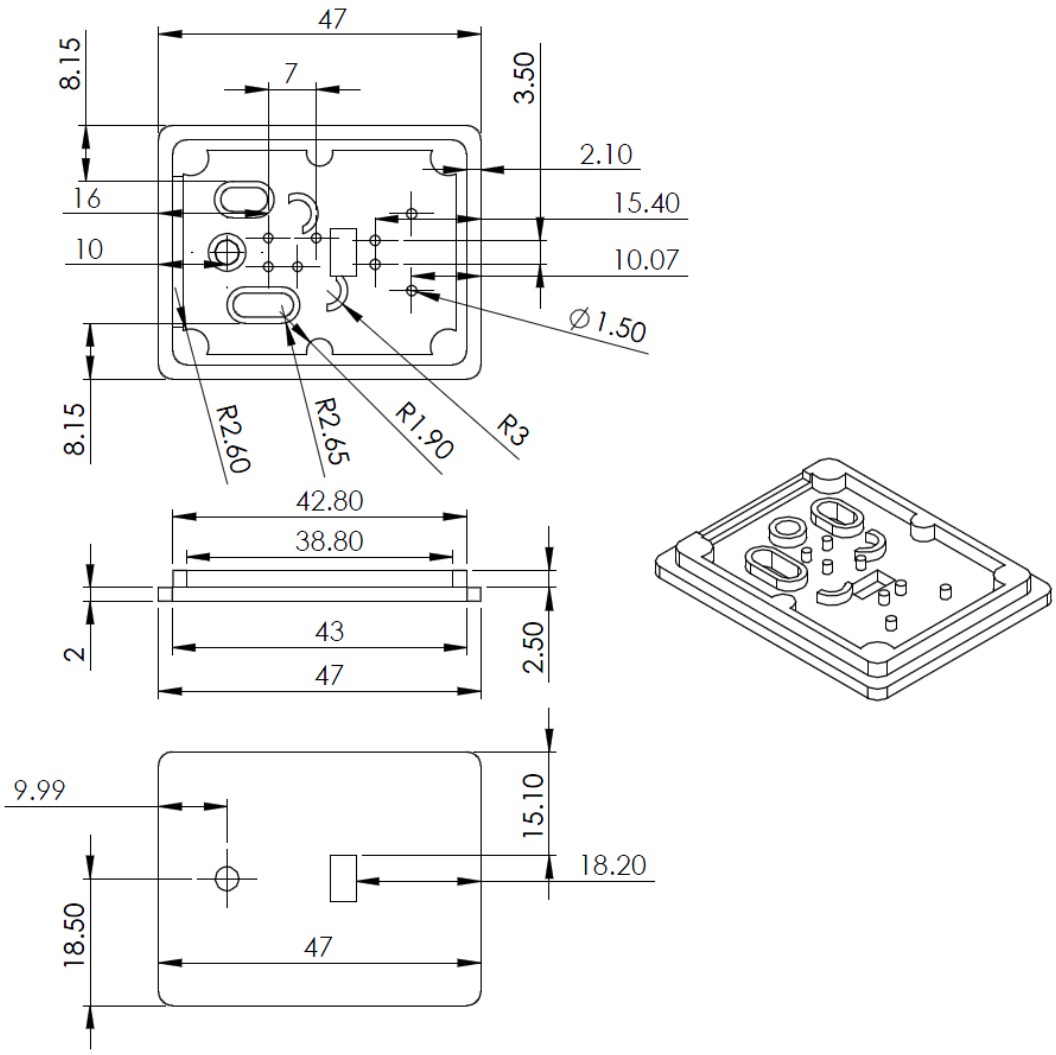

Figure A.4: Dimensions [mm] for housing (Top with reagent storing)

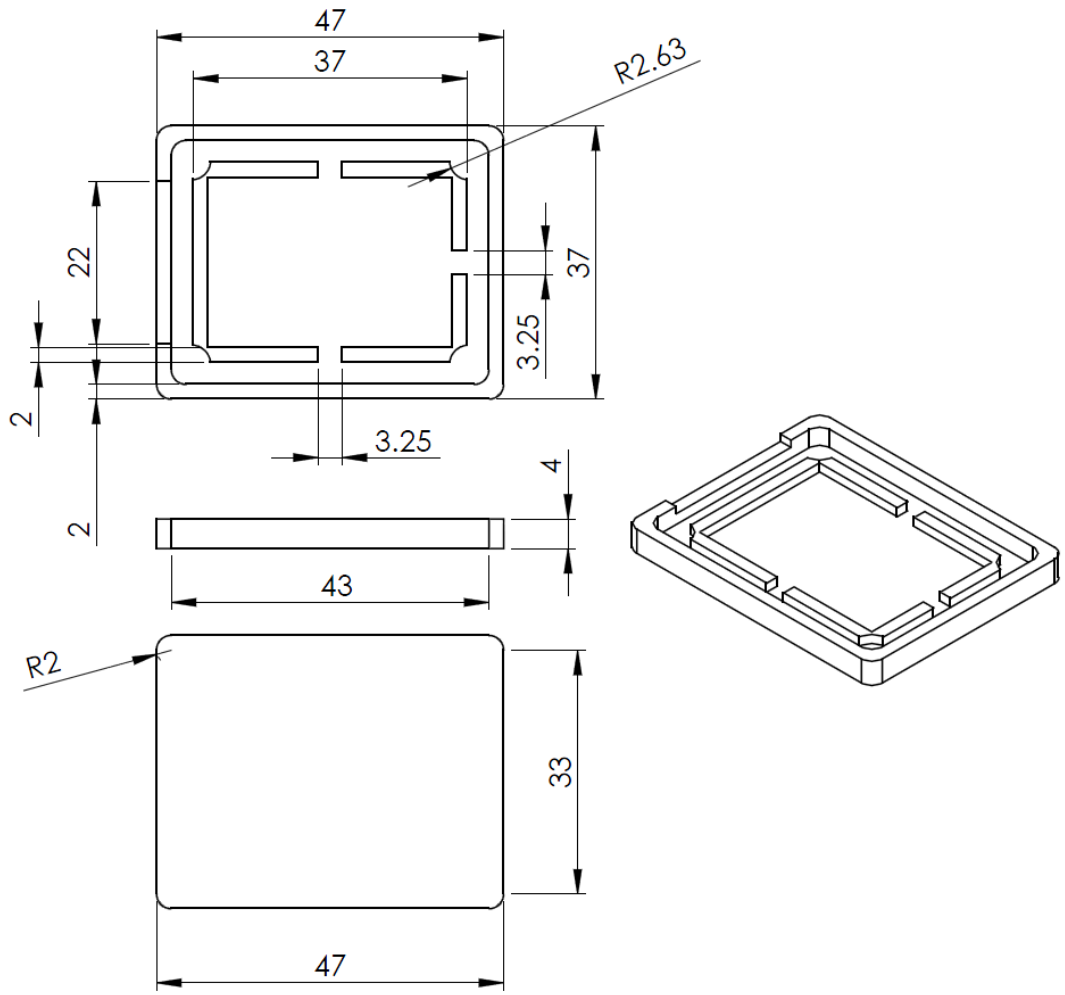

Figure A.5: Dimensions [mm] for housing (Bottom)

BIBLIOGRAPHY

[1] Ahn-Yoon, S., DeCory, T. R., Baeumner, A. J., and Durst, R. A. 2003. Ganglioside-Liposome Immunoassay for the Ultrasensitive Detection of Cholera Toxin. *Anal. Chem.* 75, 10, 2256–2261.

[2] Bonenberger, J. and Doumanas, M. 2006. Overcoming sensitivity limitations of lateral- flow with a novel labeling technique. *IVD Technology,* 5, 41–46.

[3] Chen, H., Cogswell, J., Anagnostopoulos, C., and Faghri, M. 2012. A fluidic diode, valves, and a sequential-loading circuit fabricated on layered paper. *Lab Chip* 12, 16, 2909–2913.

[4] Chen, X., Chen, J., Wang, F., Xiang, X., Luo, M., Ji, X., and He, Z. 2012. Determination of glucose and uric acid with bienzyme colorimetry on microfluidic paper-based analysis devices. *Biosensors and Bioelectronics* 35, 1, 363–368.

[5] Cheng, C.-M., Martinez, A. W., Gong, J., Mace, C. R., Phillips, S. T., Carrilho, E., Mirica, K. A., and Whitesides, G. M. 2010. Paper-Based ELISA. *Angewandte Chemie International Edition* 49, 28, 4771–4774.

[6] Cole, S. P. C., Campling, B. G., Atlaw, T., Kozbor, D., and Roder, J. C. 1984. Human monoclonal antibodies. *Mol Cell Biochem* 62, 2.

[7] Darcy, H. 1856. *Les fontaines publiques de la ville de Dijon*, Paris.

[8] Diamandis, E. P. 1990. Analytical methodology for immunoassays and DNA hybridization assays — current status and selected systems — critical review. *Clinica Chimica Acta* 194, 1, 19–50.

[9] Fernández-Sánchez, C., McNeil, C. J., Rawson, K., Nilsson, O., Leung, H. Y., and Gnanapragasam, V. 2005. One-step immunostrip test for the simultaneous detection of free and total prostate specific antigen in serum. *Journal of Immunological Methods* 307, 1-2, 1–12.

[10] Föllscher, W. 2013. *Development of a Platform for Lateral Flow Test Devices with the Capability of using Multiple Fluids*.

[11] Frost & Sullivan. 2009. *US point-of-care testing markets*.

[12] Fu, E., Ramsey, S. A., Kauffman, P., Lutz, B., and Yager, P. 2011. Transport in two-dimensional paper networks. *Microfluid Nanofluid* 10, 1, 29–35.

[13] Goldsby, R. A., Kindt, T. J., Osborne, B. A., and Kuby, J. 2003. *Immunology - Antigens (Chapter 3)*. W.H. Freeman, New York.

[14] Greg T. Hermanson. 1996. *Bioconjugate Techniques*.

[15] Hong Chen, Constantine Anagnostopoulos, Mohammad Faghri, Alex Pytka, Manuel Muller, Wilke Foellscher, Roman Gerbers, Jeremy Cogswell, Mike Franzblau. 2013. *Microfluidics with Application to Point-of-Care Diagnostics*.

[16] Horváth, I. T., Ed. 2012. *Fluorous Chemistry*. Topics in Current Chemistry. Springer Berlin Heidelberg, Berlin, Heidelberg.

[17] Hossain, S. M. Z., Luckham, R. E., Smith, A. M., Lebert, J. M., Davies, L. M., Pelton, R. H., Filipe, C. D. M., and Brennan, J. D. 2009. Development of a Bioactive Paper Sensor for Detection of Neurotoxins Using Piezoelectric Inkjet Printing of Sol−Gel-Derived Bioinks. *Anal. Chem.* 81, 13, 5474–5483.

[18] Hossain, S. M. Z., Ozimok, C., Sicard, C., Aguirre, S. D., Ali, M. M., Li, Y., and Brennan, J. D. 2012. Multiplexed paper test strip for quantitative bacterial detection. *Anal Bioanal Chem* 403, 6, 1567–1576.

[19] Hu, C., Bai, X., Wang, Y., Jin, W., Zhang, X., and Hu, S. 2012. Inkjet Printing of Nanoporous Gold Electrode Arrays on Cellulose Membranes for High-Sensitive Paper-Like Electrochemical Oxygen Sensors Using Ionic Liquid Electrolytes. *Anal. Chem.* 84, 8, 3745–3750.

[20] Janeway, C. op. 2001. *Immunobiology*. *The immune system in health and disease*. Garland, New York [etc.].

[21] Janin, J. and Chothia, C. 1990. The structure of protein-protein recognition sites. *J. Biol. Chem.* 265, 27, 16027–16030.

[22] Jokerst, J. C., Emory, J. M., and Henry, C. S. 2011. Advances in microfluidics for environmental analysis. *Analyst* 137, 1, 24.

[23] Kasahara, Y. and Ashihara, Y. 1997. Simple devices and their possible application in clinical laboratory downsizing. *Clinica Chimica Acta* 267, 1, 87–102.

[24] Lankelma, J., Nie, Z., Carrilho, E., and Whitesides, G. M. 2012. Paper-Based Analytical Device for Electrochemical Flow-Injection Analysis of Glucose in Urine. *Anal. Chem.* 84, 9, 4147–4152.

[25] Lee, B. and Richards, F. M. 1971. The interpretation of protein structures: Estimation of static accessibility. *Journal of Molecular Biology* 55, 3, 379–IN4.

[26] Lisowski, P. and Zarzycki, P. K. 2013. Microfluidic Paper-Based Analytical Devices (μPADs) and Micro Total Analysis Systems (μTAS): Development, Applications and Future Trends. *Chromatographia*.

[27] Liu, H. and Crooks, R. M. 2011. Three-Dimensional Paper Microfluidic Devices Assembled Using the Principles of Origami. *J. Am. Chem. Soc.* 133, 44, 17564–17566.

[28] Liu, H., Xiang, Y., Lu, Y., and Crooks, R. M. 2012. Aptamer-Based Origami Paper Analytical Device for Electrochemical Detection of Adenosine. *Angew. Chem. Int. Ed.* 51, 28, 6925–6928.

[29] Lode, P. von. 2005. Point-of-care immunotesting: approaching the analytical performance of central laboratory methods. *Clin. Biochem.* 38, 7, 591–606.

[30] Lu, J., Ge, S., Ge, L., Yan, M., and Yu, J. 2012. Electrochemical DNA sensor based on three-dimensional folding paper device for specific and sensitive point-of-care testing. *Electrochimica Acta* 80, 334–341.

[31] Marie Dupuy, A., Lehmann, S., and Paul Cristol, J. 2005. Protein biochip systems for the clinical laboratory. *Clinical Chemical Laboratory Medicine* 43, 12.

[32] Martinez, A. W., Phillips, S. T., Nie, Z., Cheng, C.-M., Carrilho, E., Wiley, B. J., and Whitesides, G. M. 2010. Programmable diagnostic devices made from paper and tape. *Lab Chip* 10, 19, 2499.

[33] Martinez, A. W., Phillips, S. T., and Whitesides, G. M. 2008. Three-dimensional microfluidic devices fabricated in layered paper and tape. *Proceedings of the National Academy of Sciences* 105, 50, 19606–19611.

[34] Millipore. 2008. *Rapid Lateral Flow Test Strips Considerations for Product Development*.

[35] Muller, R. H. and Clegg, D. L. 1949. Automatic Paper Chromatography. *Anal. Chem.* 21, 9, 1123–1125.

[36] Munge, B. S., Coffey, A. L., Doucette, J. M., Somba, B. K., Malhotra, R., Patel, V., Gutkind, J. S., and Rusling, J. F. 2011. Nanostructured Immunosensor for Attomolar Detection of Cancer Biomarker Interleukin-8 Using Massively Labeled Superparamagnetic Particles. *Angew. Chem. Int. Ed.* 50, 34, 7915–7918.

[37] Nery, E. W. and Kubota, L. T. 2013. Sensing approaches on paper-based devices: a review. *Anal Bioanal Chem*.

[38] Noh, H. and Phillips, S. T. 2010. Fluidic Timers for Time-Dependent, Point-of-Care Assays on Paper. *Anal. Chem.* 82, 19, 8071–8078.

[39] Piovan, E., Tosello, V., Indraccolo, S., Cabrelle, A., Baesso, I., Trentin, L., Zamarchi, R., Tamamura, H., Fujii, N., Semenzato, G., Chieco-Bianchi, L., and Amadori, A. 2005. Chemokine receptor expression in EBV-associated lymphoproliferation in hu/SCID mice: implications for CXCL12/CXCR4 axis in lymphoma generation. *Blood* 105, 3, 931–939.

[40] Posthuma-Trumpie, G. A., Korf, J., and Amerongen, A. 2009. Lateral flow (immuno)assay: its strengths, weaknesses, opportunities and threats. A literature survey. *Anal Bioanal Chem* 393, 2, 569–582.

[41] Ramasamy, S. 1998. Oxygen sensor via the quenching of room-temperature phosphorescence of perdeuterated phenanthrene adsorbed on Whatman 1PS filter paper. *Talanta* 47, 4, 971–979.

[42] Rhoades, R. and Pflanzer, R. G. 2003. *Human physiology*. Thomson; Brooks/Cole, Australia, Pacific Grove, Calif.

[43] Sarfraz, J., Tobjork, D., Osterbacka, R., and Linden, M. 2012. Low-Cost Hydrogen Sulfide Gas Sensor on Paper Substrates: Fabrication and Demonstration. *IEEE Sensors J.* 12, 6, 1973–1978.

[44] Seydack, M. 2008. Immunoassays: Basic Concepts, Physical Chemistry and Validation. In *Standardization and Quality Assurance in Fluorescence Measurements II*, U. Resch-Genger, Ed. Springer Series on Fluorescence. Springer Berlin Heidelberg, Berlin, Heidelberg, 401–428.

[45] Shrivastava, A. and Gupta, V. 2011. Methods for the determination of limit of detection and limit of quantitation of the analytical methods. *Chron Young Sci* 2, 1, 21.

[46] Szűcs, J. and Gyurcsányi, R. E. 2012. Towards Protein Assays on Paper Platforms with Potentiometric Detection. *Electroanalysis* 24, 1, 146–152.

[47] The European Agency for the Evaluation of Medicinal Products. 1995. *ICH Topic Q 2 (R1) Validation of Analytical Procedures: Text and Methodology*.

[48] The Food and Drug Administration, Center for Drug Evaluation. 2001. *Guidance for Industry – Bioanalytical Method Validation*.

[49] Thom, N. K., Yeung, K., Pillion, M. B., and Phillips, S. T. 2012. “Fluidic batteries” as low-cost sources of power in paper-based microfluidic devices. *Lab Chip* 12, 10, 1768.

[50] Tijssen P. 1985. *Practice and theory of enzyme immunoassays*. Elsevier, New York.

[51] TriMark Publications, L. L. 2012. *Point of Care Diagnostic Testing World Markets*.

[52] Vella, S. J., Beattie, P., Cademartiri, R., Laromaine, A., Martinez, A. W., Phillips, S. T., Mirica, K. A., and Whitesides, G. M. 2012. Measuring Markers of Liver Function Using a Micropatterned Paper Device Designed for Blood from a Fingerstick. *Anal. Chem.* 84, 6, 2883–2891.

[53] Wang, W., Wu, W.-Y., and Zhu, J.-J. 2010. Tree-shaped paper strip for semiquantitative colorimetric detection of protein with self-calibration. *Journal of Chromatography A* 1217, 24, 3896–3899.

[54] Warsinke, A. 2009. Point-of-care testing of proteins. *Anal Bioanal Chem* 393, 5, 1393–1405.

[55] Washburn, E. W. 1921. The Dynamics of Capillary Flow. *Phys. Rev.* 17, 3, 273–283.

[56] Whatman. 2004. *FUSION 5™ One Material, Five Functions*.

[57] Wong, R. and Tse, H. 2009. *Lateral Flow Immunoassay*. Humana Press, Totowa, NJ.

[58] X.J. Li, Z.H. Nie, C.-M. Cheng, A.B. Goodale, and G.M. Whitesides, Ed. 2010. *Paper-based electrochemical ELISA*.

[59] Xu, M., Bunes, B. R., and Zang, L. 2011. Paper-Based Vapor Detection of Hydrogen Peroxide: Colorimetric Sensing with Tunable Interface. *ACS Appl. Mater. Interfaces* 3, 3, 642–647.

[60] Yager, P., Domingo, G. J., and Gerdes, J. 2008. Point-of-care diagnostics for global health. *Annu Rev Biomed Eng* 10, 107–144.

[61] Yager, P., Edwards, T., Fu, E., Helton, K., Nelson, K., Tam, M. R., and Weigl, B. H. 2006. Microfluidic diagnostic technologies for global public health. *Nature* 442, 7101, 412–418.

[62] Yu, J., Ge, L., Huang, J., Wang, S., and Ge, S. 2011. Microfluidic paper-based chemiluminescence biosensor for simultaneous determination of glucose and uric acid. *Lab Chip* 11, 7, 1286.

[63] Zhang, D. H., Li, P. W., Zhang, Q., Yang, Y., Zhang, W., Guan, D., and Ding, X. X. 2012. Extract-free immunochromatographic assay for on-site tests of aflatoxin M1 in milk. *Anal. Methods* 4, 10, 3307.

[64] Zhong, Z. W., Wang, Z. P., and Huang, G. X. D. 2012. Investigation of wax and paper materials for the fabrication of paper-based microfluidic devices. *Microsyst Technol* 18, 5, 649–659.

[65] Zhu, J., Zou, N., Zhu, D., Wang, J., Jin, Q., Zhao, J., and Mao, H. 2011. Simultaneous Detection of High-Sensitivity Cardiac Troponin I and Myoglobin by Modified Sandwich Lateral Flow Immunoassay: Proof of Principle. *Clinical Chemistry* 57, 12, 1732–1738.